ISSN: 2738-9928 (Online)
2738-9812 (Print)

NEPAL JOURNAL OF MATHEMATICAL SCIENCES (NJMS)

Published by

SCHOOL OF MATHEMATICAL SCIENCES

Tribhuvan University, Kirtipur
Kathmandu, Nepal

Volume 4, Number 2 **August 2023**

NEPAL JOURNAL OF MATHEMATICAL SCIENCES (NJMS)

ISSN: 2738-9928 (Online), 2738-9812 (Print)
Volume-4, Number -2 (August, 2023)

Acknowledgement

The Editorial Board would like to express their sincere gratitude and special thanks to the following reviewers for their substantial contribution of time and expertise to the journal's rigorous editorial process for this volume, regardless of whether the papers are finally accepted /published or not.

- Anju Devi, *Department of Mathematics, NIILM University Kaithal, Kaithal, Haryana, India*
- Bal Krishna Bal, *Department of Computer Engineering, Kathmandu University, Dhulikhel, Nepal*
- Binod Chandra Tripathy, *Department of Mathematics, Tripura University, West Tripura, India.*
- Buddhi Sapkota, *Department of Mathematics, Ratna Rajya Campus, Tribhuvan University, Kathmandu, Nepal*
- Chet Raj Bhatta, *Central Department of Mathematics, Tribhuvan University, Kathmandu, Nepal*
- Dil Bahadur Gurung, *Department of Mathematics ,School of Natural Sciences, Kathmandu University*
- Dinesh Panthi,*Department of Mathematics, Nepal Sanskrit University, Kathmandu, Nepal*
- Gyan Prasad Paudel , *Central Campus of Science and Technology, Mid-Western University, Surkhet, Nepal*
- Harsh Vardhan Harsh , *Faculty of Sci. & Tech., ICFAI Tech. School, ICFAI University Jaipur, Rajasthan, India*
- Jhavi Lal Ghimire, *Central Department of Mathematics, Tribhuvan University, Kathmandu , Nepal*
- Kamal Chapagain, *Department of Electrical and Electronics Engineering, Kathmandu University, Dhulikhel, Nepal*
- Gajendra Sharma, *Department of Computer Science & Engineering, Kathmandu University,Dhulikhel, Nepal*
- Kazi Fayzus Salahin, *Senior Data Analyst, Eminence Associates for Social Development, Bangladesh.*
- Madhav Prasad Poudel, *School of Engineering, Central Campus, Pokhara University, Kaski, Nepal*
- Narayan Prasad Pahari, *School of Mathematical Sciences, Tribhuvan University, Kathmandu,Nepal*
- Omorodion Martins, *Associate Prof and Qualified actuary, Elizade University, Nigeria*
- Panchatcharam Mariappan, *Indian Institute of Technology (IIT), Tirupati, India*
- Pawan Shrestha, *Central Department of Mathematics, Tribhuvan University, Kathmandu, Nepal*
- Praphul Chhabra, *Department of Mathematics , University of Engineering and Management, Rajasthan*
- Ramakant Bhardwaj, *Department of Mathematics, Amity University,Kolkata, West Bengal, India*
- Ravinder Poonia, *Department of Mathematics, Govt. College Narnaund, Hisar, Haryana India*
- Sailendra Kumar Mishra, *Department of Mathematics, Pulchok Engineering Campus, Tribhuvan University,Nepal*
- Sania Qureshi , *Department of Mathematics , Mehran University of Engineering and Technology, Pakisthan*
- Santosh Ghimire, *Mathematics of Mathematics, Pulchok Engineering Campus, Tribhuvan University,Nepal*
- Soumen Kishor Nath, *Institute of Education & Research (IER), University of Chittagong , Bangladesh*
- Surendra Kumar Agarwal, *Department of Mathematics, IIS (Deemed to be University),Jaipur, India*
- Surendra Kumar Tiwari, *Dept. of Mathematics, Dr. C. V. Raman University, Kota, Bilaspur, Chhattisgarh, India*
- Suresh Kumar Sahani, *Department of Mathematics, MIT campus, Janakpurdham , Nepal*

NEPAL JOURNAL OF MATHEMATICAL SCIENCES (NJMS)

Volume-4, Number-2 (August, 2023)

The Nepal Journal of Mathematical Sciences (NJMS) is now available on NepJOL at https://www.nepjol.info/index.php/njmathsci/index

MAILING ADDRESS

Nepal Journal of Mathematical Sciences
School of Mathematical Sciences,
Tribhuvan University, Kirtipur,
Kathmandu, Nepal
Website: www.sms.tu.edu.np
Email: *njmseditor@gmail.com*

Editorial

Welcome to the second issue of Volume 4, 2023 of Nepal Journal of Mathematical Sciences (NJMS). This issue contains ten original research articles and review papers in different fields of mathematics and mathematical sciences. We are grateful to all the authors for publishing their research works on this issue. We are expressing our thankfulness to all the reviewers and editors for their support, and backing for the publication of this work. We would like to request research scholars, professors, and scientists to submit their original research articles for future issues.

August 30, 2023

Editor-in-Chief
Prof. Dr. Narayan Prasad Pahari
Nepal Journal of Mathematical Sciences
(NJMS)
Email: *njmseditor@gmail.com*

Nepal Journal of Mathematical Sciences (NJMS)
ISSN: 2738-9928 (Online), 2738-9812 (Print)
Volume 4, Number 2, August 2023

CONTENTS

1.	**On a Generalization of Chatterjee's Fixed Point Theorem in *b*-metric Space** *Chhabi Dhungana, Kshitiz Mangal Bajracharya, Narayan Prasad Pahari , & Durgesh Ojha* ***DOI:*** https://doi.org/10.3126/njmathsci.v4i2.59526	**1-6**
2.	**High School Performance Based Engineering Intake Analysis and Prediction Using Logistic Regression and Recurrent Neural Network** *Govinda Pandey, Nanda Bikram Adhikari, & Subarna Shakya* ***DOI:*** https://doi.org/10.3126/njmathsci.v4i2.59524	**7-16**
3.	**The Gradshteyn and Ryzhik's Integral and the Theoretical Computation of $GM(m,n)$ involving the Continuous Whole Life Annuities** *Ogungbenle Gbenga Michael, Ihedioha Silas Abahia, & Ogungbenle Oluwatoyin Gladys* ***DOI:*** https://doi.org/10.3126/njmathsci.v4i2.59527	**17-30**
4.	**Computational Analysis of Fractional Reaction-Diffusion Equations that Appear in Porous Media** *Vinod Gill, Harsh Vardhan Harsh , & Tek Bahadur Budhathoki* ***DOI:*** https://doi.org/10.3126/njmathsci.v4i2.59534	**31-40**
5.	**On New Space of Vector-Valued Generalized Bounded Sequences Defined on Product Normed Space** *Jagat Krishna Pokharel, Narayan Prasad Pahari , & Jhavi Lal Ghimire* ***DOI:*** https://doi.org/10.3126/njmathsci.v4i2.59531	**41-48**
6.	**Forecasting Annual Mean Temperature and Rainfall in Bangladesh Using Time Series Data** *Keya Rani Das,Preetilata Burman, Linnet Riya Barman, Mashrat Jahan, & Mst. Noorunnahar* ***DOI:*** https://doi.org/10.3126/njmathsci.v4i2.59536	**49-58**
7.	**Collocation Computational Technique For Fractional Integro-Differential Equations** *Olumuyiwa James Petera, Mfon O. Etukb, Michael Oyelami Ajisopec, & Christie Yemisi Isholad, Tawakalt Abosede Ayoolae, & Hasan S. Panigoro* ***DOI:*** https://doi.org/10.3126/njmathsci.v4i2.59539	**59-66**
8.	**Numerical Analysis of Fractional-Order Diffusion Equation** *Jeevan Kafle, Deepak Bahadur Bist, & Shankar Pariyar* ***DOI:*** https://doi.org/10.3126/njmathsci.v4i2.59538	**67-76**
9.	**On a New Application of Almost Increasing Sequence to Laguerre Series Associated with Strong Summability of Ultrapherical Series** *Suresh Kumar Sahani,Jagat Krishna Pokharel, Gyan Prasad Paudel , & S.K. Tiwari* ***DOI:*** https://doi.org/10.3126/njmathsci.v4i2.59537	**77-82**
10.	**Connection Formulas on Kummer's Solutions and their Extension on Hypergeometric Function** *Madhav Prasad Poudel, Narayan Prasad Pahari, Ganesh Basnet, & Resham Poudel* ***DOI:*** https://doi.org/10.3126/njmathsci.v4i2.60177	**83-88**

Nepal Journal of Mathematical Sciences (*NJMS*)
ISSN: 2738-9928 (*online*), 2738-9812 (*print*)
Vol. 4, No. 2, 2023 (*August*): *1-6*
DOI: https://doi.org/10.3126/njmathsci.v4i2.59526

Research Article
Received Date: February 3, 2023
Accepted Date: August 9, 2023
Published Date: August 30, 2023

On a Generalization of Chatterjee's Fixed Point Theorem in *b*-metric Space

Chhabi Dhungana[1],Kshitiz Mangal Bajracharya[2], Narayan Prasad Pahari[2] , & Durgesh Ojha[3]

[1] *Khwopa College of Engineering, Tribhuvan University, Bhaktapur, Nepal*
[2] *Central Department of Mathematics,Tribhuvan University, Kirtipur, Kathmandu, Nepal*
[3]*School of Engineering, Pokhara University, Pokhara-30, Kaski, Nepal*

Email:*chhavi039@gmail.com*[1],*nppahari@gmail.com*[2], *kshitiz.bajracharya652@gmail.com*[2], *ojhadurgesh98@gmail.com*[3]

Abstract: *Banach's Fixed Point Theorem* (*BFT*)*deals with the certain contraction mappings of a complete metric space into itself. It states sufficient conditions for the existence and uniqueness of a fixed point. In the study of fixed point theory, BCP has been extended and generalized in many different directions in usual metric spaces. One of those generalizations is a b-metric space. Such generalizations have resulted in generalizing some popular metric fixed point theorems in the context of a b-metric space. In* 2013*, Kir and Kiziltunc* [8] *attempted to generalize Chatterjee's Fixed Point Theorem* (*CFPT*) *in the context of b-metric spaces. The proof of that generalization, however, had a minor flaw and an unstated assumption. This paper attempts to fix these issues by introducing new conditions.*

Keywords: *Convergence, Compactness, Cauchy sequence, Metric space, b-Metric space.*

1. Introduction and Motivation:

The concept of fixed point theories is one of the most important results in Functional Analysis. The famous fixed point result called Banach Contraction Principle(BCP) is generalized and improved in many directions. One usual way of studying the Banach contraction principle is to replace the metric space with certain generalized metric spaces. Some problems, particularly the problem of the convergence of measurable functions with respect to measure led Czerwik[6] to a generalization of metric space and introduced the concept of b-metric space. The concept of b-metric space was generalized in different directions, for instance, we refer to a few: Alamari and Ahamad [1], Bakhtin[2], Iqbal, Batool, Ege and Sen[7], Ojha and Pahari [10] and, Shoaib, and et al [12]. Several authors proved fixed-point results of single-valued and multi-valued operators in b-metric spaces. Also, Kumar, Mishra, and Mishra [9] studied common fixed point theorems in b-metric space. In the present article, we shall study on a generalization of Chatterjee's Fixed Point Theorem studied in [4]in b-metric space.

Before proceeding with the main work, we shall define some important definitions, examples, and key results related to *b*-metric spaces, which are used in our further discussion.

Definition 1.1 (***b*-metric space**, Bakhtin **[2])** Let X be any non-empty set and $b \geq 1$ be some given real number. Let$d : X \times X \to [0, \infty)$ be a function which satisfies the following properties:

(b1) For all$x, y \in X$, $d(x, y) \geq 0$ and $d(x, y) = 0 \Leftrightarrow x = y$.
(b2) For all $x, y \in X$, $d(x, y) = d(y, x)$.
(b3) For all $x, y, z \in X$, $d(x, y) \leq b[d(x, z) + d(y, z)]$.

Then, we say that d is a b-metric defined on X and that X along with d forms a b-metric space and is denoted by the ordered pair (X, d).In some cases, if we need a distinction between b-metrics defined on different spaces, we write the space in its suffix. For example, we may write d as d_X in the above discussion. We define b as a triangular constant and refer to (b3) as relaxed triangle inequality or b-triangle inequality (Cobzas,**[5]**), and (Czerwik, **[6]**)**.**

The following are examples of b-metric spaces:

Example 1.2. Every metric space is an example of a b-metric space because we have $b = 1$ validating the condition, (b3).

Example 1.3.(Bakhtin **[2])**

The set $L_p(\mathbb{R})$ where $L_p(\mathbb{R}) = \{\{x_n\} \subseteq \mathbb{R} : \sum|x_n|^p < \infty\}$ (with $0 < p < 1$) together with the function $d : L_p(\mathbb{R}) \times L_p(\mathbb{R}) \to [0, \infty)$ defined by

$$d(x, y) = (\sum_{i=0}^{n} |x - y|^p)^{1/p}$$

where $x = \{x_n\}, y = \{y_n\} \in L_p(\mathbb{R})$ forms a b-metric with $b = 2^{1/p}$.

Example 1.4.(Bakhtin **[2])**

The space $L_p[0, 1]$ (where $0 < p < 1$) of all real functions $x(t)$, $t \in [0, 1]$ such that $\int_0^1 |x(t)|^p dt < \infty$ forms a b-metric by defining

$$d(x, y) = (\int_0^1 |x(t) - y(t)|^p)^{1/p} dt \text{ for each } x, y \in L_p[0, 1], \text{ with } b = 2^{1/p}.$$

It is clear that definition of b-metric is an extension of usual metric space. Obviously, each metric space is a b-metric space with $b = 1$. However, Czerwik [6] has shown that a b-metric on X need not be a metric on X. The following example illustrates this situation.

Example 1.5.

Let (X, d) be a metric space. Define $\rho(x, y) = [d(x, y)]^p$, where $p > 1$ is a real number. Then we can verify that ρ forms a b-metric with $b = 2^{p-1}$. However, if (X, d) is a metric space, then (X, ρ) is not necessarily a metric space.

Example 1.6 (Bota , Molnar, and Varga,**[3]**). Let X be a set with three elements. Let $X = X_1 \cup X_2$ such that X_1 has two elements and $X_1 \cap X_2 = \emptyset$. Define $d : X \times X \to \mathbb{R}$ by

$$d(x, y) = \begin{cases} 0, & for\ x = y \\ 4, & for\ x, y \in X_1 \ \ and \ \ x \neq y \\ 1, & for\ x \in X_1, y \in X_2 \ \ and \ \ x \neq y \end{cases}$$

Then (X , d) is a b-metric space but not a metric space.

It is noted that the class of b-metric spaces is larger than the class of metric spaces. The following are the concepts related to sequences which we shall use in the main result.

Definition 1.7(Bota ,Molnar, and Varga**, [3]).** Let (X, d) be a b-metric space. A sequence $(x_n)_{n=1}^{\infty}$ in X is said to converge to some $x \in X$ if for every $\varepsilon > 0$ there exists a positive integer N such that

$$n \geq N \Rightarrow d(x_n , x) < \varepsilon.$$

It is denoted by $\lim_{n \to \infty} x_n = x$.

Since $(d(x_n , x))_{n=1}^{\infty}$ is a sequence of positive real numbers, this definition suggests the convergence of this sequence to zero is a characterization of convergent sequence in b-metric space. This is analogical to a similar characterization in a metric space.

Definition 1.8 (Bota , Molnar, and Varga**, [3]).** Let (X, d) be a b-metric space. A sequence $(x_n)_{n=1}^{\infty}$ in X is said to be a Cauchy sequence if for every $\varepsilon > 0$ there exists a positive integer N such that

$$m, n \geq N \Rightarrow d(x_m, x_n) < \varepsilon.$$

Thus, just like in the case of metric spaces, we can equivalently say that $(x_n)_{n=1}^{\infty}$ in X is a Cauchy sequence if $d(x_m, x_n) \to 0$ as $m, n \to \infty$.

Definition 1.9 (Bota , Molnar, and Varga**, [3]).** If a b-metric space(X, d) is such that every Cauchy sequence in space(X, d) is convergent, then it is complete b-metric space.

Definition 1.10 (Cobzas**, [5]).** Let (X, d) be a b-metric space. Then, d is said to be continuous if for any two convergent sequences $(x_n)_{n=1}^{\infty}$ and$(y_n)_{n=1}^{\infty}$ of points in X, we have

$$\lim_{n \to \infty} d(x_n, y_n) = d(x, y), \text{ where } \lim_{n \to \infty} x_n = x \text{ and } \lim_{n \to \infty} y_n = y.$$

Definition 1.11 (Panthi,**[11]).** A point u is a fixed point of the function $f(x)$ if $f(u) = u$. In other words, $f(x)$ has a root at u iff $g(x) = x - f(x)$ has a fixed point at u.

2. A Critical Study of Kir and Kiziltunc's Generalization of Chatterjee's Fixed Point Theorem (CFPT)

Kir and Kiziltunc**[8]** gave generalizations of Banach Fixed Point Theorem (BFPT), Kannan Fixed Point Theorem (KFPT) and Chatterjee's Fixed Point Theorem (CFPT). These theorems have been listed respectively as Theorem 2.1, Theorem 2.2 and Theorem 2.3 below, in the same order as they appear in Kir and Kiziltunc**[8].**The theorems have been restructured here in order to make them consistent with the notations that we have used in this paper.

Theorem 2.1 (Kir and Kiziltunc,**[8]).** Let (X, d) be a complete b-metric space with a triangular constant $b \geq 1$. Let $T: X \to X$ be a function then there exists $\lambda > 0$such that $\lambda \in (0, 1)$ and $b\lambda < 1$ which also satisfies

$$d(Tx, Ty) \leq \lambda\, d(x, y), \quad \forall\, x, y \in X.$$

Then, T has a unique fixed point.

Theorem 2.2 (Kir and Kiziltunc,**[8]).**Let (X, d) be a complete b-metric space with a triangular constant $b \geq 1$. Let $T: X \to X$ be a function for which there exists $\lambda > 0$such that $\lambda \in \left(0, \frac{1}{2}\right)$which also satisfies

$$d(Tx, Ty) \leq \lambda\, [d(x, Tx) + d(y, Ty)], \quad \forall\, x, y \in X.$$

Then, T has a unique fixed point.

Theorem 2.3 (Kir and Kiziltunc,**[8]).**Let (X, d) be a complete b-metric space with a triangular constant $b \geq 1$. Let $T: X \to X$ be a function for which there exists $\lambda > 0$ be such that $b\lambda \in \left(0, \frac{1}{2}\right)$which also satisfies

$$d(Tx, Ty) \leq \lambda\, [d(x, Ty) + d(y, Tx)] \quad \forall\, x, y \in X.$$

Then, T has a unique fixed point.

These theorems had one more condition, which was actually a hint to construct a Cauchy sequence for the proof, rather than a condition that was needed to construct a proof. It was to choose any $x_0 \in X$ and construct a sequence $(x_n)_{n=0}^{\infty}$ by $x_n = T^n x_0$. This sequence is then shown to be a Cauchy sequence using the conditions in the theorems. This construction has not been overlooked in this paper.

The proof of the third theorem had a flaw and the proof of $(x_n)_{n=0}^{\infty}$being a Cauchy sequence has some unstated assumptions as below.

a) The flaw is that the step marked in their proof has been obtained by assuming the

continuity of the *b*-metric *d.* The theorem doesn't state that condition and it has been illustrated by Cobzas**[5]** that a *b*-metric is not necessarily continuous.

b) The proof of $(x_n)_{n=0}^{\infty}$ being a Cauchy sequence is said to be followed by using a similar method as used in the proof of Theorem 2.1 and Theorem 2.2 .Theorem 2.2 suggests the method similar to that of Theorem 2.1. So, basically the authors want us to use the procedure as used in Theorem 2.1. But while doing so, we obtain

$$d(x_m\,, x_n) \leq bk^m[1 + (bk) + (bk)^2 + \cdots + (bk)^{n-m-1}]\, d(x_0\,, x_1)$$

The authors have assumed that $bk < 1$, which leads to the conclusion that the geometric series on the right was convergent and therefore the sequence was Cauchy.

Here, *k*= $\frac{b\lambda}{1-b\lambda}$. But ,if we have $b = 20$ and $\lambda = \frac{1}{80}$? In such a case, we have

$$bk = \frac{b^2\lambda}{1 - b\lambda} = \frac{(400 \times \frac{1}{80})}{(1 - \frac{1}{4})} = \frac{20}{3} > 1\,.$$

In this case, the convergence of the said geometric sequence will not follow at all. The authors have not considered or mentioned such possibilities, which makes the proof incomplete.

Here, we wish to alter the conditions prescribed by Theorem 2.3 so that the new conditions would generalize Chatterjee's Fixed Point Theorem studied in **[4]** to a *b*-metric space and has no such questionable assumptions and flaws.

3. Main Result

After critically analyzing the proof of Theorem 2.3, it was found that to fix the flaw of continuity of *d*, we need the assumption of continuity of *d*. And, to obtain a Cauchy sequence as we wished, it sufficed to take $bk < 1$. If $bk < 1$, then it was found that we can drop the original condition that $b\lambda \in \left(0, \frac{1}{2}\right)$. The necessary “corrections" were found to be trivial. This is stated and proved formally in Theorem 3.1.

Theorem 3.1.Let (X, d) be a complete *b*-metric space with a continuous *b*-metric *d* and a triangular constant $b \geq 1$. Let $T: X \to X$ be a function for which there exists $\lambda > 0$ such that $0 < \frac{b^2\lambda}{1-b\lambda} < 1$ which also satisfies

$$d(Tx\,, Ty) \leq \lambda\,[d(x, Ty) + d(y, Tx)] \quad \forall\, x\,, y \in X\,.$$

Then, *T* has a unique fixed point.

Proof. Let the given condition hold.

Since$0 < \frac{b^2\lambda}{1-b\lambda} < 1$ and $b^2\lambda > 0$, it follows that $1 - b\lambda > 0$.

Consequently, we get

$$0 < \frac{b\lambda}{1 - b\lambda} < \frac{b^2\lambda}{1 - b\lambda} < 1$$

To construct a Cauchy sequence, let $s \in X$ be arbitrary. Define a sequence $(x_n)_{n=0}^{\infty}$ by $x_n = T^n s$ so that, in general we get $x_{n+1} = Tx_n$. This sequence will be shown to be a Cauchy sequence. Let $n \in \mathbb{N}$. Then

$$\begin{aligned} d(x_n, x_{n+1}) &= d(Tx_{n-1}, Tx_n) \\ &\leq \lambda\,[d(x_{n-1}, Tx_n) + d(x_n, Tx_{n-1})] \\ &= \lambda\, d(x_{n-1}, Tx_n) \qquad [\because\ x_n = Tx_{n-1}] \\ &= \lambda\, d(x_{n-1}, x_{n+1}) \qquad [\because\ x_{n+1} = Tx_n] \\ &\leq b\lambda\,[d(x_{n-1}, x_n) + d(x_n, x_{n+1})] \end{aligned}$$

which implies that

$$(1 - b\lambda)\, d(x_n, x_{n+1}) \leq b\,\lambda\, d(x_{n-1}, x_n)$$

and therefore,

$$d(x_n, x_{n+1}) \leq k d(x_{n-1}, x_n)$$

where, $k = \frac{b\lambda}{1-b\lambda}$, because $1 - b\lambda > 0$. Using this relation recursively, we get

$$d(x_n, x_{n+1}) \leq k^n d(s, x_1)$$

Now, let $m, n \in \mathbb{N}, n > m$ and for $0 < bk < 1$, it follows that

$$\begin{aligned} d(x_m, x_n) &\leq b[d(x_m, x_{m+1}) + d(x_{m+1}, x_n)] \\ &\leq b[k^m d(s, x_1) + d(x_{m+1}, x_n)] \\ &= bk^m d(s, x_1) + b\, d(x_{m+1}, x_n) \\ &\leq bk^m d(s, x_1) + b^2 k^{m+1} d(s, x_1) + b^2 d(x_{m+2}, x_n) \\ &\vdots \\ &\leq bk^m [1 + (bk) + (bk)^2 + \cdots + (bk)^{n-m-1}]\, d(s, x_1) \\ &= bk^m \left[\frac{1-(bk)^{n-m}}{1-(bk)}\right] d(s, x_1) \\ &\leq bk^m \left[\frac{1}{1-(bk)}\right] d(s, x_1) \end{aligned}$$

So, $(x_n)_{n=0}^{\infty}$ is a Cauchy sequence since $d(x_m, x_n) \to 0$ as $m, n \to \infty$.
Thus, by completeness of *X*, there exists $x \in X$ such that $\lim_{n\to\infty} x_n = x$.Now, we show that *x* is a fixed point of *T*. For $n \in \mathbb{N}$, we have

$$\begin{aligned} d(x, Tx) &\leq b\,[d(x, x_{n+1}) + d(x_{n+1}, Tx)] \\ &= b\, d(x, x_{n+1}) + b\, d(Tx_n, Tx)] \\ &\leq b\, d(x, x_{n+1}) + b\,\lambda\, d(x, Tx_n) + b\lambda\, d(x_n, Tx) \\ &= b\, d(x, x_{n+1}) + b\,\lambda\, d(x, x_{n+1}) + b\lambda\, d(x_n, Tx) \end{aligned}$$

Due to the continuity of *d,* we get

$$d(x_n, Tx) \to d(x, Tx) \text{ as } n \to \infty.$$

So taking limits as $n \to \infty$ in above inequality, we get

$$d(x, Tx) \leq b\lambda\, d(x, Tx).$$

Now, as $1 - b\,\lambda > 0$, we have

$$\begin{aligned} & d(x, Tx) \leq b\lambda\, d(x, Tx) \\ & \Rightarrow (1 - b\lambda) d(x, Tx) \leq 0 \\ & \Rightarrow d(x, Tx) \leq 0 \\ & \Rightarrow d(x, Tx) = 0. \end{aligned}$$

Therefore, $Tx = x$, which makes *x* a fixed point of *T*.

To establish the uniqueness, let *y* be a different fixed point than *x* so that we have $y = Ty$. As $x \neq y$, we have$d(x, y) > 0$. Since *x* and *y* are fixed points of *T*, we have

$$d(x, Ty) = d(y, Tx) = d(x, y).$$

So, we obtain

$$\begin{aligned} d(x,y) &= d(Tx,Ty) \\ &\leq \lambda\,[\,d(x,Ty)+d(y,Tx)] \\ &\leq 2\lambda\, d(x,y) \end{aligned}$$

Now, as $0 < \frac{b\lambda}{1-b\lambda} < 1$.

It follows that $b\lambda < 1 - b\lambda$ and so, $2b\lambda < 1$.

Since $b \geq 1$, it follows that $2\lambda < 2b\lambda < 1$.

Therefore, the last inequality reduces to $d(x,y) < d(x,y)$.This is absurd. Hence, x is a unique fixed point of *T*.

Conclusion

In this paper, we have introduced some existing properties of b-metric space as the usual notion of a metric space. Besides this, we have studied a generalization of Chatterjee's Fixed Point Theorem in *b*-metric space. In fact, this result can be used for further research work in fixed point theory in Metric space and extends many other authors' existing works.

Acknowledgement

The authors would like to thank the unknown referee for his/her comments that helped us to improve this paper.

References

[1] Alamari, B. ,& Ahamad,J. **(2023)**. Fixed point results in *b*-metric spaces with applications to integral equations. *AIMS Mathematics*, **8**(4): 9443-9460.

[2] Bakhtin, I. A. **(1989)**.The contraction mapping principle in quasi-metric spaces. *Funct. Anal. Unianowsk Gos. Ped. Inst.,* **30**: 26-37.

[3] Bota, M.,Molnar, A.,& Varga, C. **(2011)**. On Ekaland's variational principle in *b*-metric spaces. *International Journal on Fixed Point Theory Computation and Applications,***12**(2): 21-28.

[4] Chatterjee, S. K.**(1972)**.Fixed point theorems. *C.R. Acad. Bulgare Sci*., **25**: 727-730.

[5] Cobzas, S. **(2019)**.*b*-metric spaces, fixed points and Lipchitz functions. *arXiv*,10.48550/ARXIV.1802.02722.

[6] Czerwik, S. **(1993)**.Contraction mappings in *b*-metric Spaces. A*cta Mathematica et Informatica Universitatis Ostraviensis,* **1(**1): 5-11.

[7] Iqbal, M., Batool, A., Ege O.,& de la Sen, M.**(2020)**. Fixed point of almost contraction in b-metric space. *Hindawi Journal of Mathematics*, Article ID 3218134.

[8] Kir, M.,& Kiziltunc, H. **(2013)**. On some well known fixed point theorems in *b*-metric space. *Turkish Journal of Analysis and Number Theory,***1**(1): 13-16.

[9] Kumar, M., Mishra, L.N.,& Mishra, S.**(2017)**.Common fixed point theorems satisfying (CRL_{ST}) property in b-metric spaces. *Research India Publications*, **12**(2) : 135 – 147.

[10] Ojha, D., & Pahari, N.P.**(2021)**.A study of fixed point theory in generalized *b*-metric space. *International Journal of Mathematical Archive,* **12**(7): 4-9.

[11] Panthi, D.**(2013)**. Some fixed point in dislocated and dislocated quasi metric space. *PhD Dissertation*.

[12] Shoaib, A., Rasham ,T., Marino, G., Lee, J.R. , & Park, C.**(2020)**.Fixed point results for dominated mappings in rectangular b-metric spaces with applications. *AIMS Mathematics*, **5**: 5221 - 5229.

□□

Nepal Journal of Mathematical Sciences (*NJMS*)
ISSN: 2738-9928 (*online*), 2738-9812 (*print*)
Vol. 4, No. 2, 2023 (*August*): 7-16
DOI: https://doi.org/10.3126/njmathsci.v4i2.59524

Research Article
Received Date: July 3, 2023
Accepted Date: August 11, 2023
Published Date: August 30, 2023

High School Performance Based Engineering Intake Analysis and Prediction Using Logistic Regression and Recurrent Neural Network

Govinda Pandey[1],Nanda Bikram Adhikari[2], & Subarna Shakya[3]

[1,2,3]*Dept. of Electronics and Computer Engineering, Pulchowk Engineering Campus, Tribhuvan University, Nepal*

Email:[1]073*mscs*655.*govinda@pcampus.edu.np*,[2]*adhikari@ioe.edu.np*, [3]*drss@ioe.edu.np*

Abstract: *A student's high school performance is crucial for engineering admission in Nepal. Machine learning-based predictive models can provide valuable insights. This study aims to predict engineering entrance exam scores and admission probability based on high school academic records. In this study, we have used exam data from National Examination Board (NEB) and Institute of Engineering (IOE) containing grades, scores and results for over* 11,000 *students. Logistic Regression (LR) and Long-Short Term Memory (LSTM) models are implemented to predict pass/fail status and year-wise entrance score forecasting, respectively. In addition, the Prophet model analyzed trends in entrance score threshold averaging. The result shows that the logistic model achieved* 97% *accuracy in predicting pass/fail status and the LSTM network attained reasonable accuracy between* 65-85% *for score forecasting. The Prophet model accurately projected decreasing trends in threshold scores and admitted students' averages. Our model analyses provides actionable insights into student outcomes, complex patterns, and changing trends. Proactive interventions through upgraded curriculum, teacher training etc. could reverse declining enrolment.*

Keywords: *Education data mining, Intake prediction, Logistic regression, Long Short-Term Memory (LSTM), Student performance*

1. Introduction

In the realm of education, understanding and enhancing student performance is pivotal for fostering national development and stimulating economic growth. Educational institutions amass extensive datasets encompassing student activities, routines, backgrounds, and academic histories. However, a considerable portion of this data remains underutilized, primarily due to its sheer volume and complexity, as well as the institutions' capacity constraints in processing it. To harness the potential of this data for predictive and prescriptive purposes, the integration of advanced information technologies, notably data mining and machine learning, is imperative. The data on engineering entrance exam applicants and results over the past 5 years reveals concerning declines in both student interest and performance. Specifically, the number of applicants has steadily dropped from over 12,000 in 2017 to just 9,404 in 2022, indicative of reducing the popularity of engineering programs. However, even among those appearing for the exams, competitiveness and preparedness have worsened. The entrance score threshold has fallen from 52 down to 38 and average scores have declined from nearly 70 to around 62. This consistent downward trend in cut off marks and admitted student performance highlights deficiencies in pre-engineering preparation at the high school level. Students seem less academically equipped to handle the rigor of the entrance exams compared to

previous years. The reasons could include deteriorating quality of schooling, increased opportunities abroad, or other competing fields attracting talent. Nonetheless, the data signals the need for interventions to boost interest in engineering and bolster high school teaching and resources. Addressing these gaps proactively through counselling, upgraded curriculum, teacher training, etc. can help reverse the concerning enrolment patterns. More effective high school preparation will translate into increased applicants and better performance.

This paper aims to bridge the existing knowledge gap between high school and engineering education by developing predictive models based on high school academic records. The scope includes students applying for engineering programs at the Institute of Engineering under Tribhuvan University. The objectives are to predict entrance exam scores and admission probability using machine learning techniques. The research questions are: 1) How accurately can high school performance predict engineering entrance outcomes? 2) What are the capabilities of different machine learning models for this predictive task? Machine learning techniques like logistic regression and LSTM networks are applied to high school and entrance datasets to uncover patterns and trends that can enable data-driven decision-making around admissions.

Data mining, also known as knowledge discovery in databases (KDD), employs a multitude of techniques and algorithms to extract valuable insights from vast datasets. When applied to the educational domain, termed as "educational data mining," these techniques can unveil patterns and correlations previously unseen. Algorithms such as decision trees, neural networks, linear regression, and random forests are particularly adept at predicting outcomes based on historical data, enabling educational stakeholders to anticipate student performance trends and act proactively.

For instance, a student's performance in high school, analysed holistically across various parameters-grade-wise and subject-wise results, demographics, school type, and more-can serve as a predictive indicator of their potential success in higher education. Especially in contexts where high school graduates aspire for competitive admissions in tertiary institutions, such predictive models can be invaluable. As a case in point, for admissions to engineering programs under Tribhuvan University, students are assessed through a rigorous computer-based entrance examination by the Institute of Engineering, which evaluates proficiency in subjects like Mathematics, Physics, Chemistry, and English, all grounded in the high school curriculum. Thus, a student's high school academic record becomes a significant predictor of their entrance score and subsequent success in the program.

This paper aims to bridge the existing knowledge gap between high school and engineering education by developing a predictive model based on high school academic records. Such a model can assist in identifying students at risk, guiding admission decisions, and formulating strategies to ensure every student's optimal academic progression.

2. Background Study

Predicting student entrance scores based on prior academic performance utilizes information extraction. Analysing student data, including exam scores, enables institutions to develop predictive models for identifying students needing extra support. Educational data mining explores predictive models for academic performance using machine learning techniques (Chen et al.,[2]). Educational institutions are amassing extensive datasets encompassing student activities, attendance patterns, geographical locations, family backgrounds, and more. Nevertheless, this wealth of data typically gets harnessed for generating basic queries and conventional reports that seldom reach the appropriate individuals in a timely manner to enable informed decision-making (Kabakchieva, [8]). Dien et al. study deep learning methods for student performance prediction, considering data preprocessing strategies (Dien et al., [4]). In Nepal, research explores hyper-parameter tuning for student grade prediction using neural networks (Rimal et al., [14]). GPA prediction employs Boruta algorithm and random forest with single and multiple-layer models. Artificial neural networks forecast student performance. Educational data mining evaluates classification algorithms for student success prediction(Gochhait & Rimal, [7]; Meghji et al., [10]; Naser et al., [11]).

Machine learning is crucial for education, enhancing retention, performance prediction, and curriculum design. Waheed et al. demonstrate deep neural networks outperform logistic regression and support vector machines. A hybrid 2D CNN model predicts academic achievement. A deep neural network predicts student performance effectively. High school GPA predicts college outcomes and future income. Prophet forecasting aids resource allocation using enrolment data (Bendangnuksung & Prabu, [1]; Enughwure & Ogbise, [5]; Marte, [9]; Patayon & Crisostomo, [12]; Poudyal et al., [13]; Waheed et al., [15]). Prophet methodology is a time series forecasting approach that uses a decomposable model with three main components: trend, seasonality, and holidays (Daraghmeh et al., [3]).To our knowledge, such modelling is not found in literature in the mentioned scope, thus this research attempts the same using the following methodology.

3. Methodology

The study methodology involved collecting student academic records from the National Examination Board (NEB) and Institute of Engineering (IOE) entrance exams. The NEB data contained high school (Grade 10 and 12) grades and GPAs, while the IOE data had entrance registration details and exam scores. After joining the datasets, feature extraction and selection was done to identify the most relevant input variables like PCL subject scores.

Data pre-processing steps included handling missing values, removing outliers, encoding categorical variables, and pivoting to summarize subject marks. The final dataset contained features such as academic year, gender, NEB grades, IOE entrance scores and results for over 11000 students. Exploratory analysis using summary statistics and visualizations provided insights into score distributions.The processed data was split 70:30 into train and test sets. Three models were developed - logistic regression to predict pass/fail, LSTM networks for score regression, and Facebook Prophet for result trend forecasting. The logistic regression hyperparameters were tuned using grid search. The LSTM model architecture had input, hidden and output layers to capture temporal relationships. Prophet decomposed the time series into trend, seasonal and holiday components.

The models were implemented in Python using libraries like Pandas, Scikit-learn, Keras and Tensor Flow. Model training and performance evaluation was done on a Windows system with Core i7 processor and 16GB RAM. Key metrics like accuracy, RMSE and prediction plots were used to analyse model results.

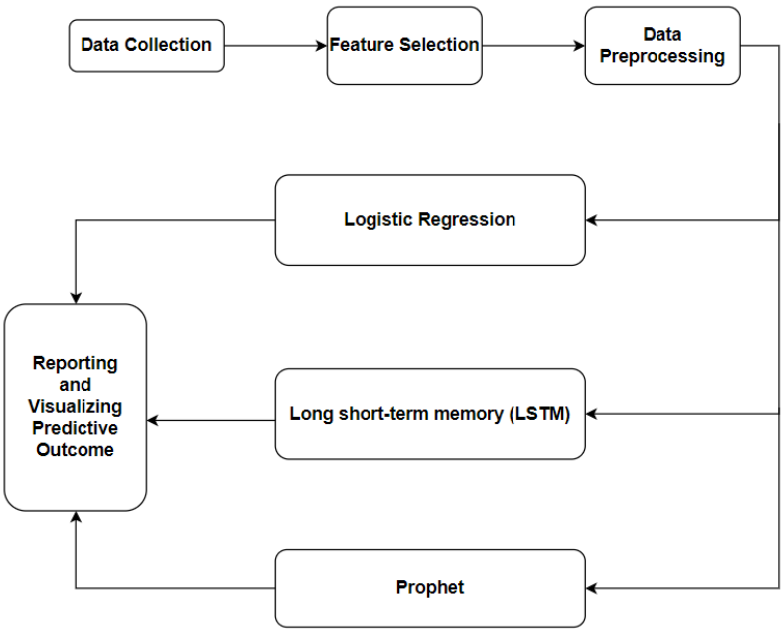

Figure 1 Methodology followed in the research

Model Development& Training

Three models were developed - logistic regression, LSTM networks, and Facebook Prophet. Logistic regression was implemented for binary classification to predict exam pass/fail. The model was trained by optimizing a cost function using gradient descent. Data preprocessing selected relevant features like PCL grades.In contrast to ordinary regression that minimizes the sum of squared errors to choose parameters, logistic regression selects parameters that maximize the probability of observing the sample values.Logistic regression generates the coefficients (and its standard errors and significance levels) of a formula to predict a logit transformation of the probability of presence of the characteristic of interest:

$$logit\ (p) = b_0 + b_1X_1 + b_2X_2 + b_3X_3 + \ldots + b_kX_k \quad (1)$$

where p is the probability of presence of the characteristic of interest, b_i is the weightage factor of inputs X_i. The logit transformation is defined as the logged odds:

$$odds = \frac{p}{1-p} = \frac{probability\ of\ presence\ of\ characteristic}{probability\ of\ absence\ of\ characteristic} \quad (2)$$

$$logit\ (p) = \ln(odds)$$

LSTM networks were designed for score regression, with input, hidden and output layers to capture temporal patterns. The LSTM architecture used sequences of past observations to make multi-step forecasts. The LSTM model had an input layer with 18 units corresponding to the 18 feature variables. This fed into an LSTM layer with 150 neural network units to capture temporal dependencies. A dense output layer with a single unit made a regression prediction of the exam score. The model was trained using the Adam optimization algorithm to minimize the binary cross-entropy loss function. Evaluation metrics calculated were prediction accuracy and mean squared error (MSE) on a held-out test set. This LSTM architecture with tuned hyperparameters was designed to leverage sequence data and learn complex relationships between past academic performance and future examscores.

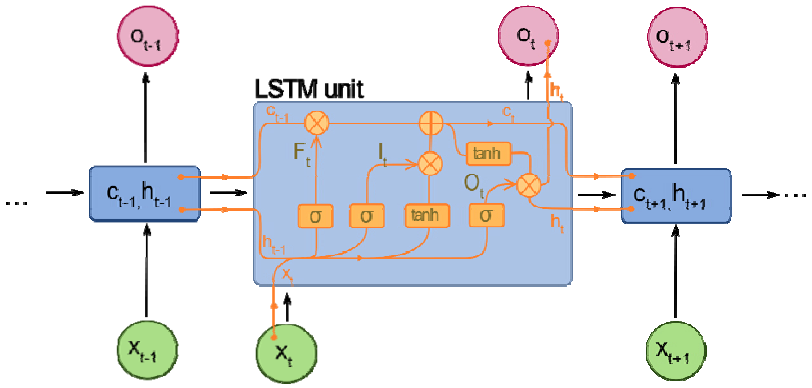

Figure 2 Long Short-Term Memory (LSTM) Architecture(fdeloche, [6])

The logistic regression model estimated the probability of passing the exam using the sigmoid function. Hyperparameters were tuned via grid search for optimal performance. The LSTM model was built using the Keras Sequential API, with layers for LSTM cells, dropout, dense connections, and activations. Binary cross-entropy loss and the Adam optimizer were used for training over multiple epochs. For new observations, the trained LSTM model generated score predictions.

The Prophet model was applied for time series forecasting of engineering entrance exam pass thresholds and average scores. It decomposes the time series into trend, seasonality, holidays, and noise components. The trend component models non-periodic changes using the beta parameter. Prophet provided interpretable forecasts along with uncertainty intervals for the time series data. Seasonality is captured by the *delta* parameter to incorporate periodic patterns. One-off events are accounted for by the *trend_params* parameter for holidays. The *sigma_obs* parameter represents noise or random variability. The model is represented by the equation:

$$Y(t) = g(t) + s(t) + h(t) + e(t), \quad (3)$$

where $g(t)$ is trend, $s(t)$ is seasonality, $h(t)$ is holidays, and $e(t)$ is noiseKey estimated parameters as, slope $k = -0.01304175$, intercept $m = 1.02369371$,noise $sigma\_obs = 0.00457194$.

Prophet automatically detected change points in the time series and modelled trend nonlinearity.It incorporated uncertainty estimates in its forecasts. The effects of holidays were captured using additional delta parameters in the model. Regularization helped avoid overfitting the training data. Overall, the three complementary models provided insights into exam outcomes, score patterns, and temporal trends.

4. Results and Discussion

The analysis demonstrated the capability of machine learning techniques for predictive modelling of engineering entrance exam outcomes. Correlation analysis using heatmaps revealed entrance scores are positively associated with high school grades. Heatmap showed entrance exam scores correlated positively with SEE (0.43) and PCL (0.39) results. Entrance math score had very strong correlation (0.89) with final entrance score, while PCL math correlation was weaker (0.19).Logistic regression achieved high accuracy of 97% in classifying pass versus fail status, as evidenced by ROC curve, precision and recall metrics. LSTM networks attained reasonable accuracy levels between 65-85% for forecasting entrance scores on a yearly basis, though performance declined in later years likely due to irrelevant training data and potential COVID-19 impacts.

Facebook Prophet excelled at forecasting decreasing temporal trends in both the entrance score threshold and average scores of admitted candidates based on historical data. Prophet model accurately forecasted decreasing trend in entrance score thresholds, from 52 in 2017 to 38 in 2022.Prophet also predicted declining trend in average scores of eligible candidates, from 69.60 in 2017 to 61.71 in 2022.For threshold forecasting, Prophet model achieved MAE of 3.279, MSE of 13.820, and RMSE of 3.717.For average score forecasting, Prophet model obtained MAE of 2.694, MSE of 8.484, and RMSE of 2.912.Prophet obtained mean absolute errors around 3 for threshold and 2.7 for average score predictions. Overall, the complementarity of logistic regression, LSTM and Prophet models provided insights into student outcomes, complex score patterns, and changing trends to support data-driven decision making around admissions.

Logistic Regression

Table 1. Confusion matrix for performance of Logistic Regression model

	Predicted (Yes)	Predicted (No)
Actual (Yes)	TP=1495	FN=40
Actual (No)	FP=27	TN=780

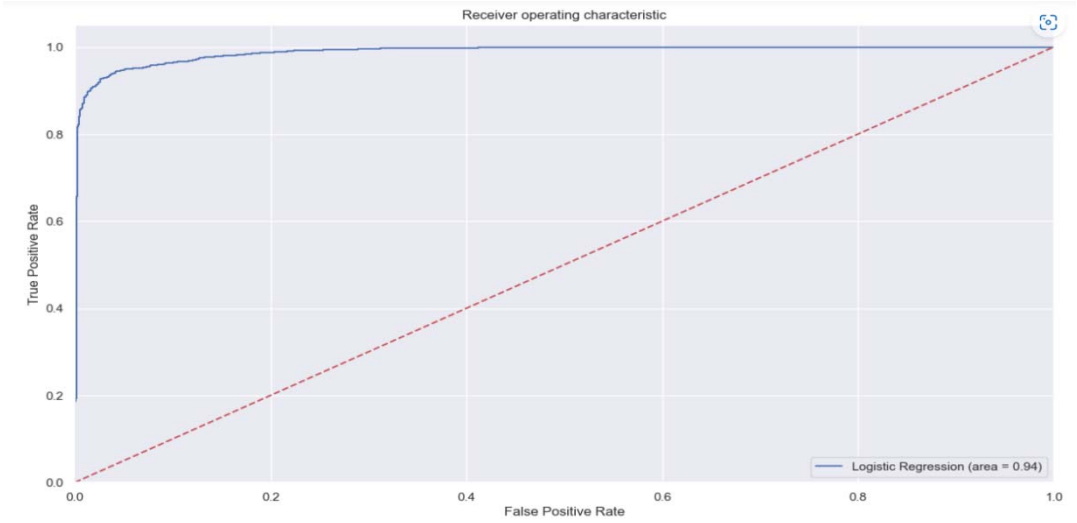

Figure 3 AUC ROC curve for performance of Logistic Regression

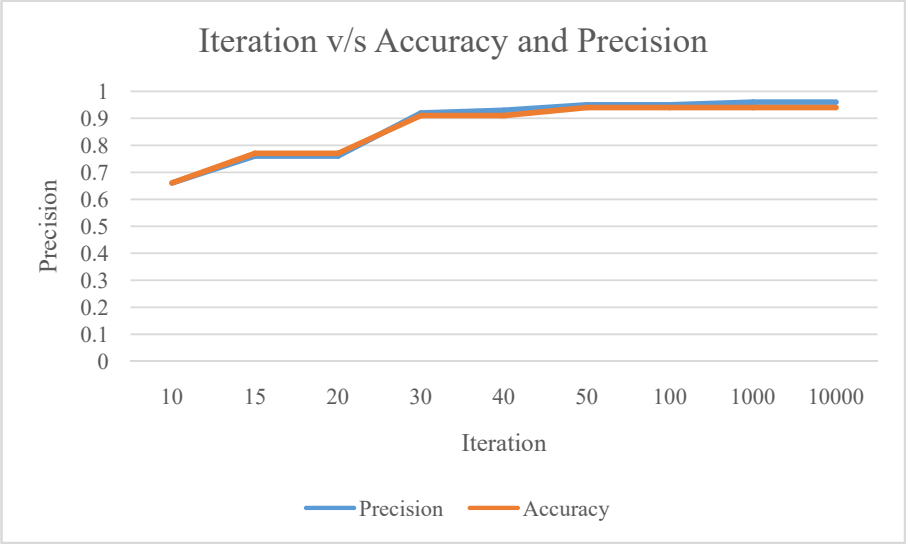

Figure 4. *Iteration wise precision and accuracy curve for performance of Logistic Regression*

Figure 4 depicts precision over training iterations for the logistic regression model, showing a high precision consistently maintained between 0.97-0.99. This highlights the model's capability for accurate positive predictions throughout the training process. A flat accuracy line of 0.97 across iterations, indicating an unchanging high accuracy rapidly attained within the first few iterations, without improvement from extended training.

LSTM

Table 2 Actual and predicted (using LSTM) values of entrance score for randomly selected students

SN	Actual Entrance Score (A)	Predicted Entrance Score (P)	Ratio = P/A
1	103	77.88	0.756
2	61.9	51.28	0.828
3	79.5	62.6	0.787
4	46.5	44.04	0.947
5	89	73.65	0.827
6	113.5	98.07	0.864
7	129	98.97	0.767
8	99.5	84.15	0.845

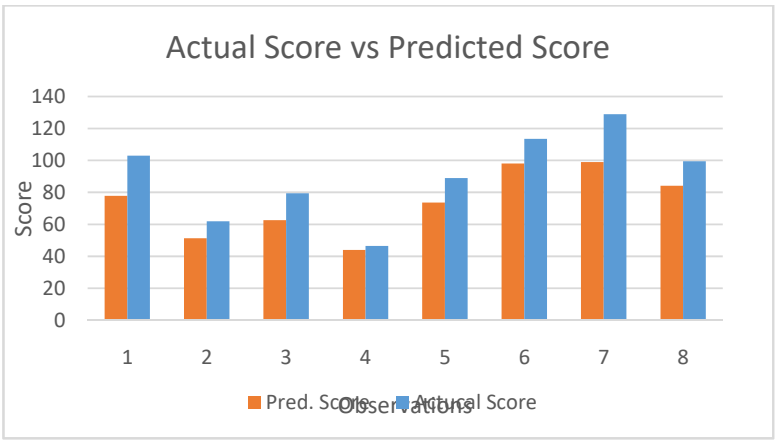

Figure 5 Plot of actual and predicted values of entrance score from table 2

Figure 5 plots the actual versus predicted entrance scores for 8 sample students to demonstrate the LSTM model's score forecasting capability. The predicted scores align fairly closely to the actual values, with some minor variability. This indicates the LSTM network can reasonably predict entrance exam performance for individual students based on their academic history, though some variance persists between actual and predicted scores.

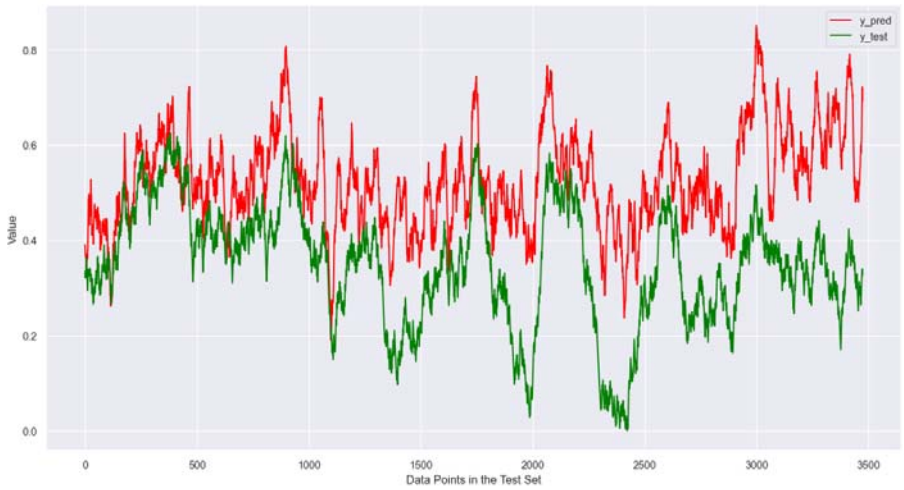

Figure 6 Prediction Plot: Prediction Values & actual values using LSTM

Figure 6 visually evaluates the trained LSTM model's overall predictive accuracy on the test set through a regression plot. The tight fit of predicted scores to the ideal $y = x$ line and high R-squared of 0.89 highlight excellent correlation between true and predicted outcomes. This shows the LSTM model attains strong predictive capabilities, able to generalize well to new unseen data.

Prophet

Table 3 Historical records of year wise Threshold Score and Average Score of Eligible Applicants

Year	**2017**	**2018**	**2019**	**2020**	**2021**	**2022**
No of Applicants	12309	11184	NA	12708	11037	9404
No of Eligible Candidates	6377	6335	NA	6725	6879	6722
Entrance Threshold Score	52	49	NA	46	42	38
Average Score of Eligible Candidates	69.60	68.42	NA	65.98	64.52	61.71

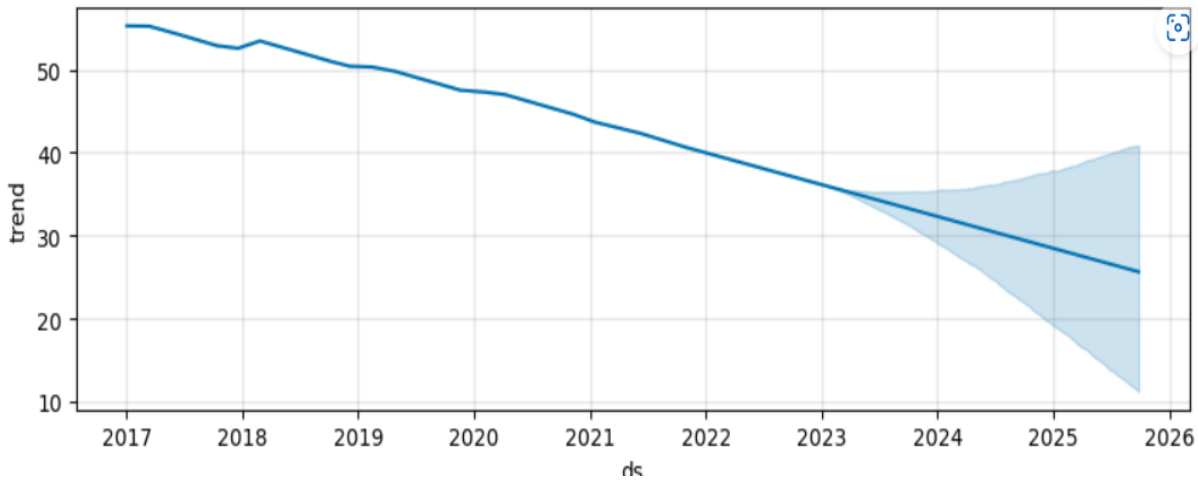

Figure 7 Trend of Entrance Threshold Score as forecasted by Prophet Model

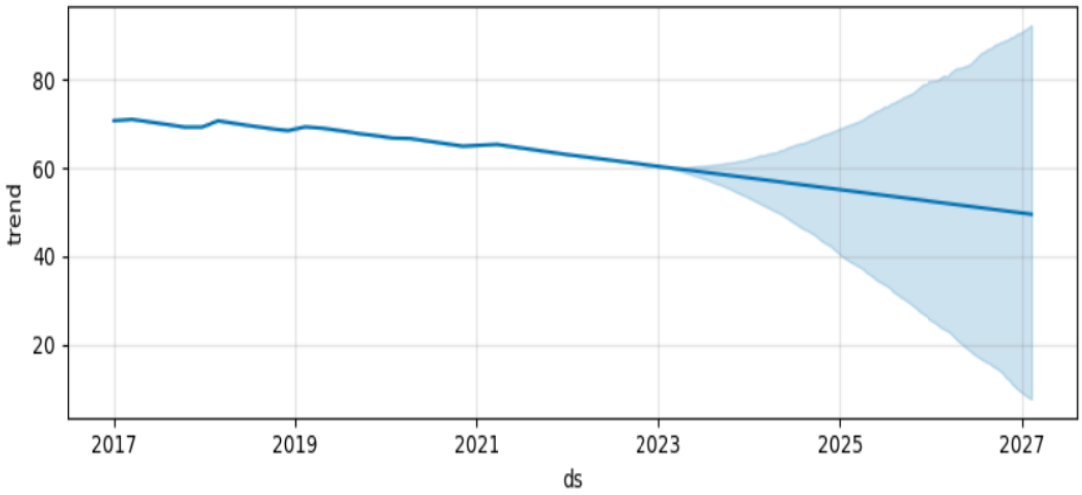

Figure 8: *Trend of Entrance Average Score as forecasted by Prophet Model*

Figures 7 and 8 utilize Facebook Prophet to forecast temporal trends in the engineering entrance exam threshold cut-off and average scores over a 5-year period. Prophet projects decreasing trajectories for both metrics, implying worsening competitiveness and academic preparedness among aspirants over time. The accurate capture of these downward trends demonstrates Prophet's effectiveness at analysing historical time series data to reveal insights into changing exam patterns.

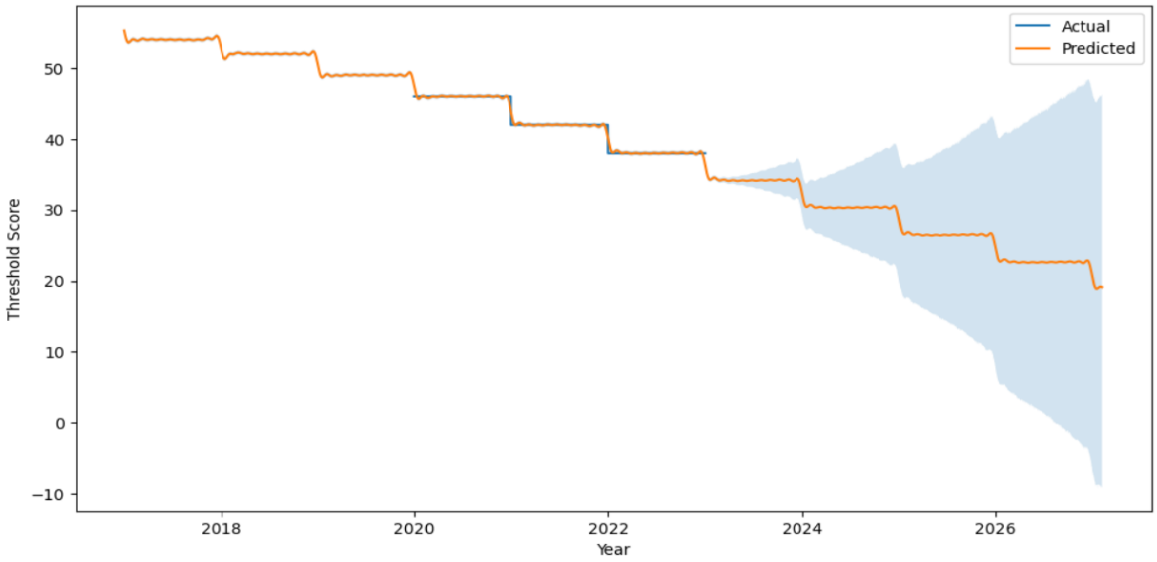

Figure 9: *Actual vs Predicted Entrance Threshold Score over Time*

Lastly, Figures 9 and 10 compare Prophet's predicted threshold and average scores to the actual values over time. The close alignment to the real data with minor errors illustrates Prophet's ability to precisely forecast the trends and fluctuations in these key exam metrics. The accurate predictions highlight the model's suitability for making data-driven projections to support planning around admission requirements and applicant preparedness.

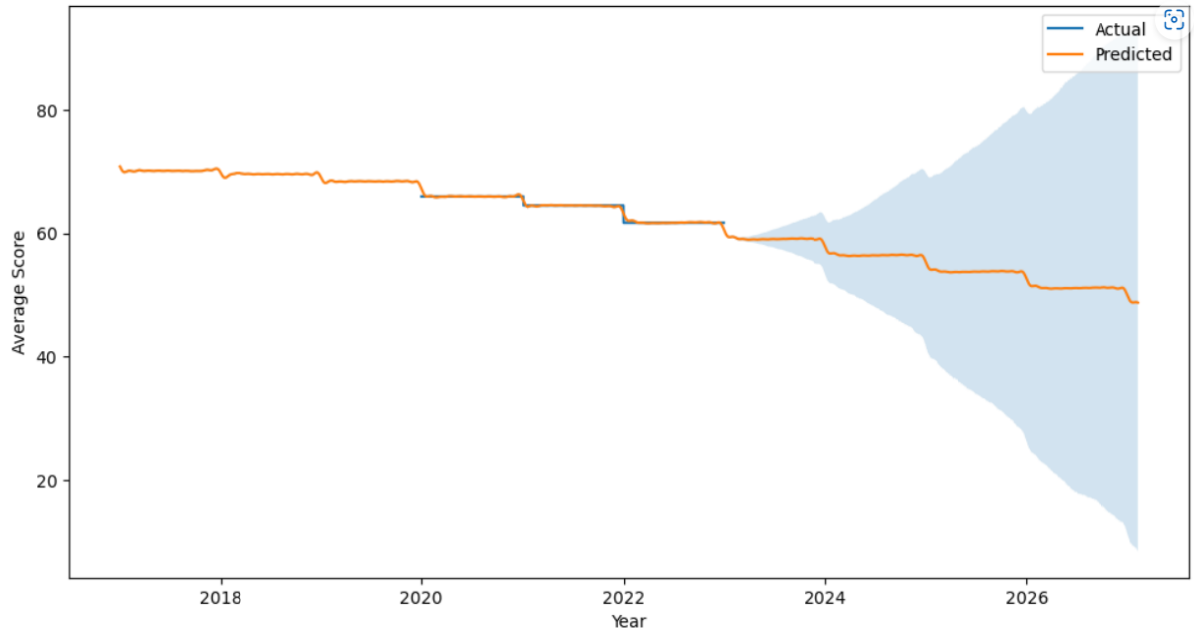

Figure 10: *Actual vs Predicted Entrance Average Score over Time*

5. Conclusion

The logistic regression model demonstrated satisfactory performance for predicting engineering admission probability based on high school results, attaining an R-score of 0.8733 and accuracy of 97.13%. These metrics indicate the model's reliability for estimating intake likelihood. Meanwhile, the LSTM network exhibited potential for high prediction accuracy up to 85% for forecasting engineering entrance scores using prior academic records. However, model accuracy may be influenced by various factors including student behaviours, backgrounds, activities, and potential impacts of events like COVID-19. Hence, the LSTM model could also achieve a lower accuracy of 65% for a given year. Both approaches can be justified based on their respective evaluation metrics. The Prophet model accurately forecasted declining future trends in entrance threshold scores and average scores. The findings provide insights for policymakers and educators regarding performance gaps across education levels. Addressing such gaps through improved instruction quality and resource allocation is critical. Entrance authorities need to examine reasons for the consistent threshold and score declines each year, implying reduced engineering education interest and substandard schooling.

This study centred solely on high school students applying for engineering programs at the Institute of Engineering. Student behaviours, backgrounds, and geographic parameters were not considered, which may influence performance due to educational access disparities. Future work should broaden the scope across other academic domains like medicine, sciences, and international education trends. Incorporating supplemental factors such as socioeconomics, culture, family settings, and extra-curriculars could enrich the research. Overall, this study offers a foundation for future efforts to expand predictive modelling and provide enhanced insights into student transitions to higher education. A multifaceted approach accounting for a wider array of student attributes and environments would further advance this research domain.

In summary, machine learning techniques like logistic regression and LSTM networks are recommended for admission screening and score prediction using high school records. Prophet aids in projecting threshold trends for planning. Overall, these data-driven methods offer actionable insights to enhance student outcomes through early intervention and streamlined admission processes.

Acknowledgement

Authors are highly thankful to the referee for his valuable suggestions in improvement of this paper.

References

[1] Bendangnuksung, & Prabu, D. **(2018)**. Students' performance prediction using deep neural network. *International Journal of Applied Engineering Research*, **13**(2): 1171–1176. http://www.ripublication.com

[2] Chen, X., Peng, Y., Gao, Y., & Cai, S. (**2022**). A competition model for prediction of admission scores of colleges and universities in Chinese college entrance examination. *PLoS ONE*, 17(10), e0274221. DOI: https://doi.org/10.1371/journal.pone.0274221

[3] Daraghmeh, M., Agarwal, A., Manzano, R., & Zaman, M. (**2021**). Time series forecasting using facebook prophet for cloud resource management. *IEEE International Conference on Communications Workshops* (ICC Workshops), 1–6. DOI: https://doi.org/10.1109/ICCWorkshops50388.2021.9473607

[4] Dien, T. T., Luu, S. H., Thanh-Hai, N., & Thai-Nghe, N. (**2020**). Deep learning with data transformation and factor analysis for student performance prediction. *International Journal of Advanced Computer Science and Applications*, **11**(8): 711–721. DOI: https://doi.org/10.14569/IJACSA.2020.0110886

[5] Enughwure, A. A., & Ogbise, M. E. (**2020**). Application of Machine Learning Methods to Predict Student Performance: A Systematic Literature Review. 07(05), 11.

[6] fdeloche. (**2017**). English: A diagram for a one-unit Long Short-Term Memory (LSTM). From bottom to top: input state, hidden state and cell state, output state. Gates are sigmoïds or hyperbolic tangents. Other operators: element-wise plus and multiplication. Weights are not displayed. Inspired from Understanding LSTM, Blog of C. Olah. https://commons.wikimedia.org/wiki/File:Long_Short-Term_Memory.svg

[7] Gochhait, Dr. S., & Rimal, Y. (**2021**). The Comparison of Forward and Backward Neural Network Model – A Study on the Prediction of Student Grade. *WSEAS Transactions on Systems and Control*, **16**: 422–429. DOI: https://doi.org/10.37394/23203.2021.16.37

[8] Kabakchieva, D. (**2012**). Student Performance Prediction by Using Data Mining Classification Algorithms. 1(4).

[9] Marte, J. (**2021**). Here's how much your high school grades predict your future salary. *Washington Post*. https://www.washingtonpost.com/news/wonk/wp/2014/05/20/heres-how-much-your-high-school-grades-predict-how-much-you-make-today/

[10] Meghji, A. F., Mahoto, N. A., Ali Unar, M., & Akram Shaikh, M. (**2019**). Predicting Student Academic Performance using Data Generated in Higher Educational Institutes. 3*C Tecnología*, 366–383. DOI: https://doi.org/10.17993/3ctecno.2019.specialissue2.366-383

[11] Naser, S. A., Zaqout, I., Ghosh, M. A., Atallah, R., & Alajrami, E. (**2015**). Predicting Student Performance Using Artificial Neural Network: in the Faculty of Engineering and Information Technology. *International Journal of Hybrid Information Technology*, **8**(2): 221–228. DOI: https://doi.org/10.14257/ijhit.2015.8.2.20

[12] Patayon, U. B., & Crisostomo, R. V. (**2022**). Time Series Analysis on Enrolment Data: A case in a State University in Zamboanga del Norte, Philippines. *International Conference on Advanced Computer Science and Information Systems* (*ICACSIS*), 13–18. DOI: https://doi.org/10.1109/ICACSIS56558.2022.9923436

[13] Poudyal, S., Mohammadi-Aragh, M. J., & Ball, J. E. (**2022**). Prediction of student academic performance using a hybrid 2D CNN model. *Electronics*, **11**(7): 1005. DOI: https://doi.org/10.3390/electronics11071005

[14] Rimal, Y., Pandit, P., Gocchait, S., Butt, S. A., & Obaid, A. J. (**2021**). Hyperparameter determines the best learning curve on single, multi-layer and deep neural network of student grade prediction of Pokhara university. Nepal. *J. Phys.: Conf. Ser*., 1804(1), 12054. DOI: https://doi.org/10.1088/1742-6596/1804/1/012054

[15] Waheed, H., Hassan, S. U., Aljohani, N. R., Hardman, J., Alelyani, S., & Nawaz, R. (**2020**). Predicting academic performance of students from VLE big data using deep learning models. *Computers in Human Behavior*, 104. DOI: https://doi.org/10.1016/j.chb.2019.106189

□□

Nepal Journal of Mathematical Sciences (NJMS)
ISSN: 2738-9928 (online), 2738-9812 (print)
Vol. 4, No. 2, 2023 (August): 17-30
DOI: https://doi.org/10.3126/njmathsci.v4i2.59527

Research Article
Received Date: May 3, 2023
Accepted Date: August 2, 2023
Published Date: August 30, 2023

The Gradshteyn and Ryzhik's Integral and the Theoretical Computation of *GM* (*m*,*n*) Involving the Continuous Whole Life Annuities

[1]Ogungbenle Gbenga Michael, [2]Ihedioha Silas Abahia , & [3]Ogungbenle Oluwatoyin Gladys

[1]Department of Actuarial Science, Faculty of Management Sciences, University of Jos, Nigeria
[2]Department of Mathematics, Faculty of Natural Sciences, Plateau State University Bokkos, Nigeria
[3]Student, Department of Nursing, Faculty of Clinical Sciences, University of Ilorin, Nigeria

[1]Corresponding email: *moyosiolorun@gmail.com*

Abstract: *Considering the risk connected with the expectation of life at retirement as a result of the unavailable actuarially modeled life annuity to price life insurance products, this study explores the gains in an annuity that would be advantageous to lives who choose life annuity option at retirement under defined condition of actuarially fair annuity value. When continuous parsimonious parametric mortality intensities are Makehamised, then the life table functions used in computing the actuarial present values of the fully continuous whole life insurance and the fully continuous life annuity could be expressed in terms of special functions such as Gamma, Incomplete lower Gamma and Incomplete upper Gamma functions for a homogeneous insured population. In this study, the objective is to*
(i) *Construct mathematical estimations through single life parameterization through algebraic technique*
(ii) *Apply the mean value theorem to construct modification theorems under the framework of policy alterations*
(iii) *Employ the properties of the aforementioned special functions to construct estimations which could permit us to compute closed-form expressions for continuous whole life insurance and continuous whole life expectancy applicable in classical life contingencies.*
(iv) *Apply the commutation function to develop a mathematical model for the employer liability.*
From our results, Gradshteyn and Ryzhik's analytic integral technique presents an advanced technique for computing life insurance biometric functions and ignores the need for any algorithmic numerical procedures.

Keywords: $GM(1,2)$, *Whole life insurance, whole life annuity, Gradshteyn and Ryzhik's integral, Gamma functions*.

1. Introduction to *GM* (*m*,*n*) Class

In human mortality, intensity is applied to define the trends of mortality where the management of life office assets and liability depend on the death rate of the insured Siswono, Azmi, and Syaifudin(2021). Following Lageras, 2009; Missov and Lennart (2013), continuous parametric functions such as assume that the mortality rate increases as age advances. However, the intensity law adds an age-

independent parameter that is not associated with senescence. In human populations, issues connected with overestimation in observed death rates at senescence in mortality trajectories aroused the study of continuous parsimonious parametric mortality models which are responsible for the unobserved heterogeneity and consequently, the cohort population is then partitioned into strata in accordance with an observed measure of insured's exposure to the risk of death. However, in Dragan(2022), we have observed that the methods of generating mortality tables were initially developed for cohorts whose members have varying characteristics in connection with longevity measures.

Numerical Computation of the $GM(1,2)$ Parameters

In Debon, Montes and Sala (2005); Debon, Montes and Sala (2005), the $GM(1,2)$ is defined as

$$\mu_x = \rho + GH^x \tag{1}$$

Let $\zeta = e^{\rho}$ and $G = -\log_e \delta \log_e H$, $\zeta > 0$ and $\delta > 0$

The right hand side must be multiplied by (-1) throughout by definition of the force of mortality

$$\mu_x = -\log_e \zeta + (-\log_e \delta \log_e H)H^x \tag{2}$$

$$\mu_x = -\frac{1}{l_x}\frac{dl_x}{d_x} = -\frac{d\log_e l_x}{dx} \tag{3}$$

$$\mu_x = -\frac{d\log_e l_x}{dx} = -\log_e \zeta + (-\log_e \delta \log_e H)H^x \tag{4}$$

$$-\int \frac{d\log_e l_x}{dx}dx = \int -\log_e \zeta + (-\log_e \delta \log_e H)H^x dx + K \tag{5}$$

$$\log_e l_x = x\log_e \zeta + (\log_e \delta \log_e H)\frac{H^x}{\log_e H} + \log_e \lambda \tag{6}$$

$K = \log_e \lambda$; taking K as the constant of integration

$$\log_e l_x = \log_e \zeta^x + (\log_e \delta \log_e H)\frac{H^x}{\log_e H} + \log_e \lambda \tag{7}$$

$$\log_e l_x = \log_e \zeta^x + (\log_e \delta)H^x + \log_e \lambda \tag{8}$$

where $\log_e \lambda$, is the constant of integration.

$$\log_e l_x = \log_e \zeta^x + \left(\log_e \delta^{H^x}\right) + \log_e \lambda = \log_e \lambda \zeta^x \delta^{H^x} \tag{9}$$

Now, equating both sides, we have

$$l_x = \lambda \zeta^x \delta^{H^x} \Rightarrow \int_0^{\infty} l_{x+s}\mu_{x+s}ds = \lambda \zeta^x \delta^{H^x} \tag{10}$$

Note that the age of the insured is chronological. We can take four of such age with equal intervals at the points $\{x+0, x+s, x+2s, x+3s\}$ to have four systems of simultaneous equations

$$l_{x+s} = \lambda \zeta^{x+\mathbf{s}} \delta^{H^{x+\mathbf{s}}} \tag{11}$$

$$l_{x+2s} = \lambda \zeta^{x+2s} \delta^{H^{x+2s}} \tag{12}$$

$$l_{x+3s} = \lambda \zeta^{x+3s} \delta^{H^{x+3s}} \tag{13}$$

$${}_sP_x = \frac{l_{x+s}}{l_x} = \frac{\lambda \zeta^{x+s} \delta^{H^{x+s}}}{\lambda \zeta^x \delta^{H^x}} = \frac{\zeta^s \delta^{H^{x+s}}}{\delta^{H^x}} = \zeta^s \delta^{H^x\left(H^S-1\right)} \tag{14}$$

Considering 4 consecutive values of function $\log_e l_x$

$$\log_e l_{x+0} = x \log_e \zeta + \left(\log_e \delta\right) H^x + \log_e \lambda \tag{15}$$

$$\log_e l_{x+s} = \left(x+s\right) \log_e \zeta + \left(\log_e \delta\right) H^{x+s} + \log_e \lambda \tag{16}$$

$$\log_e l_{x+2s} = \left(x+2s\right) \log_e \zeta + \left(\log_e \delta\right) H^{x+2s} + \log_e \lambda \tag{17}$$

$$\log_e l_{x+3s} = \left(x+3s\right) \log_e \zeta + \left(\log_e \delta\right) H^{x+3s} + \log_e \lambda \tag{18}$$

$$\begin{aligned} &\log_e l_{x+s} - \log_e l_x = \left(x+s\right) \log_e \zeta + \left(\log_e \delta\right) H^{x+s} + \log_e \lambda \\ &-x \log_e \zeta + \left(\log_e \delta\right) H^x + \log_e \lambda \end{aligned} \tag{19}$$

$$\log_e l_{x+s} - \log_e l_x = \left(s \log_e \zeta\right) + \left(\log_e \delta\right) H^s H^x - \left(\log_e \delta\right) H^x \tag{20}$$

$$\log_e l_{x+s} - \log_e l_x = s \log_e \zeta + H^x \left(H^s - 1\right) \log_e \delta \tag{21}$$

$$\log_e l_{x+2s} - \log_e l_{x+s} = s \log_e \zeta + H^{x+s} \left(H^s - 1\right) \log_e \delta \tag{22}$$

$$\log_e l_{x+3s} - \log_e l_{x+2s} = s \log_e \zeta + H^{x+2s} \left(H^s - 1\right) \log_e \delta \tag{23}$$

$$\begin{aligned} &\log_e l_{x+2s} - 2 \log_e l_{x+s} + \log_e l_x = \left(x+2s\right) \log_e \zeta + \left(\log_e \delta\right) H^{x+2s} + \log_e \lambda - \\ &2\left[\left(x+s\right)\left(\log_e \zeta\right) + \left(\log_e \delta\right) H^{x+s} + \log_e \lambda\right] + x\left(\log_e \zeta\right) + \left(\log_e \delta\right) H^x + \left(\log_e \lambda\right) \end{aligned} \tag{24}$$

$$\begin{aligned} &\log_e l_{x+2s} - 2 \log_e l_{x+s} + \log_e l_x = x \log_e \zeta + 2s \log_e \zeta + \left(\log_e \delta\right) H^{x+2s} + \log_e \lambda \\ &-2x \log_e \zeta - 2s \log_e \zeta - 2\left(\log_e \delta\right) H^{x+s} - 2 \log_e \lambda + x \log_e \zeta + \left(\log_e \delta\right) H^x + \log_e \lambda \end{aligned} \tag{25}$$

$$\log_e l_{x+2s} - 2 \log_e l_{x+s} + \log_e l_x = \left(\log_e \delta\right) H^{x+2s} - 2\left(\log_e \delta\right) H^{x+s} + \left(\log_e \delta\right) H^x \tag{26}$$

$$\log_e l_{x+2s} - 2 \log_e l_{x+s} + \log_e l_x = \left(\log_e \delta\right) H^x \left[H^{2s} - 2H^s + 1\right] \tag{27}$$

Let $U = H^s$, then

$$\log_e l_{x+2s} - 2 \log_e l_{x+s} + \log_e l_x = \left(\log_e \delta\right) U \left[U^2 - 2U^s + 1\right] \tag{28}$$

$$\log_e l_{x+2s} - 2\log_e l_{x+s} + \log_e l_x = (\log_e \delta) U (U-1)^2 \tag{29}$$

$$\log_e l_{x+2s} - 2\log_e l_{x+s} + \log_e l_x = (\log_e \delta) H^x \left(H^x - 1\right)^2 \tag{30}$$

Similarly,

$$\begin{aligned}&\log_e l_{x+3s} - 2\log_e l_{x+2s} + \log_e l_{x+s} = (x+3s)\log_e \zeta + (\log_e \delta) H^{x+3s} + \log_e \lambda \\ &-2\left[(x+2s)\log_e \zeta + (\log_e \delta) H^{x+2s} + \log_e \lambda\right] + (x+s)\log_e \zeta + (\log_e \delta) H^{x+s} + \log_e \lambda\end{aligned} \tag{31}$$

$$\begin{aligned}&\log_e l_{x+3s} - 2\log_e l_{x+2s} + \log_e l_{x+s} = x\log_e \zeta + 3s\log_e \zeta + (\log_e \delta) H^{x+3s} + \log_e \lambda \\ &-2x\log_e \zeta - 4s\log_e \zeta - 2(\log_e \delta) H^{x+2s} - 2\log_e \lambda + x\log_e \zeta + s\log_e \zeta + (\log_e \delta) H^{x+s} \\ &+\log_e \lambda\end{aligned} \tag{32}$$

$$\log_e l_{x+3s} - 2\log_e l_{x+2s} + \log_e l_{x+s} = (\log_e \delta) H^{x+3s} - 2(\log_e \delta) H^{x+2s} + (\log_e \delta) H^{x+s} \tag{33}$$

$$\log_e l_{x+3s} - 2\log_e l_{x+2s} + \log_e l_{x+s} = (\log_e \delta) H^{x+s} \left[H^{2s} - 2H^s + 1\right] \tag{34}$$

$$\log_e l_{x+3s} - 2\log_e l_{x+2s} + \log_e l_{x+s} = H^{x+s} \left(H^s - 1\right)^2 \log_e \delta \tag{35}$$

$$\frac{\log_e l_{x+3s} - 2\log_e l_{x+2s} + \log_e l_{x+s}}{\log_e l_{x+2s} - 2\log_e l_{x+s} + \log_e l_x} = \frac{= H^{x+s} \left(H^s - 1\right)^2 \log_e \delta}{H^x \left(H^s - 1\right)^2 \log_e \delta} = H^x \tag{36}$$

Let $\log_e l_{x+2s} - 2\log_e l_{x+s} + \log_e l_x = \alpha$ (37)

$$\log_e l_{x+3s} - 2\log_e l_{x+2s} + \log_e l_{x+s} = \beta \tag{38}$$

$$H^x \left(H^s - 1\right)^2 \log_e \delta = \alpha \tag{39}$$

$$H^{x+s} \left(H^s - 1\right)^2 \log_e \delta = \beta \tag{40}$$

Taking logarithms of the two equations above, we have

$$x\log_e H + 2\log_e \left(H^s - 1\right) + \log_e \log_e \delta = \log_e \alpha \tag{41}$$

$$(x+s)\log_e H + 2\log_e \left(H^s - 1\right) + \log_e \log_e \delta = \log_e \beta \tag{42}$$

Subtracting equation (41) from(42), we obtain

$$\begin{aligned}&x\log_e H + s\log_e H + 2\log\left(H^s - 1\right) + \log_e \log_e \delta - x\log_e H - 2\log_e \left(H^s - 1\right) - \log_e \log_e \delta \\ &= \log_e \beta - \log_e \alpha\end{aligned} \tag{43}$$

$$s\log_e H = \log_e \beta - \log_e \alpha \tag{44}$$

$$\log_e H = \frac{\log_e \beta - \log_e \alpha}{s} = \frac{\log_e \frac{\beta}{\alpha}}{s} \tag{45}$$

$$x \log_e H + 2\log_e \left(H^s - 1\right) + \log_e \log_e \delta = \log_e \alpha \tag{46}$$

substitute (45) into(41)

$$\frac{x}{s}\log_e \frac{\beta}{\alpha} + 2\log_e \left(H^s - 1\right) + \log_e \log_e \delta = \log_e \alpha \tag{47}$$

$$\log_e \log_e \delta = \log_e \alpha - \frac{x}{s}\log_e \frac{\beta}{\alpha} - 2\log_e \left(H^s - 1\right) \tag{48}$$

$$\log_e \left[\log_e \delta\right] = \log_e \alpha + \log_e \left(\frac{\beta}{\alpha}\right)^{-\frac{x}{s}} + \log_e \left(H^s - 1\right)^{-2} = \log_e \left(\frac{\beta}{\alpha}\right)^{-\frac{x}{s}} \left(H^s - 1\right)^{-2} \tag{49}$$

Equation (49) then becomes $\log_e \delta = \alpha \left(\frac{\beta}{\alpha}\right)^{-\frac{x}{s}} \left(H^s - 1\right)^{-2}$ (50)

$$x \log_e H + 2\log_e \left(H^s - 1\right) + \log_e \log_e \delta = \log_e \alpha \tag{51}$$

Eqn (46) is re-expressed as

$$x \log_e H + \log_e \left(H^s - 1\right) + \log_e \log_e \delta = \log_e \alpha - \log_e \left(H^s - 1\right) \tag{52}$$

$$\log_e \left[H^x \left(H^s - 1\right) \log_e \delta\right] = \log_e \frac{\alpha}{\left(H^s - 1\right)} \tag{53}$$

$$H^x \left(H^s - 1\right) \log_e \delta = \frac{\alpha}{\left(H^s - 1\right)} \tag{54}$$

$$\log_e l_{x+s} - \log_e l_x = s \log_e \zeta + H^x \left(H^s - 1\right) \log_e \delta \tag{55}$$

Substituting equation (54) in (55), we have

$$\log_e l_{x+s} - \log_e l_x = s \log_e \zeta + \frac{\alpha}{\left(H^s - 1\right)} \tag{56}$$

$$s \log_e \zeta = \log_e l_{x+s} - \log_e l_x - \frac{\alpha}{\left(H^s - 1\right)} \tag{57}$$

$$\log_e \zeta = \left[\frac{\log_e l_{x+s} - \log_e l_x - \frac{\alpha}{\left(H^s - 1\right)}}{s}\right] \tag{58}$$

Recall from (52) that $x \log_e H + \log_e \left(H^s - 1\right) + \log_e \log_e \delta = \log_e \alpha - \log_e \left(H^s - 1\right)$ (59)

$$x\log_e H + \log_e \log_e \delta = \log_e \alpha + \log_e \left(H^s - 1\right)^{-2} \tag{60}$$

$$\log_e \left[H^x \log_e \delta \right] = \log_e \alpha \left(H^s - 1\right)^{-2} \tag{61}$$

$$H^x \log_e \delta = \alpha \left(H^s - 1\right)^{-2} \tag{62}$$

$$H^x = \frac{\alpha}{\log_e \delta}\left(H^s - 1\right)^{-2} \tag{63}$$

Recall that $x\log_e \zeta + \left(\log_e \delta\right)H^x + \log_e \lambda = \log_e l_x$ (64)

$$\log_e \lambda = \log_e l_x - x\log_e \zeta - \left(\log \delta\right)H^x \tag{65}$$

Inserting (58), (63) into (64)

$$\log_e \lambda = \log_e l_x - x\left[\frac{\log_e l_{x+s} - \log_e l_x - \dfrac{\alpha}{\left(H^s - 1\right)}}{s}\right] - \alpha\left(H^s - 1\right)^{-2} \tag{66}$$

$$\log_e \zeta = \rho$$

$$\rho = \left[\frac{\log_e l_{x+s} - \log_e l_x - \dfrac{\alpha}{\left(H^s - 1\right)}}{s}\right] \tag{67}$$

and by the initial definition $G = -\log_e \delta \log_e H$

recall $\log_e H = \dfrac{\log_e \dfrac{\beta}{\alpha}}{s} = \log_e \left(\dfrac{\beta}{\alpha}\right)^{\frac{1}{s}}$ (68)

$$H = \left(\frac{\beta}{\alpha}\right)^{\frac{1}{s}} \tag{69}$$

Note that $G = \dfrac{\left(-\log_e \delta\right)}{s}\log_e \dfrac{\beta}{\alpha}$ (70)

And $H^x = \dfrac{\alpha}{\log_e \delta}\left(H^s - 1\right)^{-2}$ (71)

$\mu_x = \rho + GH^x$ becomes

$$\mu_x = \left[\frac{\log_e l_{x+s} - \log_e l_x - \dfrac{\alpha}{\left(H^s - 1\right)}}{s} \right] + \left[\frac{\left(-\log_e \delta\right)}{s} \log_e \frac{\beta}{\alpha} \right] \left(\frac{\beta}{\alpha} \right)^{\frac{x}{s}} \tag{72}$$

$$\mu_x = \left[\frac{\log_e \dfrac{l_{x+s}}{l_x} - \dfrac{\alpha}{\left(H^s - 1\right)}}{s} \right] + \left(\frac{\beta}{\alpha} \right)^{\frac{x}{s}} \frac{\left(-\log_e \delta\right)}{s} \log_e \frac{\beta}{\alpha} \tag{73}$$

$$\mu_x = \left[\frac{\log_e \left({}_s P_x \right) - \dfrac{\alpha}{\left(H^s - 1\right)}}{s} \right] + \left(\frac{\beta}{\alpha} \right)^{\frac{x}{s}} \frac{\left(-\log_e \delta\right)}{s} \log_e \frac{\beta}{\alpha} \tag{74}$$

$$\mu_x = \left[\frac{\log_e \zeta^2 \delta^{H^x \left(H^s - 1\right)} - \dfrac{\alpha}{\left(H^s - 1\right)}}{s} \right] + \left(\frac{\beta}{\alpha} \right)^{\frac{x}{s}} \frac{\left(-\log_e \delta\right)}{s} \log_e \frac{\beta}{\alpha} \tag{75}$$

Recall $H = \left(\dfrac{\beta}{\alpha} \right)^{\frac{1}{s}} \Rightarrow H^s = \left(\dfrac{\beta}{\alpha} \right)$ (76)

So when $s = x$, we have

$$H^x = \left(\frac{\beta}{\alpha} \right) \tag{77}$$

$$\frac{\log_e l_{x+3s} - 2\log_e l_{x+2s} + \log_e l_{x+s}}{\log_e l_{x+2s} - 2\log_e l_{x+s} + \log_e l_x} = \frac{H^{x+s} \left(H^s - 1\right)^2 \log_e \delta}{H^x \left(H^s - 1\right)^2 \log_e \delta} = H^x = \left(\frac{\beta}{\alpha} \right) \tag{78}$$

Inserting Equation (37) and (38) into equation (78), we have

Hence, we obtain $\mu_x = \left\{ \begin{array}{l} \left[\dfrac{\log_e \zeta^2 \delta^{H^x \left(H^s - 1\right)} - \dfrac{\alpha}{\left(H^s - 1\right)}}{s} \right] + \\ \left(\dfrac{\beta}{\alpha} \right)^{\frac{x}{s}} \dfrac{\left(-\log_e \delta\right)}{s} \log_e \dfrac{\left(\log_e l_{x+3s} - 2\log_e l_{x+2s} \log_e l_{x+s}\right)}{\log_e l_{x+2s} - 2\log_e l_{x+s} + \log_e l_x} \end{array} \right\}$ (79)

$$\mu_x = \left[\frac{\log_e \zeta^s \delta^{H^x\left(H^s-1\right)} - \dfrac{\alpha}{\left(H^s-1\right)}}{s}\right] + \left(\frac{\beta}{\alpha}\right)^{\frac{x}{s}} \frac{\left(-\log_e \delta\right)}{s} \log_e \frac{\left(\log_e \lambda\zeta^{x+3s}\delta^{H^{x+3s}} - 2\log_e \lambda\zeta^{x+2s}\delta^{H^{x+2s}} + \log_e \lambda\zeta^{x+s}\delta^{H^{x+s}}\right)}{\log_e \lambda\zeta^{x+2s}\delta^{H^{x+3s}} - 2\log_e \lambda\zeta^{x+s}\delta^{H^{x+s}} + \log_e \lambda\zeta^{x}\delta^{H^{x}}} \tag{80}$$

$$\mu_x = \left[\frac{\log_e \zeta^s \delta^{H^x\left(H^s-1\right)} - \dfrac{\alpha}{\left(H^s-1\right)}}{s}\right] + \left(\frac{\beta}{\alpha}\right)^{\frac{x}{s}} \frac{\left(-\log_e \delta\right)}{s} \log_e \frac{\left(\begin{array}{l}\log_e \lambda\zeta^{x+3s}\delta^{H^{x+3s}} - \log_e \lambda\zeta^{x+2s}\delta^{H^{x+2s}} + \log_e \lambda\zeta^{x+s}\delta^{H^{x+s}} \\ -\log_e \lambda\zeta^{x+2s}\delta^{H^{x+2s}}\end{array}\right)}{\begin{array}{l}\log_e \lambda\zeta^{x+2s}\delta^{H^{x+3s}} - \log_e \lambda\zeta^{x+s}\delta^{H^{x+s}} + \log_e \lambda\zeta^{x}\delta^{H^{x}} \\ -\log_e \lambda\zeta^{x+s}\delta^{H^{x+s}}\end{array}} \tag{81}$$

$$\mu_x = \left[\frac{\log_e \zeta^s \delta^{H^x\left(H^X-1\right)} - \dfrac{\alpha}{\left(H^s-1\right)}}{s}\right] + \left(\frac{\beta}{\alpha}\right)^{\frac{x}{s}} \frac{\left(-\log_e \delta\right)}{s} \log_e \frac{\left(\log_e \dfrac{\lambda\zeta^{x+3s}\delta^{H^{x+3s}}}{\log_e \lambda\zeta^{x+2s}\delta^{H^{x+2s}}} + \log_e \dfrac{\lambda\zeta^{x+s}\delta^{H^{x+s}}}{\lambda\zeta^{x+2s}\delta^{H^{x+2s}}}\right)}{\log_e \dfrac{\lambda\zeta^{x+2s}\delta^{H^{x+3s}}}{\log_e \lambda\zeta^{x+s}\delta^{H^{x+s}}} + \log \dfrac{\log_e \lambda\zeta^{x}\delta^{H^{x}}}{\lambda\zeta^{x+s}\delta^{H^{x+s}}}} \tag{81a}$$

$$\mu_x = \left[\frac{\log_e \zeta^s \delta^{H^x\left(H^X-1\right)} - \dfrac{\alpha}{\left(H^s-1\right)}}{s}\right] + \left(\frac{\beta}{\alpha}\right)^{\frac{x}{s}} \frac{\left(-\log_e \delta\right)}{s} \log_e \left[\frac{\left(\log_e \dfrac{\delta^{H^{x+3s}}}{\delta^{H^{x+2s}}} \dfrac{\delta^{H^{x+s}}}{\delta^{H^{x+2s}}}\right)}{\log_e \dfrac{\delta^{H^{x+3s}}}{\delta^{H^{x+s}}} \dfrac{\delta^{H^{x}}}{\delta^{H^{x+s}}}}\right] \tag{82}$$

Materials and Methods

Let $\sigma = \log_e(1+i)$ be the force of interest where i is the valuation interest rate

Following Neil (1979); Chowdhury (2012); Kara (2021); Patricio, Castellares and Queiroz (2023), the continuous whole life annuity. Suppose, Ω is the maximum age in a mortality table, then

$$\mathbf{E}\left(a_{\overline{T}|}\right) = \bar{a}_x = \frac{1}{l_x}\int_0^{\Omega-x} v^t l_{x+t}\,dt \tag{83}$$

$$\bar{a}_x = \int_0^{\Omega-x} e^{-\sigma t}\left({}_tP_x\right)dt \tag{84}$$

$$\bar{a}_x = \int_0^{\Omega-x} \zeta^t \delta^{H^x\left(H^t-1\right)} e^{-\sigma t}\,dt \tag{85}$$

$${}_tP_x e^{-\sigma t} = e^{-\sigma t}\zeta^t \delta^{H^x\left(H^t-1\right)} = e^{-\sigma t}\zeta^t \delta^{\left(H^{x+t}-H^x\right)} = \frac{e^{-\sigma t}\zeta^t \delta^{\left(H^{x+t}\right)}}{\delta^{H^x}} \tag{86}$$

$${}_tP_x e^{-\sigma t} = e^{-\sigma t}\zeta^t \delta^{H^x\left(H^t-1\right)} = \frac{e^{-\sigma t}\zeta^t \delta^{\left(H^{x+t}\right)}}{\delta^{H^x}} = \frac{\exp\left(H^t H^x \log_e \delta + t\log_e\left(e^{-\sigma}\zeta\right)\right)}{\delta^{H^x}} \tag{87}$$

Observe that $H^t = e^{\log_e H^t} = e^{t\log_e H}$ (88)

$${}_tP_x e^{-\sigma t} = e^{-\sigma t}\zeta^t \delta^{H^x\left(H^t-1\right)} = \frac{e^{-\sigma t}\zeta^t g^{\left(H^{x+t}\right)}}{\delta^{H^x}} = \frac{\exp\left(\left(e^{t\log_e H}\right)\left(H^x \times \log_e g\right) + t\log_e e^{-\sigma}\zeta\right)}{\delta^{H^x}} \tag{89}$$

$$\bar{a}_x = \int_0^{\Omega-x} \frac{\exp\left(\left(e^{t\log_e H}\right)\left(H^x \times \log_e \delta\right) + t\log_e e^{-\sigma}\zeta\right)}{\delta^{H^x}}dt \tag{90}$$

Let $\eta = t\log_e H \Rightarrow \dfrac{\eta}{\log_e H} = t$ (91)

When $t = 0$, $\eta = 0$

When $t = \Omega - x$, $\eta = (\Omega - x)\log_e H = \log_e H^{(\Omega-x)}$ (92)

$$\frac{d\eta}{dt} = \log_e H \Rightarrow d\eta = \log_e H dt \Rightarrow \frac{d\eta}{\log_e H} = dt \tag{93}$$

$$\bar{a}_x = \int_0^{\log_e H^{(\Omega-x)}} \frac{\exp\left(e^{\eta}\left(H^x \times \log_e \delta\right) + \dfrac{\eta}{\log_e H} \times \log_e e^{-\sigma}\zeta\right)}{\delta^{H^x}} \frac{d\eta}{\log_e H} \tag{94}$$

$$\bar{a}_x = \frac{1}{\left(\log_e H\right)\left(\delta^{H^x}\right)} \int_0^{\log_e H^{(\Omega-x)}} \exp\left(\left(e^{\eta} \times H^x \times \log_e \delta\right) + \frac{\eta}{\log_e H} \times \log_e e^{-\sigma\zeta}\right) d\eta \tag{95}$$

$$\bar{a}_x = \frac{1}{\left(\log_e H\right)\left(\delta^{H^x}\right)} \int_0^{\log_e H^{(\Omega-x)}} \exp\left(\left(H^x \times \log_e \delta\right) e^{\eta} + \left(\frac{\log_e e^{-\sigma\zeta}}{\log_e H}\right)\eta\right) d\eta \tag{96}$$

Following Gradshteyn and Ryzhik (n.d, pp. 356, formula, $ETI147(37)$) (97)

$$\int_0^{\infty} \exp\left(-\alpha e^{Y} - \bar{\delta} Y\right) dY = \alpha^{\delta} \Gamma\left(-\bar{\delta}, \alpha\right) \tag{98}$$

Where $\Gamma(.)$ is the gamma function

$$\alpha = a + ib,\ i = \sqrt{-1} \text{ and } a > 0 \text{ and } a \le \mathrm{Re}|\alpha| \tag{99}$$

$$\bar{a}_x = \frac{1}{\left(\log_e H\right)\left(\delta^{H^x}\right)} \int_0^{\log_e H^{(\Omega-x)}} \exp\left(-\left(-H^x \times \log_e \delta\right) e^{\eta} - \left(-\frac{\log_e e^{-\sigma\zeta}}{\log_e H}\right)\eta\right) d\eta \tag{100}$$

$$\int_0^{\infty} \exp\left(-\left(-H^x \times \log_e \delta\right) e^{\eta} - \left(-\frac{\log_e e^{-\sigma\zeta}}{\log_e H}\right)\eta\right) d\eta =$$

$$\left\{\begin{array}{l} \int_0^{\log_e H^{(\Omega-x)}} \exp\left(-\left(-H^x \times \log_e \delta\right) e^{\eta} - \left(-\frac{\log_e e^{-\sigma\zeta}}{\log_e H}\right)\eta\right) d\eta \\ + \int_{\log_e H^{(\Omega-x)}}^{\infty} \exp\left(-\left(-H^x \times \log_e \delta\right) e^{\eta} - \left(-\frac{\log_e e^{-\sigma\zeta}}{\log_e H}\right)\eta\right) d\eta \end{array}\right\} \tag{101}$$

Consequently,

$$\bar{a}_x = \frac{\left\{\begin{array}{l} \int_0^{\infty} \exp\left(-\left(-H^x \times \log_e \delta\right) e^{\eta} - \left(-\frac{\log_e e^{-\sigma\zeta}}{\log_e H}\right)\eta\right) d\eta - \\ \int_{\log_e H^{(\Omega-x)}}^{\infty} \exp\left(-\left(-H^x \times \log_e \delta\right) e^{\eta} - \left(-\frac{\log_e e^{-\sigma\zeta}}{\log_e H}\right)\eta\right) d\eta \end{array}\right\}}{\left(\log_e H\right)\left(\delta^{H^x}\right)} \tag{101}$$

$$\bar{a}_x = \frac{1}{\left(\log_e H\right)\left(\delta^{H^x}\right)} \left\{\begin{array}{l} \int_0^{\infty} \exp\left(-\left(-H^x \times \log_e \delta\right) e^{\eta} - \left(-\frac{\log_e e^{-\sigma\zeta}}{\log_e H}\right)\eta\right) d\eta - \\ \int_{\log_e H^{(\Omega-x)}}^{\infty} \exp\left(-\left(-H^x \times \log_e \delta\right) e^{\eta} - \left(-\frac{\log_e e^{-\sigma\zeta}}{\log_e H}\right)\eta\right) d\eta \end{array}\right\} \tag{102}$$

$$J_1 = \int_0^{\infty} \exp\left(-\left(-H^x \times \log_e \delta\right) e^{\eta} - \left(-\frac{\log_e e^{-\sigma}\zeta}{\log_e H} \right) \eta \right) d\eta = \left[\left(-H^x \times \log_e \delta\right) \right]^{\left(-\frac{\log_e \zeta}{\log_e H} \right)} \Gamma\left(-\left(-\frac{\log_e e^{-\sigma}\zeta}{\log_e H} \right), \left(-H^x \times \log_e \delta\right) \right) \tag{103}$$

$$J_2 = \int_{\log_e H^{(\Omega - x)}}^{\infty} \exp\left(-\left(-H^x \times \log_e \delta\right) e^{\eta} - \left(-\frac{\log_e e^{-\sigma}\zeta}{\log_e H} \right) \eta \right) d\eta \tag{104}$$

Let $\xi = \eta - \log_e H^{\Omega - x}$ (105)

Let $\xi + \log_e H^{\Omega - x} = \eta$ (106)

$d\xi = d\eta$ (107)

When $\eta = \infty$, $\xi = \infty$ and when $\eta = \log_e H^{\Omega - x}$, $\xi = 0$

Therefore, $J_2 = \int_0^{\infty} \exp\left(-\left(-H^x \times \log_e \delta\right) e^{\xi + \log_e H^{\Omega - x}} - \left(-\frac{\log_e e^{-\sigma}\zeta}{\log_e H} \right) \left(\xi + \log_e H^{\Omega - x} \right) \right) d\xi$ (108)

$$J_2 = \int_0^{\infty} \exp\left\{ -\left(-H^x \times \log_e \delta\right) e^{\log_e H^{\Omega - x}} e^{\xi} - \left(\left(-\frac{\log_e e^{-\sigma}\zeta}{\log_e H} \right) \xi + \left(\left(-\frac{\log_e e^{-\sigma}\zeta}{\log_e H} \right) \right) \log_e H^{\Omega - x} \right) \right\} d\xi \tag{109}$$

$$J_2 = \int_0^{\infty} \exp\left\{ -\left(-H^x \times \log_e \delta\right) H^{\Omega - x} e^{\xi} + -\left(-\frac{\log_e e^{-\sigma}\zeta}{\log_e H} \right) \xi - \left(-\frac{\log_e e^{-\sigma}\zeta}{\log_e H} \right) \left(\Omega - x\right) \left(\log_e H\right) \right\} d\xi \tag{110}$$

$$J_2 = \int_0^{\infty} \exp\left\{ -\left(-\log_e \delta\right) H^{\Omega} e^{\xi} + -\left(-\frac{\log_e e^{-\sigma}\zeta}{\log_e H} \right) \xi - \left(-\log_e e^{-\sigma}\zeta\right) \left(\Omega - x\right) \right\} d\xi \tag{111}$$

$$J_2 = \int_0^{\infty} \exp\left\{ -\left(-\log_e \delta\right) H^{\Omega} e^{\xi} + -\left(-\frac{\log_e e^{-\sigma}\zeta}{\log_e H} \right) \xi + \log_e \zeta^{\Omega - x} \right\} d\xi \tag{112}$$

$$J_2 = \int_0^{\infty} \exp\left\{ -\left(-\log_e \delta\right) H^{\Omega} e^{\xi} + -\left(-\frac{\log_e e^{-\sigma}\zeta}{\log_e H} \right) \xi + \log_e e^{-\sigma(\Omega - x)} \right\} d\xi \tag{113}$$

$$J_2 = \int_0^{\infty} \exp\left\{ -\left(-\log_e \delta\right) H^{\Omega} e^{\xi} + -\left(-\frac{\log_e e^{-\sigma}\zeta}{\log_e H} \right) \xi - \sigma\left(\Omega - x\right) \right\} d\xi \tag{114}$$

$$J_2 = e^{-\sigma(\Omega - x)} \int_0^{\infty} \exp\left\{ -\left(-\log_e \delta\right) H^{\Omega} \times e^{\xi} - \left(-\frac{\log_e e^{-\sigma}\zeta}{\log_e H} \right) \xi \right\} d\xi \tag{115}$$

$$J_2 = e^{-\sigma(\Omega-x)}\int_0^{\infty}\exp\left\{-\left(-\log_e\delta\right)H^{\Omega}\times e^{\xi}-\left(-\frac{\log_e e^{-\sigma}\zeta}{\log_e H}\right)\xi\right\}d\xi = \\ e^{-\sigma(\Omega-x)}\left[\left(-\log_e\delta\right)H^{\Omega}\right]^{\left(-\frac{\log_e e^{-\sigma}\zeta}{\log_e H}\right)}\Gamma\left(-\left(-\frac{\log_e e^{-\sigma}\zeta}{\log_e H}\right),\left(-\log_e\delta\right)H^{\Omega}\right) \tag{116}$$

$$\bar{a}_x = \frac{1}{\left(\log_e H\right)\left(\delta^{H^x}\right)}\left(J_1 - J_2\right) \tag{117}$$

$$\bar{a}_x = \frac{1}{\left(\log_e H\right)\left(\delta^{H^x}\right)}\left\{\begin{array}{l}\left[\left(-H^x\times\log_e\delta\right)\right]^{\left(-\frac{\log_e e^{-\sigma}\zeta}{\log_e H}\right)}\Gamma\left(-\left(-\frac{\log_e e^{-\sigma}\zeta}{\log_e H}\right),\left(-H^x\times\log_e\delta\right)\right)- \\ e^{-\sigma(\Omega-x)}\left[\left(-\log_e\delta\right)H^{\Omega}\right]^{\left(-\frac{\log_e e^{-\sigma}\zeta}{\log_e H}\right)}\Gamma\left(-\left(-\frac{\log_e e^{-\sigma}\zeta}{\log_e H}\right),\left(-\log_e\delta\right)H^{\Omega}\right)\end{array}\right\} \tag{118}$$

$$\bar{a}_x = \frac{1}{\left(\log_e H\right)\left(\delta^{H^x}\right)}\left\{\begin{array}{l}\left[\left(-H^x\times\log_e\delta\right)\right]^{\left(-\frac{\log_e e^{-\sigma}\zeta}{\log_e H}\right)}\Gamma\left(\left(\frac{\log_e e^{-\sigma}\zeta}{\log_e H}\right),\left(-H^x\times\log_e\delta\right)\right)- \\ e^{-\sigma(\Omega-x)}\left[\left(-\log_e\delta\right)H^{\Omega}\right]^{\left(-\frac{\log_e e^{-\sigma}\zeta}{\log_e H}\right)}\Gamma\left(\left(\frac{\log_e e^{-\sigma}\zeta}{\log_e H}\right),\left(-\log_e\delta\right)H^{\Omega}\right)\end{array}\right\} \tag{119}$$

Where $H^x = \frac{\alpha}{\log_e\delta}\left(H^s-1\right)^{-2}$ (120)

$$\log_e\zeta = \left[\frac{\log_e l_{x+s}-\log_e l_x-\frac{\alpha}{\left(H^s-1\right)}}{s}\right] \Rightarrow \zeta = e^{\left(\frac{\log_e l_{x+s}-\log_e l_x-\frac{\alpha}{\left(H^s-1\right)}}{s}\right)} \tag{121}$$

$$\log_e\delta = \frac{\alpha\left(H^s-1\right)^{-2}}{H^x} \Rightarrow H^x\log_e\delta = \alpha\left(H^s-1\right)^{-2} \Rightarrow \log_e\delta^{H^x} = \alpha\left(H^s-1\right)^{-2} \tag{122}$$

$$\Rightarrow \delta^{H^x} = e^{\alpha\left(H^s-1\right)^{-2}}$$

$$H^x = \frac{\alpha}{\log_e\delta}\left(H^s-1\right)^{-2} \tag{123}$$

$$\bar{a}_x = \frac{1}{\left(\log_e H\right)\left(\delta^{H^x}\right)}\left\{\begin{array}{l}\left[\left(-H^x\times\log_e\delta\right)\right]^{\left(-\frac{\log_e e^{-\sigma}\zeta}{\log_e H}\right)}\Gamma\left(\left(\frac{\log_e e^{-\sigma}\zeta}{\log_e H}\right),\left(-H^x\times\log_e\delta\right)\right)- \\ e^{-\sigma(\Omega-x)}\left[\left(-\log_e\delta\right)H^{\Omega}\right]^{\left(-\frac{\log_e e^{-\sigma}\zeta}{\log_e H}\right)}\Gamma\left(\left(\frac{\log_e e^{-\sigma}\zeta}{\log_e H}\right),\left(-\log_e\delta\right)H^{\Omega}\right)\end{array}\right\} \tag{124}$$

If $l_x = \int_0^\infty l_{x+s}\mu_{x+s}ds$ and $l_{x+\xi} = \int_0^\infty l_{x+s+\xi}\mu_{x+s}(\xi)d\xi$, then following de Souza (2018), the continuous annuity in equation (124) is bounded as follows

$$\left(\frac{l_{x+n} - l_{x+n}e^{-\delta n} + l_{x+n}\delta e^{-\delta n}\bar{a}_{x+n}}{\delta l_x}\right) \leq \bar{a}_x \leq \left(\frac{l_x - l_x e^{-\delta n} + \delta l_{x+n}e^{-\delta n}\bar{a}_{x+n}}{l_x \delta}\right) \tag{125}$$

Discussion of results

$$\lim_{\sigma\to 0}\bar{a}_x = \int_0^\infty {}_\xi p_x d\xi = \bar{e}_x \tag{126}$$

$$\lim_{\sigma\to 0}\bar{a}_x = \frac{1}{\left(\log_e H\right)\left(\delta^{H^x}\right)}\lim_{\sigma\to 0}\left\{\begin{array}{l}\left[\left(-H^x\times\log_e\delta\right)\right]^{\left(-\frac{\log_e e^{-\sigma}\zeta}{\log_e H}\right)}\Gamma\left(\left(\frac{\log_e e^{-\sigma}\zeta}{\log_e H}\right),\left(-H^x\times\log_e\delta\right)\right)- \\ e^{-\sigma(\Omega-x)}\left[\left(-\log_e\delta\right)H^\Omega\right]^{\left(-\frac{\log_e e^{-\sigma}\zeta}{\log_e H}\right)}\Gamma\left(\left(\frac{\log_e e^{-\sigma}\zeta}{\log_e H}\right),\left(-\log_e\delta\right)H^\Omega\right)\end{array}\right\} \tag{127}$$

$$\int_0^\infty {}_\xi p_x d\xi = \frac{1}{\left(\log_e H\right)\left(\delta^{H^x}\right)}\left\{\begin{array}{l}\left[\left(-H^x\times\log_e\delta\right)\right]^{\left(-\frac{\log_e\zeta}{\log_e H}\right)}\Gamma\left(\left(\frac{\log_e\zeta}{\log_e H}\right),\left(-H^x\times\log_e\delta\right)\right)- \\ \left[\left(-\log_e\delta\right)H^\Omega\right]^{\left(-\frac{\log_e\zeta}{\log_e H}\right)}\Gamma\left(\left(\frac{\log_e\zeta}{\log_e H}\right),\left(-\log_e\delta\right)H^\Omega\right)\end{array}\right\} \tag{128}$$

Conclusion

Life annuity plays an important role in defined benefits schemes under defined contribution pension plans and hence it represents a modified version of a defined benefit structure. Consequently, it lends itself as a good alternative measure to defined benefits schemes to assist retirees in earning income streams provided the annuitant survives. This paper contributes to this field by providing an analytical technique for computing the fully continuous life annuities and continuous life insurance under the framework of mortality rate intensity defining the trend of human mortality. The development of actuarially robust analytical computation of fully continuous life annuities and fully continuous life insurance has continually posed core challenges for actuaries and life offices. In insured populations having reasonably good track records of death statistics, there seems to be disturbances in the function of a low number of events representing limitations in the information on the survival data at different ages. The applicable pricing assumptions available in life insurance especially in annuity-linked securities take into account changes in demographic statistics and mortality changes. The mathematical technique through the Gamma function is used to evaluate attempts to model and generate mortality rate intensities further employed in computing pension and death benefits. The continuous life annuities in a probabilistic mortality model aptly defines the actuarial present value of the underlying death density function such that the analytically closed form solution for the annuity integral contains special function in the form Gamma, upper Incomplete Gamma, and Lower Incomplete Gamma function. In particular, the lower Incomplete Gamma function was constructed with series representation to allow approximations of first-order and second-order basis when the initial level of mortality is infinitesimally small.

References

[1] Castro-Perez, J., Aguilar-Sanchez G.P., & Gonzalez-Nucamendi A. **(2020)**. Approximate integration through remarkable points using the intermediate value theorem. *Scientiaet TechnicaAno XXV,* **25**(1): 142-149.

[2] Chowdhury M. **(2012)**. A brief study on Gompertz-Makeham model and some aspects on agricultural growth of Assam. *International Journal of Mathematical Archive*, **3**(6)

[3] Debon, A., Montes, F., &Sala, R. **(2005)**. A comparison of parametric models for mortality graduation. Application to mortality data for the Valencia Region (Spain). *Sort*. **29**(2): 269-288

[4] Dragan, M. **(2022)**. Some general Gompertz and Gompertz-Makeham life expectancy models. *Sciendo,* **30**(3): 117-142. DOI:10.2478/auom-2022-0037

[5] Gradshteyn I.S., &Ryzhik I.M **(2007)**. *Table of integrals, series and products*. Academic Press, New York.

[6] Kara E.K. **(2021)**. A study on modelling of lifetime with right-truncated composite lognormal Pareto distribution: Actuarial premium calculations. *Gazi University Journal of Science.* **34**(1): 272-288, doi:10.35378/gujs.646899

[7] Lageras, A.N. **(2009)**. Analytical and easily calculated expressions for continuous commutation functions under Gompertz-Makeham mortality. *airXiv: 0902.4855v1 [math.PR]*, pp. 1-4

[8] Missov, M.I.,&Lennart, L.A **(2013)**. Gompertz-Makeham life expectancies: Expressions and applications. *Theoretical Population Biology,* **90 :** 29-35. http://dx.doi.org/10.1016/j.tpb.2013.09.013

[9] Neil, A. **(1979)**. *Life contingencies*. The Institute of Actuaries and Faculty of Actuaries, special edition.

[10] Patricio, S.C, Castellares, F., &Queiroz, B. **(2023)**. Mortality modelling at old-age: An mixture model approach. *arXiv:2301.01693v1* [stat.AP] Jan 2023: 1-16

[11] Siswono, G.O., Azmi, U., &Syaifudin W.H. **(2021)**. Mortality projection on Indonesia's abridged life table to determine the EPV of term annuity. *Journal Varian.* **4**(2): 159-168. doi: https://doi.org/10.30812/varian.v412.1094

[12] Walters, H.R., &Wilkie A.D. **(1987)**. A short note on the construction of life tables and multiple decrement tables. *Journal Institute of Actuaries,* **114** :569-580.

□□

Nepal Journal of Mathematical Sciences (NJMS)
ISSN: **2738-9928 (*online*), 2738-9812 (*print*)**
Vol. 4, No. 2, 2023 (August): 31-40
DOI: https://doi.org/10.3126/njmathsci.v4i2.59534

Research Article
Received Date: April 3, 2023
Accepted Date: August 14, 2023
Published Date: August 30, 2023

Computational Analysis of Fractional Reaction-Diffusion Equations that Appear in Porous Media

Vinod Gill[1], Harsh Vardhan Harsh[2] , & Tek Bahadur Budhathoki[3]

[1]*Department of Mathematics*, *Govt. College Nalwa(Hisar)*, *Haryana-125037*, *India*
[2]*Faculty of Sci. & Tech.*, *ICFAI Tech. School*, *ICFAI University Jaipur*, *Rajasthan*, *India*
[3]*Department of Applied Sciences*, *Thapathali Campus*, *Tribhuvan University* , *Kathmandu*, *Nepal*

Email: [1]*vinod.gill08@gmail.com*, [2]*harshvardhanharsh@gmail.com*, [3]*bbctek@ioe.edu.np*

Corresponding Author: Vinod Gill

Abstract: *The Elzaki Transform Homotopy Perturbation Method (ETHPM)*, *a modified computational technique*, *is used in this article to solve the time-fractional reaction-diffusion equation that emerges in porous media. Herein fractional-order derivatives are considered in Caputo sense. To show how simple and effective the suggested method is*, *some specific and understandable examples are provided. The numerical results produced by the suggested technique show that the method is accurate and easy to use. The graphical illustrations of the approximate solutions to the porous media equation for different particular cases are the key characteristics of the current research. The solution obtained is very useful and significant to analyze the many physical phenomena.*

Keywords: *Fractional calculus*, *Elzaki Transform Homotopy Perturbation Method (ETHPM)*, *Fractional reaction-diffusion equations*

1. Introduction

Numerous problems in the real world have been solved using the theory and fundamental concepts of fractional calculus. As an extension of the conventional integer-order differential equations, fractional-order differential equations are being utilized more often to describe problems in the domains of engineering, mechanics, fluid flow, biology, and physics. Fractional partial differential equations (FPDEs) are widely used in science and engineering, and as a result, research on FPDEs has grown significantly over the past several decades. The theory of fractional partial differential equations can be used to more accurately and systematically translate real-world problems. A novel automated brain segmentation technique for magnetic resonance imaging was developed by Ahlgren et al. [1] employing fractional signal modeling of a spoiled gradient-recalled echo (SPGR) sequence acquired at different flip angles. Sun et al. [2] presented fractional and fractal derivative models for temporary anomalous diffusion. Here, four models are thoroughly compared with one another. In order to solve the time-fractional Navier-Stokes equation in a tube, Kumar et al. [3] devised a unique homotopy perturbation transform method. Murio [4] suggested an implicit unconditionally stable numerical strategy to address the one-dimensional linear time-fractional diffusion issue. The fractional-order diffusion equations were solved by Shah et al.

[5] using the Natural transform decomposition technique. The best approach for q-homotopy analysis was used by Darzi et al. [6] to solve partial differential equations with time-fractional derivatives. A space-time fractional order non-linear Cahn-Hilliard issue was resolved by Pandey et al. [7] using an operational matrix approach and Laguerre polynomials. Pandey et al. [8] recommended an effective Laguerre collocation technique to generate the approximate order non-linear reaction-advection-diffusion equations. The first basic solutions of general fractional-order diffusion equations within the negative Prabhakar kernel were taken into consideration by Yang et al. [9]. The symmetry analysis approach to determine the symmetry of the time-fractional diffusion equation has been covered by Liu et al. [10].

As a chemical moves from a zone of high concentration to one of low concentration, the diffusion process takes place. The dynamics of density profiles during the diffusion of a material are depicted by the diffusion type equation, which is a partial differential equation [11]. Fractional reaction-diffusion equations may be used to describe both shallow water waves in seas and ion-acoustic waves in plasma.

The present study deals with the following time- fraction reaction-diffusion equation which arises in porous media [12]

$$\frac{\partial^{\rho}}{\partial\tau^{\rho}}\chi(\zeta,\tau) = \mathrm{D}\frac{\partial^{\alpha_1}}{\partial\zeta^{\alpha_1}}\chi(\zeta,\tau) - \varsigma\chi^{\mathrm{m}}\frac{\partial^{\alpha_2}}{\partial\zeta^{\alpha_2}}\chi^{\mathrm{n}}(\zeta,\tau) + \mathrm{k}\chi(1-\chi) + \mathrm{f}(\zeta,\tau)\,, \tag{1}$$

Where $0 \le \zeta \le 1,\ 0 \le \tau \le 1,\ 0 < \rho \le 1, \alpha_1 > 1, \alpha_2 \ge 2$; with IC

$$\chi(\zeta,0) = \chi_0(\zeta). \tag{2}$$

Here, $\chi(\zeta,\tau)$ is a state variable and describes the concentration of a substance/solute profile, D denotes the diffusion coefficient, average velocity of fluid is denoted by $\varsigma > 0, k$ denotes the reaction coefficient and m, n are integers.

Here we will be applying ETHPM to find the approximate numerical solution of time-fractional reaction-diffusion equation (1)-(2). The correctness and effectiveness of the provided technique are demonstrated by the three test examples.

2. Basic definitions of fractional calculus and Elzaki Transform

In this section, we present some basic definitions of fractional calculus that will be incorporated into this study, as follows [13-15].

Definition 1. A real function $f(t)$, $t > 0$ is said to be in the space C_μ if $\mu \in R$, there exists a real number $p > \mu$ and the function $f_1(t) \in C[0,\infty)$ such that $f(t) = t^p f_1(t)$. Moreover, if

$f^{(n)} \in C_\mu$, then $f(t)$ is said to be in the space $C_\mu^n, n \in N$.

Definition 2. The Riemann-Liouville fractional integral of order $\alpha \ge 0$ for a function $f(t)$ is defined as

$$\mathrm{I}^{\alpha}f(t) = \begin{cases} \dfrac{1}{\Gamma(\alpha)}\displaystyle\int_0^t (t-\tau)^{\alpha-1}f(\tau)d\tau, & \alpha > 0 \\ f(t), & \alpha = 0 \end{cases}$$

Where $\Gamma(\cdot)$ denotes the Gamma function.

Definition 3. The Riemann-Liouville fractional derivative of order $\alpha > 0$ for a function $f(t)$ is defined as

$$\mathrm{D}^{\alpha} f(t) = \frac{d^n}{dt^n} I^{n-\alpha} f(t),$$

$$= I^{n-\alpha} \frac{d^n}{dt^n} f(t), \quad n \in N, n-1 < \alpha \leq n.$$

Definition 4. The Caputo fractional derivative of order $\alpha > 0$ is defined as

$$\mathrm{D}^{\alpha} f(t) = \begin{cases} \frac{d^n f(t)}{dt^n}, & \alpha = n, \ n \in N \\ \frac{1}{\Gamma(\mathrm{n}-\alpha)} \int_0^t \frac{f^{(n)}(\tau)}{(t-\tau)^{\alpha-n+1}} d\tau, & 0 \leq n-1 < \alpha < n, \end{cases}$$

where n is an integer, $t > 0$ and $f(t) \in C_1^n$.

Definition 5. The Elzaki transform of $f(t)$ is defined [16] as

$$E[f(t)] = E[f(t), v] = T(v) = v \int_0^{\infty} f(t) e^{-\frac{t}{v}} dt, \ k_1 < v < k_2, k_1, k_2 > 0, 0 \leq t < \infty, \tag{3}$$

where $f(t)$ is taken from the set A, which is defined as

$$A = \left\{ f(t); \ \exists \, M, k_j > 0, \ j = 1, 2, |f(t)| < M e^{\frac{|t|}{k_j}}, if \ t \in (-1)^j \times [0, \infty) \right\}, \tag{4}$$

here, constant M must be a finite number, k_1 and k_2 may be finite or infinite.

Using duality of Laplace [17], Elzaki transform of the Caputo fractional derivative (given in definition 4) of order $\alpha > 0$, can be obtained [18] and get as

$$E[D^{\alpha} f(t), v] = \frac{T(v)}{v^{\alpha}} - \sum_{k=0}^{n-1} v^{k-\alpha+2} f^{(k)}(0), \quad n-1 < \alpha \leq n, \tag{5}$$

In Eq. (5), $T(v)$ is the Elzaki transform of the function $f(t)$.

Elzaki transform has many useful and important properties like linear property, scale property, shifting property, duality with Laplace transform ,and so forth. Further detail and properties about this transform can be found in [16-19].

3. Elzaki Transform Homotopy Perturbation Method

To illustrate the basic idea of this method, we consider a general form of nonlinear, non-homogeneous partial differential equation as follows:

$$D_t^{\alpha} u(x,t) = Lu(x,t) + Nu(x,t) + f(x,t), \ \alpha > 0 \tag{6}$$

With the following initial conditions

$$D_0^k u(x,0) = g_k, k = 0, \ldots, n-1, \ D_0^n u(x,0) = 0, \text{and } n = \lfloor \alpha \rfloor \tag{7}$$

In eq. (6), D_t^{α} denotes without loss of generality the Caputo fractional derivative operator, L represents a linear differential operator, N stands for nonlinear differential operator and $f(x,t)$ is a known function.

Taking Elzaki transform on both sides of eq. (6), to get

$$E[D_t^{\alpha}u(x,t)] = E[Lu(x,t)] + E[Nu(x,t)] + E[f(x,t)], \quad (8)$$

Using the differentiation property of Elzaki transform[16-19] and above initial conditions, we have

$$E[u(x,t)] = v^{\alpha}E[Lu(x,t)] + v^{\alpha}E[Nu(x,t)] + g(x,t) \quad (9)$$

Applying the inverse Elzaki transform on both sides of eq. (9), we obtain

$$u(x,t) = G(x,t) + E^{-1}\left[v^{\alpha}E[Lu(x,t)] + v^{\alpha}E[Nu(x,t)]\right] \quad (10)$$

Where $G(x,t)$ represents the term arising from the known function $f(x,t)$ and the prescribed initial condition.

Now, we implement the homotopy perturbation method, (see [20-22])

$$u(x,t) = \sum_{n=0}^{\infty} p^n u_n(x,t) \quad (11)$$

And the nonlinear term can be decomposed as

$$N[u(x,t)] = \sum_{n=0}^{\infty} p^n H_n(u) \quad (12)$$

Where $H_n(u)$ are He's polynomials (see, [23-24]) and given by

$$H_n(u_0, u_1, \dots, u_n) = \frac{1}{n!}\frac{\partial^n}{\partial p^n}\left[N\left(\sum_{i=0}^{\infty} p^i u_i\right)\right]_{p=0}, \quad n = 0, 1, 2, \dots \quad (13)$$

Substituting equations (11) and (12) in equation (10), we get

$$\sum_{n=0}^{\infty} p^n u_n(x,t) = G(x,t) + p\{E^{-1}[v^{\alpha}E(L\sum_{n=0}^{\infty} p^n u_n(x,t) + \sum_{n=0}^{\infty} p^n H_n(u))]\}. \quad (14)$$

This is the coupling of the Elzaki transform and the Homotopy perturbation method using He's polynomials. Comparing the coefficients of like powers of p in eq. (14) on both sides, we obtain the following approximations as

$p^0: u_0(x,t) = G(x,t)$

$p^1: u_1(x,t) = E^{-1}\{v^{\alpha}E[Lu_0(x,t) + H_0(u)]\}$

$p^2: u_2(x,t) = E^{-1}\{v^{\alpha}E[Lu_1(x,t) + H_1(u)]\}$

$p^3: u_3(x,t) = E^{-1}\{v^{\alpha}E[Lu_2(x,t) + H_2(u)]\}$

……..

$p^n: u_n(x,t) = E^{-1}\{v^{\alpha}E[Lu_{n-1}(x,t) + H_{n-1}(u)]\}$.

Similarly, we can find rest of the terms and hence, we obtain the desired series solution. Thus, we approximate the analytical solution $u(x,t)$ as

$$u(x,t) = \lim_{N\to\infty} \sum_{n=0}^{N} u_n(x,t). \quad (15)$$

The series solution (15) converges very fast in a very few terms.

4. Solution of the time-fractional Reaction-Diffusion Equations

In this part of the article, we have solved some fractional order one-dimensional non-linear partial differential equations that originate in porous media by using ETHPM as mentioned in section 3.

Example 1. The following non-linear fractional order PDE has many uses in rotating flow of liquid in a tube, waves in plasma, etc.

$$\frac{\partial^\rho}{\partial\tau^\rho}\chi(\zeta,\tau)+\frac{\partial}{\partial\zeta}\left(\frac{\chi^2(\zeta,\tau)}{2}\right)-\frac{\partial^3}{\partial\zeta^2\partial\tau}\chi(\zeta,\tau)=0\,,\quad \tau>0,0\le\zeta\le 1,0<\rho\le 1 \tag{16}$$

with IC

$$\chi(\zeta,0)=\zeta. \tag{17}$$

On putting $\rho=1$, then exact solution of (16) is $\chi(\zeta,\tau)=\frac{\zeta}{1+\tau}$.

Applying the Elzaki transform on (16), get as

$$E\left[\frac{\partial^\rho}{\partial\tau^\rho}\chi(\zeta,\tau)\right]+E\left[\frac{\partial}{\partial\zeta}\left(\frac{\chi^2(\zeta,\tau)}{2}\right)-\frac{\partial^3}{\partial\zeta^2\partial\tau}\chi(\zeta,\tau)\right]=0,$$

By using the results of Elzaki transform and simultaneously using IC (17), we get

$$E[\chi(\zeta,\tau)]-v^2\zeta+v^\rho E\left[\frac{\partial}{\partial\zeta}\left(\frac{\chi^2(\zeta,\tau)}{2}\right)-\frac{\partial^3}{\partial\zeta^2\partial\tau}\chi(\zeta,\tau)\right]=0, \tag{18}$$

Employing inverse Elzaki transform on (18), it yields

$$\chi(\zeta,\tau)=\ \zeta-E^{-1}\left(v^\rho E\left[\frac{\partial}{\partial\zeta}\left(\frac{\chi^2(\zeta,\tau)}{2}\right)-\frac{\partial^3}{\partial\zeta^2\partial\tau}\chi(\zeta,\tau)\right]\right)=0, \tag{19}$$

Again incorporating the homotopy perturbation method, (see [20, 21, 22])

$$\chi(\zeta,\tau)=\ \sum_{n=0}^{\infty}p^n\chi_n(\zeta,\tau) \tag{20}$$

And the decomposition of nonlinear term as

$$N[\chi(\zeta,\tau)]=\ \sum_{n=0}^{\infty}p^nH_n(\chi) \tag{21}$$

Substituting (20) and (21), in (19), it reduces to

$$\sum_{n=0}^{\infty}p^n\chi_n(\zeta,\tau)=\ \zeta-p\left\{E^{-1}\left[v^\rho E\left(\sum_{n=0}^{\infty}p^nH_n(\chi)-\frac{\partial^3(\sum_{n=0}^{\infty}p^n\chi_n(\zeta,\tau))}{\partial\zeta^2\partial\tau}\right)\right]\right\}, \tag{22}$$

Where $H_n(\chi)$ are He's polynomials (see, [23, 24]). Some He's polynomials factors are

$$H_0(\chi)=\frac{\partial}{\partial\zeta}\left(\frac{{\chi_0}^2(\zeta,\tau)}{2}\right)$$

$$H_1(\chi)=\frac{\partial}{\partial\zeta}\left(\chi_0(\zeta,\tau)\chi_1(\zeta,\tau)\right)$$

$$H_2(\chi)=\frac{\partial}{\partial\zeta}\left(\chi_0(\zeta,\tau)\chi_2(\zeta,\tau)+\frac{{\chi_1}^2(\zeta,\tau)}{2}\right)$$

……..

Comparing the coefficients of like powers of p in eq. (22), its yields

$$p^0\colon \chi_0(\zeta,\tau)=\zeta\,,$$

$$p^1\colon \chi_1(\zeta,\tau)=-E^{-1}\left\{v^\rho E\left[\frac{\partial}{\partial\zeta}\left(\frac{{\chi_0}^2(\zeta,\tau)}{2}\right)-\frac{\partial^3}{\partial\zeta^2\partial\tau}\chi_0(\zeta,\tau)\right]\right\},$$

On little simplification, we get

p^1: $\chi_1(\zeta,\tau) = -\frac{\zeta\tau^\rho}{\Gamma(\rho+1)}$,

p^2: $\chi_2(\zeta,\tau) = -E^{-1}\left\{v^\rho E\left[\frac{\partial}{\partial\zeta}\left(\chi_0(\zeta,\tau)\chi_1(\zeta,\tau)\right) - \frac{\partial^3}{\partial\zeta^2\partial\tau}\chi_1(\zeta,\tau)\right]\right\}$,

On putting previously obtained value and after that little simplification, get as

p^2: $\chi_2(\zeta,\tau) = \frac{2\zeta\tau^{2\rho}}{\Gamma(2\rho+1)}$,

Similarly

p^3: $\chi_3(\zeta,\tau) = -E^{-1}\left\{v^\rho E\left[\frac{\partial}{\partial\zeta}\left(\chi_0(\zeta,\tau)\chi_2(\zeta,\tau) + \frac{{\chi_1}^2(\zeta,\tau)}{2}\right) - \frac{\partial^3}{\partial\zeta^2\partial\tau}\chi_2(\zeta,\tau)\right]\right\}$,

On putting previously obtained value and after that little simplification, get as

p^3: $\chi_3(\zeta,\tau) = -\zeta\left[4 + \frac{\Gamma(2\rho+1)}{\left(\Gamma(\rho+1)\right)^2}\right]\frac{\tau^{3\rho}}{\Gamma(3\rho+1)}$,

……..

Using the same procedure, we can extract more values, and by substituting the aforementioned values in (15), we get an approximate solution in the form of a series

$$\chi(\zeta,\tau) = \zeta - \frac{\zeta\tau^\rho}{\Gamma(\rho+1)} + \frac{2\zeta\tau^{2\rho}}{\Gamma(2\rho+1)} - \zeta\left[4 + \frac{\Gamma(2\rho+1)}{\left(\Gamma(\rho+1)\right)^2}\right]\frac{\tau^{3\rho}}{\Gamma(3\rho+1)} + \cdots. \quad (23)$$

Putting $\rho = 1$ in (23), we get

$$\chi(\zeta,\tau) = \zeta - \zeta\tau + \zeta\tau^2 - \zeta\tau^3 + \cdots. \quad (24)$$

This is identical to exact solution

$$\chi(\zeta,\tau) = \frac{\zeta}{1+\tau}. \quad (25)$$

Example 2. Taking a non-linear fractional order PDE which is a specific occurrence(**non-conservative case $k \neq 0$**) of our concern equation i.e. (1).

On putting D $= \varsigma = \alpha_2 = k = 1$ and $\alpha_1 = 1.5$ in (1), it reduces into

$$\frac{\partial^\rho}{\partial\tau^\rho}\chi(\zeta,\tau) = \frac{\partial^{1.5}}{\partial\tau^{1.5}}\chi(\zeta,\tau) - \frac{\partial}{\partial\zeta}\left(\chi^2(\zeta,\tau)\right) + \left(1-\chi(\zeta,\tau)\right)\chi(\zeta,\tau), \quad (26)$$

with the initial condition $\chi(\zeta,0) = \zeta^2$. Jointly with this IC the exact solution of (26) is

$\chi(\zeta,\tau) = \zeta^2 + \tau^2$.

On using the computational technique (given in section 3) as applied for getting the solution of Example 1, obtain the coefficients of power of p as below

p^0: $\chi_0(\zeta,\tau) = \zeta^2$,

p^1: $\chi_1(\zeta,\tau) = \left(\frac{4\sqrt{\zeta}}{\sqrt{\pi}} + \zeta^2 - 4\zeta^3 - \zeta^4\right)\frac{\tau^\rho}{\Gamma(\rho+1)}$,

p^2: $\chi_2(\zeta,\tau) = \left(\frac{8\sqrt{\zeta}}{\sqrt{\pi}} - \frac{52}{\sqrt{\pi}}\zeta^{\frac{3}{2}} - \frac{24}{5\sqrt{\pi}}\zeta^{\frac{5}{2}} + \zeta^2 - 12\zeta^3 + 37\zeta^4 + 20\zeta^5 + 6\zeta^6\right)\frac{\tau^{2\rho}}{\Gamma(2\rho+1)}$,

……..

Similar obtain further values; on putting these obtained values in (15), get solution of (26), in series form

$$\chi(\zeta,\tau)=\zeta^2+\tau^2-\left(\frac{4\sqrt{\zeta}}{\sqrt{\pi}}+\zeta^2-4\zeta^3-\zeta^4\right)\frac{\tau^{\rho}}{\Gamma(\rho+1)}+\left(\frac{8\sqrt{\zeta}}{\sqrt{\pi}}-\frac{52}{\sqrt{\pi}}\zeta^{\frac{3}{2}}-\frac{24}{5\sqrt{\pi}}\zeta^{\frac{5}{2}}+\zeta^2-12\zeta^3+37\zeta^4+20\zeta^5+6\zeta^6\right)\frac{\tau^{2\rho}}{\Gamma(2\rho+1)}+\cdots. \quad (27)$$

Example 3. Taking a non-linear fractional order PDE which is a specific occurrence(**conservative case $k=0$**) of our concern equation i.e. (1).

On putting $D=\varsigma=\alpha_2=1$ and $\alpha_1=1.5,\ k=0,m=0,n=2$ in (1), it reduce into

$$\frac{\partial^{\rho}}{\partial\tau^{\rho}}\chi(\zeta,\tau)=\frac{\partial^{1.5}}{\partial\tau^{1.5}}\chi(\zeta,\tau)-\frac{\partial}{\partial\zeta}\left(\chi^2(\zeta,\tau)\right), \quad (28)$$

With the initial condition $\chi(\zeta,0)=\zeta-\zeta^2$.

On using the computational technique (given in section 3) as applied for solution of Example 1, get the coefficients of power of p as

p^0: $\chi_0(\zeta,\tau)=\zeta-\zeta^2$,

p^1: $\chi_1(\zeta,\tau)=\left(-\frac{4\sqrt{\zeta}}{\sqrt{\pi}}-2\zeta+6\zeta^2-4\zeta^3\right)\frac{\tau^{\rho}}{\Gamma(\rho+1)}$,

p^2: $\chi_2(\zeta,\tau)=\left(\frac{36}{\sqrt{\pi}}\sqrt{\zeta}-\frac{52}{\sqrt{\pi}}\zeta^{\frac{3}{2}}+4\zeta-40\zeta^2+80\zeta^3-40\zeta^4\right)\frac{\tau^{2\rho}}{\Gamma(2\rho+1)}$,

……..

Similar obtain further values; on putting these obtained values in (15), get solution of (28), in series form

$$\chi(\zeta,\tau)=\zeta-\zeta^2+\left(-\frac{4\sqrt{\zeta}}{\sqrt{\pi}}-2\zeta+6\zeta^2-4\zeta^3\right)\frac{\tau^{\rho}}{\Gamma(\rho+1)}+\left(\frac{36}{\sqrt{\pi}}\sqrt{\zeta}-\frac{52}{\sqrt{\pi}}\zeta^{\frac{3}{2}}+4\zeta-40\zeta^2+80\zeta^3-40\zeta^4\right)\frac{\tau^{2\rho}}{\Gamma(2\rho+1)}+\cdots. \quad (29)$$

5. Graphical Analysis of the Approximate Results

In this section we are presenting some graphical analysis of the obtained approximate results as

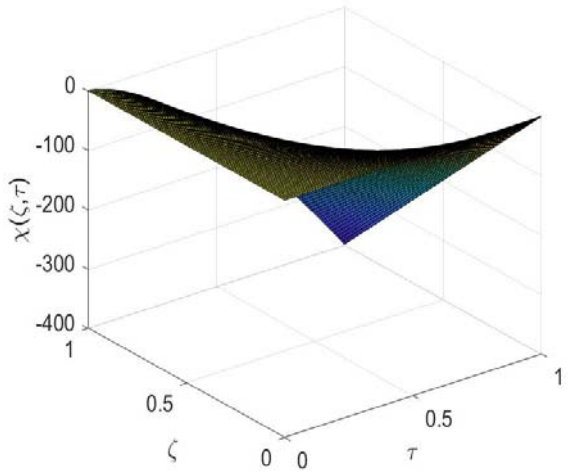

Fig. 1: The surface shows the ETHPM solution $\chi(\zeta,\tau)$ for Example 1, when $\rho=0.5$

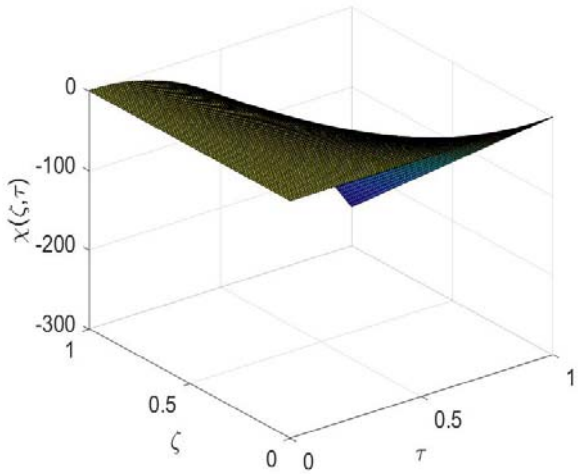

Fig. 2: The surface shows the ETHPM solution $\chi(\zeta,\tau)$ for Example 1, when $\rho=0.7$

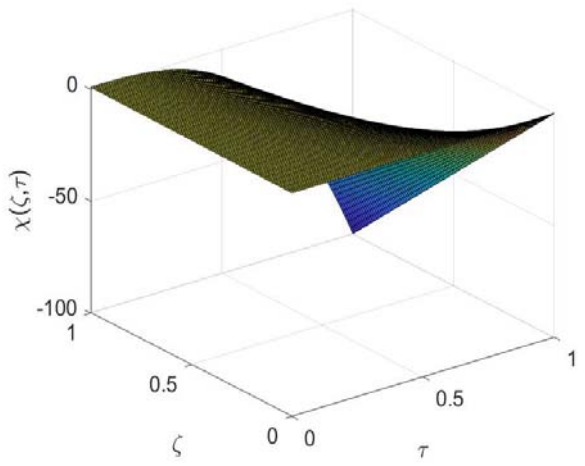

Fig. 3: The surface shows the ETHPM solution $\chi(\zeta,\tau)$ for Example 1, when $\rho = 1$

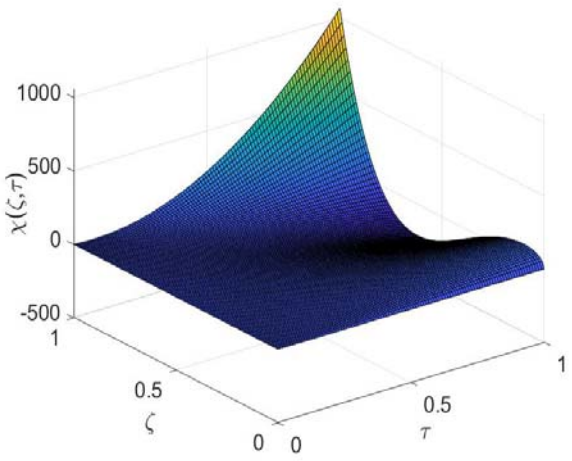

Fig. 4: The surface shows the ETHPM solution $\chi(\zeta,\tau)$ for Example 2, when $\rho = 1$

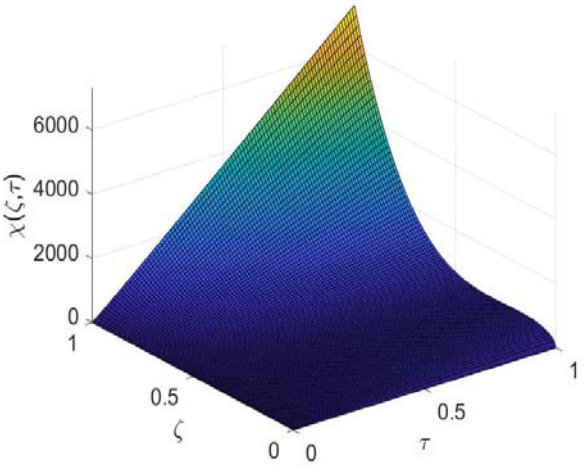

Fig. 5: The surface shows the ETHPM solution $\chi(\zeta,\tau)$ for Example 3, when $\rho = 0.5$

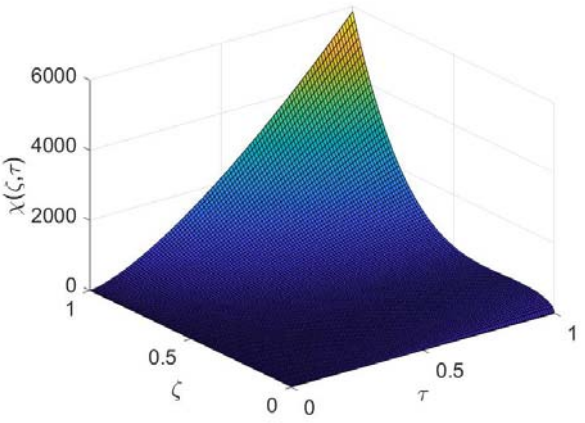

Fig. 6: The surface shows the ETHPM solution $\chi(\zeta,\tau)$ for Example 3, when $\rho = 0.7$

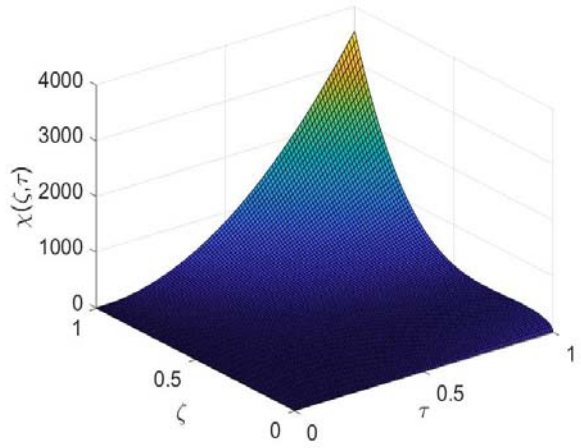

Fig. 7: The surface shows the ETHPM solution $\chi(\zeta,\tau)$ for Example 3, when $\rho = 1$

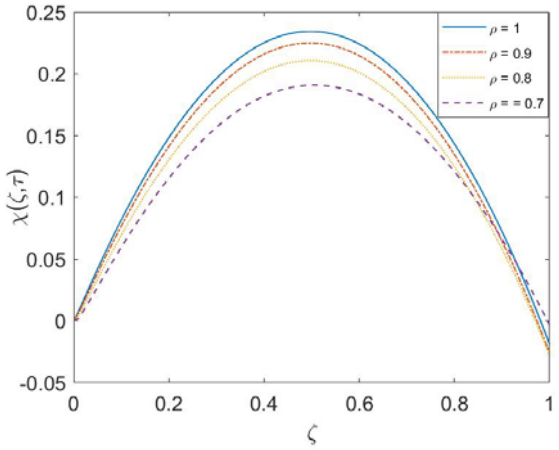

Fig. 8: The behavior of Solute concentration $\chi(\zeta,\tau)$ vs. ζ at $\tau = 1$, for different values of ρ for Example 3

It has been observed from all graphs that the fractional order is better to describe the solution of the time-fractional Reaction-Diffusion Equations, and give a free hand to adjust and control accordingly.

6. Conclusion

The major objective of this study is to demonstrate the usefulness of the combination of the homotopy perturbation technique and the novel integral transform "Elzaki transform" for obtaining both approximate and accurate solutions for nonlinear time-fractional reaction-diffusion equations. Graphs for different fractional order have been plotted to examine the various effects on solute concentration. The numerical result shows that the method used is very simple and straightforward to implement. Our findings provide interesting unifications and extensions of many results, hither to scattered in the literature. At the end, we can conclude that the ETHPM has nice refinement in all numerical methods and it can be used in solving many real world-problems.

References

[1] Ahlgren, A., Wirestam, R., Ståhlberg, F. and Knutsson, L. **(2014)**. Automatic brain segmentation using fractional signal modeling of a multiple flip angle, spoiled gradient-recalled echo acquisition. *Magnetic Resonance Materials in Physics*, *Biology and Medicine*, **27** (6): 551–565.

[2] Sun, H., Li, Z. Zhang, Y. and Chen, W. **(2017)**. Fractional and fractal derivative models for transient anomalous diffusion: Model comparison. *Chaos*, *Solitons & Fractals*, **102**: 346–353.

[3] Kumar, D., Singh, J. and Kumar, S. **(2015)**. A fractional model of Navier–stokes equation arising in unsteady flow of a viscous fluid. *Journal of the Association of Arab Universities for Basic and Applied Sciences*, **17** (1): 14–19.

[4] Murio, D. A. **(2008)**. Implicit finite difference approximation for time-fractional diffusion equations. *Computers & Mathematics with Applications*, **56** (4): 1138–1145.

[5] Shah, R., Khan, H., Mustafa, S., Kumam, P. and Arif, M. **(2019)**. Analytical solutions of fractional-order diffusion equations by natural transform decomposition method. *Entropy*, **21**(6): 557.

[6] Darzi, R. and Agheli, B. **(2018)**. Analytical approach to solving fractional partial differential equation by optimal q-homotopy analysis method. *Numer. Anal. Appl.*, **11**(2): 134−145.

[7] Pandey, P., Kumar, S., Jafari H. and Das, S. (2019). An operational matrix for solving time-fractional order cahn-hilliard equation. *Thermal Science*, **23**(6): S2045-S2052.

[8] Pandey, P., Kumar, S. and Das, S. **(2019)**. Approximate analytical solution of coupled fractional-order reaction-advection- diffusion equations. *The European Physical Journal Plus*, **134**(7): Article Number 364.

[9] Yang, X. J., Gao, F., Ju, Y. and Zhou, H. W. **(2018)**. Fundamental solutions of the general fractional-order diffusion equations. *Mathematical Methods in the Applied Sciences*, **41**(18): 9312–9320.

[10] Liu, J. G., Yang, X. J., Feng, Y. Y. and Zhang, H. Y. **(2019)**. On the generalized time fractional diffusion equation: Symmetry analysis, conservation laws, optimal system and exact solutions. *International Journal of Geometric Methods in Modern Physics*, **17** (1): 2050013–28.

[11] Luchko, Y. **(2009)**. Maximum principle for the generalized time-fractional diffusion equation. *Journal of Mathematical Analysis and Applications*, **351**(1): 218–223.

[12] Panday, P., Kumar, S., Gomez –Aguilar, J.F. and Baleanu, D. **(2020)**. An efficient technique for solving the space-time fractional reaction-diffusion equation in porous media, *Chinese Journal of Physics*, 68: 483-492.

[13] Kilbas, A. A., Srivastava, H. M. and Trujillo, J. J. **(2006)**. *Theory and Applications of Fractional Differential Equations*. Elsevier: San Diego, CA, USA.

[14] Podlubny, I. **(1999)**. *Fractional Differential Equations*. Academic Press, California, USA.

[15] Miller, K. S. and Ross, B. **(1993)**. An introduction to the fractional calculus and fractional differential equations. John Wiley and Sons, New York, 1993.

[16] Elzaki, Tarig M. **(2011)**. The new integral transform 'Elzaki Transform'. *Global Journal of Pure and Applied Mathematics*, **7**(1): 57-64.

[17] Elzaki, T. M. and Elzaki, S. M. **(2011)**. On the connections between Laplace and Elzaki transform. *Advances in Theoretical and Applied Mathematics*, **6**(1): 1-11.

[18] Devi, A. and Jakhar, M. **(2020)**. A novel approach for solving fractional Bagley-Torvik Equations. *South East Asian J. of Mathematics and Mathematical Sciences*, **16**(1): 177-188.

[19] Elzaki, T. M. and Elzaki, S. M. **(2011)**. On Elzaki Transform and ordinary differential equation with variable coefficients. *Advances in Theoretical and Applied Mathematics*, **6**(1): 13-18.

[20] He, J.H. **(1999)**. Homotopy perturbation technique. *Computer Methods in Applied Mechanics Engineering*, **178**: 257–262.

[21] Sweilam, N. H. and Khader, M. M. **(2009)**. Exact solutions of some coupled nonlinear partial differential equations using the homotopy perturbation method. *Computers & Mathematics with Applications*, **58**: 2134–2141.

[22] Saberi-Nadjafi, J. and Ghorbani, A. **(2009)**. He's homotopy perturbation method: an effective tool for solving nonlinear integral and integro-differential equations. *Computers & Mathematics with Applications*, **58**: 1345–1351.

[23] Ghorbani, A. **(2009)**. Beyond adomian's polynomials: He polynomials. *Chaos Solitons and Fractals*. **39**: 1486- 1492.

[24] Mohyud-Din, S. T., Noor, M. A. and Noor, K. I. **(2009)**. Traveling wave solutions of seventh-order generalized KdV equation using He's polynomials. *International Journal of Nonlinear Sciences and Numerical Simulation*, **10**: 227-233.

□□

Nepal Journal of Mathematical Sciences (NJMS)
ISSN: 2738-9928 (online), 2738-9812 (print)
Vol. 4, No. 2, 2023 (August): 41-48
DOI: https://doi.org/10.3126/njmathsci.v4i2.59531

Research Article
Received Date: May 3, 2023
Accepted Date: August 9, 2023
Published Date: August 30, 2023

On New Space of Vector-Valued Generalized Bounded Sequences Defined on Product Normed Space

Jagat Krishna Pokharel[1,2] , Narayan Prasad Pahari[2] , and Jhavi Lal Ghimire[3]

[1]*Department of Mathematics Education, Sanothimi Campus, Tribhuvan University, Nepal*
[2,3]*Central Department of Mathematics, Tribhuvan University, Kirtipur, Kathmandu, Nepal.*

Email: [1] *jagatpokhrel.tu@gmail.com* ,[2]*nppahari @gmail.com* , and [3]*jhavighimire@gmail.com*

Corresponding Author*:* Jagat Krishna Pokharel

Abstract: *In this paper, we introduce and study a new vector valued sequence space* $\ell_\infty(X\times Y, \overline{\gamma}, \overline{u}, \|.\|)$ *with its terms from a product normed space* $X\times Y$*. Beside investigating the linear space structure of* $\ell_\infty(X\times Y, \overline{\gamma}, \overline{u}, \|.\|)$ *with respect to co-ordinatewise vector operations, our primarily interest is to explore the conditions in terms of* $\overline{u}$ *and* $\overline{\gamma}$ *so that a class* $\ell_\infty(X\times Y, \overline{\gamma}, \overline{u}, \|.\|)$ *is contained in or equal to another class of same kind .*

Keywords: *Sequence space, Generalized sequence space, Product-normed space*.

1. Introduction and Preliminaries

So far, a large number of research projects have been carried out in mathematical structures built with real or complex numbers. In recent years, many researchers have investigated many results on vector valued sequence space defined on normed space. Many researchers are motivated towards further investigation and application on product-normed space.

In this section, we give some definitions regarding to the product-normed linear space.

Let X be a normed space over $\mathbb{C}$, the field of complex numbers and let $\omega(X)$ denote the linear space of all sequences $\overline{x} = (x_k)$ with $x_k \in X$, $k \geq 1$ with usual coordinate-wise operations .We shall denote $\omega(\mathbb{C})$ by ω . Any subspace S of ω is then called a sequence space. A vector valued sequence space or a generalized sequence space is a linear space consisting of sequences with their terms from a vector space.

The various types of vector and scalar valued single sequence spaces has been significantly developed by several workers for instances, Köthe (1970), Kamthan and Gupta (1980), Maddox (1980), Ruckle (1981), Malkowski and Rakocevic (2004), Khan (2008), Kolk (2011), Pahari (2012), (2014), Srivastava and Pahari (2012) etc. Recently, Ghimire and Pahari (2022),(2023) studied various types of vector valued sequence spaces defined by Orlicz function. Paudel and Pahari (2021),(2022) extended the work related to scalar valued single sequences in fuzzy metric space.

Let $(X, \|.\|_X)$ and $(Y, \|.\|_Y)$ be Banach spaces over the field $\mathbb{C}$ of complex numbers. Clearly the linear space structure of X and Y provides the Cartesian product of X and Y given by

$$X\times Y = \{ <x, y> : x \in X, y \in Y \}$$

forms a normed linear space over $\mathbb{C}$ under the algebraic operations

$$< x_1, y_1 > + < x_2, y_2 > = < x_1 + x_2, y_1 + y_2 > \quad \text{and } \alpha < x, y > = < \alpha x, \alpha y >$$

with the norm

$$|| < x, y > || = \max \{|| x ||_X, || y ||_Y \},$$

where $< x_1, y_1 >, < x_2, y_2>, < x, y > \in X \times Y$ and $\alpha \in \mathbb{C}$.

Moreover since $(X, || \, . \, ||_X)$ and $(Y, || \, . \, ||_Y)$ are Banach spaces therefore $(X \times Y, || < . \, , \, . > ||)$ is also a Banach space.

Sanchezl *et al*(2000), Castillo *et al* (2001) and Yilmaz *et al*(2004) and many others have introduced and examined some properties of bilinear vector valued sequence spaces defined on product normed space which generalize many sequence spaces.

2. The Space $\ell_\infty (X \times Y, \overline{\gamma}, \overline{u}, || \, . \, ||)$

Let $\overline{u} = (u_k)$ and $\overline{v} = (v_k)$ be any sequences of strictly positive real numbers and $\overline{\gamma} = (\gamma_k)$ and $\overline{\mu} = (\mu_k)$ be sequences of non-zero complex numbers.

We now introduce and study the following class of Normed space $X \times Y$ -valued sequences:

$$\ell_\infty (X \times Y, \overline{\gamma}, \overline{u}, || \, . \, ||) = \{\overline{u} = (< x_k , y_k >) : < x_k , y_k > \in X \times Y, \ \sup_k || \gamma_k < x_k , y_k > ||^{u_k} < \infty\}.$$

Further, when $\gamma_k = 1$ for all k, then $\ell_\infty (X \times Y, \overline{\gamma}, \overline{u}, || \, . \, ||)$ will be denoted by $\ell_\infty (X \times Y, \overline{u}, || \, . \, ||)$ and when $u_k = 1$ for all k then $\ell_\infty (X \times Y, \overline{\gamma}, \overline{u}, || \, . \, ||)$ will be denoted by $\ell_\infty (X \times Y, \overline{\gamma}, || \, . \, ||)$.

In fact, this class is the generalization of the space introduced and studied by Srivastava and Pahari (2012) to the product normed space.

3. Main Results

In this section we shall derive the linear space structure of the class $\ell_\infty (X \times Y, \overline{\gamma}, \overline{u}, || \, . \, ||)$ over the field $\mathbb{C}$ of complex numbers and thereby investigate conditions in terms of $\overline{u}$, $\overline{v}$, $\overline{\gamma}$ and $\overline{\mu}$ so that a class is contained in or equal to another class of same kind .

As far as the linear space structure of $\ell_\infty (X \times Y, \overline{\gamma}, \overline{u}, || \, . \, ||)$ over $\mathbb{C}$ is concerned we throughout take the co-ordinatewise vector operations i.e., for $\overline{w} = (< x_k , y_k >)$, $\overline{z} = (< x'_k , y'_k >)$ in $\ell_\infty (X \times Y, \overline{\gamma}, \overline{u}, || \, . \, ||)$ and scalar α, we have

$$\overline{w} + \overline{z} = (< x_k , y_k >) + (< x'_k , y'_k >) = (< x_k + x'_k, y_k + y'_k >)$$

$$\text{and } \alpha\overline{u} = (\alpha < x_k , y_k >) = (< \alpha x_k , \alpha y_k >).$$

The zero element of the space will be denoted by

$$\overline{\theta} = (< 0, 0 >, < 0, 0 >, < 0, 0 >, ...).$$

Further, by $\overline{u} = (u_k) \in \ell_\infty$, we mean $\sup_k u_k < \infty$.

We see below that $\sup_k u_k < \infty$ is the necessary condition for linearity of the space. Moreover, we shall denote $M = \max (1, \sup_k u_k)$ and $A(\alpha) = \max(1, |\alpha|)$.

Theorem 3.1: $\ell_\infty (X \times Y, \overline{\gamma}, \overline{u}, || \, . \, ||)$ **forms a linear space over** $\mathbb{C}$ **if and only if** $\overline{u} = (u_k) \in \ell_\infty$.

Proof:

For the sufficiency, assume that $\overline{u} = (u_k) \in \ell_\infty$ and $\overline{w} = (< x_k , y_k >)$ and

$\bar{z} = (< x'_k , y'_k >) \in \ell_\infty(X \times Y, \bar{\gamma}, \bar{u}, \| . \|)$.

So that we have

$$\sup_k \| \gamma_k < x_k , y_k > \|^{uk} < \infty \text{ and } \sup_k \| \gamma_k < x'_k , y'_k > \|^{uk} < \infty.$$

Thus considering

$$\sup_k \| \gamma_k (< x_k , y_k > + < x'_k , y'_k >) \|^{uk/M} \leq \sup_k \| \gamma_k < x_k , y_k > \|^{uk/M} + \sup_k \| \gamma_k < x'_k , y'_k > \|^{uk/M}$$

and we see that

$$\sup_k \| \gamma_k (< x_k , y_k > + < x'_k , y'_k >) \|^{uk/M} < \infty.$$

and hence $\bar{w} + \bar{z} \in \ell_\infty(X \times Y, \bar{\gamma}, \bar{u}, \| . \|)$.

Similarly for any scalar α, $\alpha\bar{w} \in \ell_\infty(X \times Y, \bar{\gamma}, \bar{u}, \| . \|)$ since

$$\begin{aligned} \sup_k \| \alpha\gamma_k < x_k , y_k > \|^{uk/M} &= \sup_k |\alpha|^{uk/M} \| \gamma_k < x_k , y_k > \|^{uk/M} \\ &\leq A(\alpha) \sup_k \| \gamma_k < x_k , y_k > \|^{uk/M} < \infty. \end{aligned}$$

Conversely if $\bar{u} = (u_k) \notin \ell_\infty(X \times Y, \bar{\gamma}, \bar{u}, \| . \|)$ then we can find a sequence $(k(n))$ of positive integers with $k(n) < k(n+1)$, $n \geq 1$ such that $u_{k(n)} > n$ for each $n \geq 1$.

Now taking $< r, t > \in X \times Y$, $\| < r, t > \| = 1$ we define a sequence $\bar{w} = (< x_k , y_k >)$ by

$$< x_k , y_k > = \begin{cases} \lambda_{k(n)}^{-1} n^{-rk(n)} < r, t >, \text{ for } k = k(n), n \geq 1 \text{ , and} \\ < 0, 0 >, \text{ otherwise.} \end{cases}$$

where $< r, t > \in X \times Y$ with $\| < r, t > \| = 1$, then we have

$$\begin{aligned} \sup_k \| \gamma_k < x_k , y_k > \|^{uk} &= \sup_n \| \gamma_{k(n)} < x_{k(n)}, y_{k(n)} > \|^{uk(n)} \\ &= \sup_n \| n^{-rk(n)} < r, t > \|^{uk(n)} \\ &= \sup_n \frac{1}{n} = 1. \end{aligned}$$

Thus we easily see that $\bar{w} \in \ell_\infty(X \times Y, \bar{\gamma}, \bar{u}, \| . \|)$ but on the other hand for $k = k(n)$, $n \geq 1$ and for the scalar $\alpha = 2$,we have

$$\begin{aligned} \sup_k \| \gamma_k (\alpha < x_k , y_k >) \|^{uk} &= \sup_k \| \gamma_{k(n)} (\alpha < x_{k(n)} , y_{k(n)} >) \|^{uk(n)} \\ &= \sup_n |2|^{uk(n)} \| n^{-rk(n)} < r, t > \|^{uk(n)} \\ &= \sup_n |2|^{uk(n)} \cdot \frac{1}{n} \\ &> \sup_n \frac{2^n}{n} \geq 1 \end{aligned}$$

This shows that $\alpha \bar{w} \notin \ell_\infty(X \times Y, \bar{\gamma}, \bar{u}, \| . \|)$. Hence $\ell_\infty(X \times Y, \bar{\gamma}, \bar{u}, \| . \|)$ forms a linear space if and only if $\bar{u} = (u_k) \in \ell_\infty$.

Theorem 3.2: For any $\bar{u} = (u_k)$, $\ell_\infty(X \times Y, \bar{\gamma}, \bar{u}, \| . \|) \subset \ell_\infty(X \times Y, \bar{\mu}, \bar{u}, \| . \|)$ if and only if

$$\liminf_k \left| \frac{\gamma_k}{\mu_k} \right|^{uk} > 0.$$

Proof : Suppose $\liminf_k \left| \frac{\gamma_k}{\mu_k} \right|^{uk} > 0$, and $\bar{w} = (< x_k , y_k >) \in \ell_\infty(X \times Y, \bar{\gamma}, \bar{u}, \| . \|)$. Then there exists $m > 0$, such that $m|\mu_k|^{uk} < |\gamma_k|^{uk}$ for all sufficiently large values of k. Thus

$$\sup_k \| \mu_k < x_k , y_k > \|^{uk} \leq \sup_k \frac{1}{m} \| \gamma_k < x_k , y_k > \|^{uk} < \infty$$

for all sufficiently large values of k, implies that $\overline{w} \in \ell_\infty(X \times Y, \overline{\mu}, \overline{u}, \| . \|)$. Hence

$$\ell_\infty(X \times Y, \overline{\gamma}, \overline{u}, \| . \|) \subset \ell_\infty(X \times Y, \overline{\mu}, \overline{u}, \| . \|).$$

Conversely, let $\ell_\infty(X \times Y, \overline{\gamma}, \overline{u}, \| . \|) \subset \ell_\infty(X \times Y, \overline{\mu}, \overline{u}, \| . \|)$ but $\liminf_k \left| \frac{\gamma_k}{\mu_k} \right|^{uk} = 0$.

Then we can find a sequence $(k(n))$ of positive integers with $k(n) < k(n+1)$, $n \geq 1$ such that

$$\left| \frac{\gamma_k}{\mu_k} \right|^{uk} < \frac{1}{n} \quad \text{i.e., } |\mu_{k(n)}|^{uk(n)} > n |\gamma_{k(n)}|^{uk(n)}.$$

So, if we take the sequence $\overline{w} = (< x_k , y_k >)$ defined by

$$< x_k , y_k > = \begin{cases} \gamma_{k(n)}^{-1} < r, t >, \text{ for } k = k(n), n \geq 1 \text{ , and} \\ < 0, 0 >, \text{ otherwise.} \end{cases}$$

where $< r, t > \in X \times Y$ with $\| < r, t > \| = 1$, then we easily see that

$$\sup_k \| \gamma_k < x_k , y_k > \|^{uk} = \sup_n \| \gamma_{k(n)} < x_{k(n)}, y_{k(n)} > \|^{uk(n)}$$
$$= \sup_n \| < r, t > \|^{uk(n)} = 1$$

and , $\sup_k \|\mu_k < x_k , y_k > \|^{uk} = \sup_n \|\mu_{k(n)} < x_{k(n)}, y_{k(n)} > \|^{uk(n)}$

$$= \sup_n \left\{ \left| \frac{\mu_{k(n)}}{\gamma_{(n)}} \right|^{uk(n)} \| < r, t > \|^{uk(n)} \right\} > \sup_n n = \infty.$$

Hence $\overline{w} \in \ell_\infty(X \times Y, \overline{\gamma}, \overline{u}, \| . \|)$ but $\overline{w} \notin \ell_\infty(X \times Y, \overline{\mu}, \overline{u}, \| . \|)$, a contradiction. This completes the proof.

Theorem 3.3: For any $\overline{u} = (u_k)$, $\ell_\infty(X \times Y, \overline{\mu}, \overline{u}, \| . \|) \subset \ell_\infty(X \times Y, \overline{\gamma}, \overline{u}, \| . \|)$

if and only if $\limsup_k \left| \frac{\gamma_k}{\mu_k} \right|^{uk} < \infty$.

Proof :

For the sufficiency, suppose $\limsup_k \left| \frac{\gamma_k}{\mu_k} \right|^{uk} < \infty$, and $\overline{w} = (< x_k , y_k >) \in \ell_\infty(X \times Y, \overline{\mu}, \overline{u}, \| . \|)$.

Then there exists $L > 0$, such that $\left| \frac{\gamma_k}{\mu_k} \right|^{uk} < L$ i.e., $L|\mu_k|^{uk} > |\gamma_k|^{uk}$

for all sufficiently large values of k.

Thus $\sup_k \| \gamma_k < x_k , y_k > \|^{uk} \leq \sup_k L \| \mu_k < x_k , y_k > \|^{uk} < \infty$,

for all sufficiently large values of k, implies that $\overline{w} \in \ell_\infty(X \times Y, \overline{\gamma}, \overline{u}, \| . \|)$. Hence

$$\ell_\infty(X \times Y, \overline{\mu}, \overline{u}, \| . \|) \subset \ell_\infty(X \times Y, \overline{\gamma}, \overline{u}, \| . \|).$$

For the necessity, suppose that $\ell_\infty(X \times Y, \overline{\mu}, \overline{u}, \| . \|) \subset \ell_\infty(X \times Y, \overline{\gamma}, \overline{u}, \| . \|)$

but $\limsup_k \left| \frac{\gamma_k}{\mu_k} \right|^{uk} = \infty$. Then we can find a sequence $(k(n))$ of positive integers $k(n) < k(n+1)$, $n \geq 1$ such that

$$n|\mu_{k(n)}|^{uk(n)} < |\gamma_{k(n)}|^{uk(n)}, \text{ for each } n \geq 1$$

For $< r, t > \in X \times Y$ with $\| < r, t > \| = 1$ we define sequence $\overline{w} = (< x_k , y_k >)$ such that

$$< x_k , y_k > = \begin{cases} \mu_{k(n)}^{-1} < r, \ t >, \text{ for } k = k(n), \ n \geq 1 \ , \text{ and} \\ < 0, 0 >, \text{ otherwise.} \end{cases}$$

Then we easily see that

$$\sup_k \| \mu_k < x_k , y_k > \|^{uk} = \sup_n \| \mu_{k(n)} < x_{k(n)}, y_{k(n)} > \|^{uk(n)}$$
$$= \sup_n \| < r, t > \|^{uk(n)} \quad = 1$$

and $$\sup_k \|\gamma_k < x_k , y_k > \|^{uk} = \sup_n \|\gamma_{k(n)} < x_{k(n)}, y_{k(n)} > \|^{uk(n)}$$
$$= \sup_n \left\{ \left| \frac{\gamma_{k(n)}}{\mu_{(n)}} \right|^{uk(n)} \| < r, \ t > \|^{uk(n)} \right\}$$
$$> \sup_n n = \infty.$$

Hence $\overline{w} \in \ell_\infty (X \times Y, \overline{\mu}, \overline{u}, \| \ . \ \|)$ but $\overline{w} \notin \ell_\infty (X \times Y, \overline{\gamma}, \overline{u}, \| \ . \ \|)$, , which leads to a contradiction.

This completes the proof.

When Theorems 3.2 and 3.3 are combined, we get

Theorem 3.4: For any $\overline{u} = (u_k)$, $\ell_\infty (X \times Y, \overline{\gamma}, \overline{u} \ , \| \ . \ \|) = \ell_\infty (X \times Y, \overline{\mu}, \overline{u} \ , \| \ . \ \|)$

if and only if $0 < \liminf_k \left| \frac{\gamma_k}{\mu_k} \right|^{uk} \leq \limsup_k \left| \frac{\gamma_k}{\mu_k} \right|^{uk} < \infty.$

Corollary 3.5: For any $\overline{u} = (u_k)$,

(i) $\ell_\infty (X \times Y, \overline{\gamma}, \overline{u} \ , \| \ . \ \|) \subset \ell_\infty (X \times Y, \overline{u}, \| \ . \ \|)$ if and only if $\liminf_k |\gamma_k|^{uk} > 0$;

(ii) $\ell_\infty (X \times Y, \overline{u}, \| \ . \ \|) \subset \ell_\infty (X \times Y, \overline{\gamma}, \overline{u}, \| \ . \ \|)$ if and only if $\limsup_k |\gamma_k|^{uk} < \infty$;

(iii) $\ell_\infty (X \times Y, \overline{\gamma}, \overline{u}, \| \ . \ \|) = \ell_\infty (X \times Y, \overline{u}, \| \ . \ \|)$ if and only if

$$0 < \liminf_k \ |\gamma_k|^{uk} \leq \limsup_k |\gamma_k|^{uk} < \infty.$$

Proof :

Proof follows if we take $\mu_k = 1$ for all k in Theorems 3.2, 3.3 and 3.4.

Theorem 3.6: For any $\overline{\gamma} = (\gamma_k)$, $\ell_\infty (X \times Y, \overline{\gamma}, \overline{u} \ , \| \ . \ \|) \subset \ell_\infty (X \times Y, \overline{\gamma}, \overline{v}, \| \ . \ \|)$

if and only if $\limsup_k \frac{v_k}{u_k} < \infty.$

Proof: Let the condition hold. Then there exists $L > 0$ such that $\frac{v_k}{u_k} < L$ for all sufficiently large values of k. Thus $\sup_k \| \gamma_k < x_k , y_k > \|^{uk} \leq N$ for some $N > 1$ implies that

$$\sup_k \| \gamma_k < x_k , y_k > \|^{vk} \leq N^L,$$

and hence $\ell_\infty (X \times Y, \overline{\gamma}, \overline{u} \ , \| \ . \ \|) \subset \ell_\infty (X \times Y, \overline{\gamma}, \overline{v}, \| \ . \ \|)$.

Conversely, let the inclusion hold but $\limsup_k \frac{v_k}{u_k} = \infty.$

Then there exists a sequence $(k(n))$ of positive integers with $k(n) < k(n + 1)$, $n \geq 1$ such that

$$\frac{v_{k(n)}}{u_{k(n)}} > n \quad \text{i.e., } v_{k(n)} > n \, u_{k(n)} \ , \ n \geq 1.$$

We now define a sequence $\overline{w} = (< x_k , y_k >)$ as follows:

$$< x_k , y_k > = \begin{cases} \gamma_{k(n)}^{-1} 2^{1/uk(n)} < r, \ t >, \text{ for } k = k(n),\ n \geq 1 \ , \text{ and} \\ < 0, 0 >, \text{ otherwise.} \end{cases}$$

where $< r, t > \in X \times Y$ with $\| < r, t > \| = 1$.

Then for $k = k(n)$, $n \geq 1$, we easily see that

$$\sup_k \| \gamma_k < x_k , y_k > \|^{uk} = \sup_n \| \gamma_{k(n)} < x_{k(n)}, y_{k(n)} > \|^{uk(n)}$$

$$= 2 \sup_n \| \ < r, t > \|^{uk(n)} \quad = 2$$

and , $\sup_k \|\gamma_k < x_k , y_k > \|^{vk} = \sup_n \|\gamma_{k(n)} < x_{k(n)}, y_{k(n)} > \|^{vk(n)}$

$$= \sup_n \| 2^{1/uk(n)} < r, \ t > \|^{vk(n)}$$

$$> \sup_n 2^n = \infty.$$

Hence $\overline{w} \in \ell_\infty(X \times Y, \overline{\gamma}, \overline{u}, \| \ . \ \|)$ but $\overline{w} \notin \ell_\infty(X \times Y, \overline{\gamma}, \overline{v}, \| \ . \ \|)$, a contradiction.

This completes the proof.

Theorem 3.7: For any $\overline{\gamma} = (\gamma_k)$, $\ell_\infty(X \times Y, \overline{\gamma}, \overline{v}, \| \ . \ \|) \subset \ell_\infty(X \times Y, \overline{\gamma}, \overline{u}, \| \ . \ \|)$

if and only if $\liminf_k \frac{v_k}{u_k} > 0$.

Proof : Let the condition hold and $\overline{w} = (< x_k , y_k >) \in \ell_\infty(X \times Y, \overline{\gamma}, \overline{v} , \| \ . \ \|)$.Then there exists $m > 0$ such that $v_k < m\ u_k$ for all sufficiently large values of k and

$$\sup_k \| \gamma_k < x_k , y_k > \|^{vk} \leq N \text{ for some } N > 1.$$

This implies that

$$\sup_k \| \gamma_k < x_k , y_k > \|^{uk} \leq N^{1/m} \text{ i.e, } \overline{w} = (< x_k , y_k >) \notin \ell_\infty(X \times Y, \overline{\gamma}, \overline{u})$$

and hence $\ell_\infty(X \times Y, \overline{\gamma}, \overline{v}, \| \ . \ \|) \subset \ell_\infty(X \times Y, \overline{\gamma}, \overline{u} , \| \ . \ \|)$.

Conversely let the inclusion hold but $\liminf_k \frac{v_k}{u_k} = 0$. Then we can find a sequence $(k(n))$ of positive integers with $k(n) < k(n + 1)$, $n \geq 1$ such that $\frac{v_{k(n)}}{u_{k(n)}} < \ n$ i.e., $v_{k(n)} < u_{k(n)}$, $n \geq 1$.

Now taking $< r, t > \in X \times Y$ with $\| < r, t > \| = 1$, we define the sequence $\overline{w} = (< x_k , y_k >)$ by

$$< x_k , y_k > = \begin{cases} \gamma_{k(n)}^{-1} 2^{1/vk(n)} < r, \ t >, \text{ for } k = k(n),\ n \geq 1 \ , \text{ and} \\ < 0, 0 >, \text{ otherwise.} \end{cases}$$

Then for $k = k(n)$, $n \geq 1$, we easily see that

$$\sup_k \| \gamma_k < x_k , y_k > \|^{vk} = \sup_n \| \gamma_{k(n)} < x_{k(n)}, y_{k(n)} > \|^{vk(n)}$$

$$= 2 \sup_n \| \ < r, t > \|^{vk(n)}$$

$$= 2$$

and $\sup_k \|\gamma_k < x_k , y_k > \|^{uk} = \sup_n \|\gamma_{k(n)} < x_{k(n)}, y_{k(n)} > \|^{uk(n)}$

$$= \sup_n \| 2^{1/vk(n)} < r, \ t > \|^{uk(n)}$$

$$> \sup_n 2^n = \infty.$$

Hence $\overline{w} \in \ell_\infty(X \times Y, \overline{\gamma}, \overline{v} , \| \ . \ \|)$ but $\overline{w} \notin \ell_\infty(X \times Y, \overline{\gamma}, \overline{u} , \| \ . \ \|)$, a contradiction.

This completes the proof.

On combining Theorems 3.6 and 3.7,we get the following theorem:

Theorem 3.8: For any $\overline{\gamma} = (\gamma_k)$, $\ell_\infty(X \times Y, \overline{\gamma}, \overline{u}, \|\ .\ \|) = \ell_\infty(X \times Y, \overline{\gamma}, \overline{v}, \|\ .\ \|)$

if and only if $0 < \liminf_k \frac{v_k}{u_k} \leq \limsup_k \frac{v_k}{u_k} < \infty$.

Corollary 3.9: For any $\overline{\gamma} = (\gamma_k)$,

(i) $\ell_\infty(X \times Y, \overline{\gamma}, \|\ .\ \|) \subset \ell_\infty(X \times Y, \overline{\gamma}, \overline{u}, \|\ .\ \|)$ if and only if $\limsup_k u_k < \infty$;

(ii) $\ell_\infty(X \times Y, \overline{\gamma}, \overline{u}, \|\ .\ \|) \subset \ell_\infty(X \times Y, \overline{\gamma}, \|\ .\ \|)$ if and only if $\liminf_k u_k > 0$;

(iii) $\ell_\infty(X \times Y, \overline{\gamma}, \overline{u}, \|\ .\ \|) = \ell_\infty(X \times Y, \overline{\gamma}, \|\ .\ \|)$ if and only if $0 < \liminf_k u_k \leq \limsup_k v_k < \infty$.

Proof :

Proof easily follows when we take $u_k = 1$ and $v_k = u_k$ for all k in theorem 3.6, 3.7 and 3.8.

Theorem 3.10: For any sequences $\overline{\gamma} = (\gamma_k)$, $\overline{\mu} = (\mu_k)$, $\overline{u} = (u_k)$ and $\overline{v} = (v_k)$,

$$\ell_\infty(X \times Y, \overline{\gamma}, \overline{u}, \|\ .\ \|) \subset \ell_\infty(X \times Y, \overline{\mu}, \overline{v}, \|\ .\ \|)$$

if and only if (i) $\liminf_k \left|\frac{\gamma_k}{\mu_k}\right|^{uk} > 0$, and

(ii) $\limsup_k \frac{v_k}{u_k} < \infty$.

Proof : Proof directly follows from Theorems 3.2 and 3.6.

In the following example we show that $\ell_\infty(X \times Y, \overline{\gamma}, \overline{u}, \|\ .\ \|)$ is strictly contained in $\ell_\infty(X \times Y, \overline{\gamma}, \overline{v}, \|\ .\ \|)$ however (i) and (ii) of Theorem 3.10 are satisfied.

Example 3.11:

Let $\overline{w} = (< x_k , y_k >)$ be a sequence in normed space $X \times Y$ such that $\|< x_k , y_k >\| = k^k$.

Take $u_k = \frac{1}{k}$ if k is odd integer and $u_k = \frac{1}{k^2}$, if k is even integer, $v_k = \frac{1}{k^2}$ for all values of k, $\gamma_k = 3^k$ for all values of k ;and $\mu_k = 2^k$, for all values of k. Then

$$\left|\frac{\gamma_k}{\mu_k}\right|^{uk} = \frac{3}{2} \text{ if } k \text{ is odd integer}$$

$$\text{and } \left|\frac{\gamma_k}{\mu_k}\right|^{uk} = \left(\frac{3}{2}\right)^{1/2}, \text{ if } k \text{ is even integer.}$$

Thus $\liminf_k \left|\frac{\gamma_k}{\mu_k}\right|^{uk} = 1$ i.e. condition (i) of Theorem 3.10 is satisfied.

Further since $\frac{v_k}{u_k} = \frac{1}{k}$, if k is odd integer and $\frac{v_k}{u_k} = 1$, if k is even integer, therefore condition (ii) of Theorem 3.10 is also satisfied as $\limsup_k \frac{v_k}{u_k} = 1$.

We now see that $\overline{w} = (< x_k , y_k >) \in \ell_\infty(X \times Y, \overline{\mu}, \overline{v})$ for all $k \geq 1$ as

$$\sup_k \| \mu_k < x_k , y_k > \|^{vk} = \sup_k (2k)^{1/k} < 2,$$

but $\overline{w} = (< x_k , y_k >) \notin \ell_\infty(X \times Y, \overline{\gamma}, \overline{u}, \|\ .\ \|)$, when k is odd integer as

$$\sup_k \| \gamma_k < x_k , y_k > \|^{uk} = \sup_k 3k = \infty.$$

This shows that the condition (i) and (ii) are satisfied but $\ell_\infty(X \times Y, \overline{\gamma}, \overline{u}, \|\ .\ \|)$ is strictly contained in $\ell_\infty(X \times Y, \overline{\gamma}, \overline{v}, \|\ .\ \|)$.

References

[1] Castillo, J., Garcia, R. and Jaramillo, J.**(2001)**. Extension of bilinear forms on Banach spaces. *Proceedings of the American Mathematical Society*, **129**(12): 3647- 3656.

[2] Ghimire, J.L and Pahari, N.P.**(2022)**. On certain linear structures of Orlicz space $c_0(M,(X, \|.\|), \overline{a}, \overline{\alpha})$ of vector valued difference sequences *The Nepali Mathematical Sciences Report*, **39**(2): 36-44.

[3] Ghimire, J.L. & Pahari,N.P.**(2023)**. On some difference sequence spaces defined by Orlicz function and ideal convergence in 2-normed space. *Nepal Journal of Mathematical Sciences*, **4**(1): 77-84.

[4] Kamthan, P.K. and Gupta, M. **(1980)**. *Sequence and Series* , *Lecture Notes*; 65 Marcel Dekker Inc.

[5] Khan, V.A.**(2008)**. On a new sequence space defined by Orlicz functions. *Common Fac. Sci. Univ. Ank-series*, **57**(2): 25–33.

[6] Kolk,E. **(2011)**. Topologies in generalized Orlicz sequence spaces. *Filomat*, **25**(4): 191-211.

[7] Köthe, G. **(1970)**. *Topological Vector Spaces*. Springer Verlag, Berlin Heidelberg, New York.

[8] Maddox, I.J.**(1980)**. *Infinite Matrices of Operators*; *Lecture Notes in Mathematics* 786, Springer-Verlag Berlin, Heidelberg, New York.

[9] Malkowski, E. and Rakocevic, V. **(2004)**. *An introduction into the theory of sequence spaces and measures of non-compactness*.

[10] Pahari, N.P.**(2011)**. On Banach space valued sequence space $l_\infty(X,M, \overline{l}, \overline{p}, L)$ defined by Orlicz function. *Nepal Journal of Science and Technology,* **12**: 252–259.

[11] Pahari, N. P. (**2014**). On normed space valued total paranormed Orlicz space of null sequences and its topological structures. *Internal Journal of Mathematics Trends and Technology*, **6**: 105-112.

[12] Paudel, G. P., and Pahari, N. P. (**2021**). On fundamental properties in Fuzzy metric space. *Academic Journal of Mathematics Education*, **4**(1): 20-25.

[13] Paudel, G. P., Pahari, N. P. and Kumar, S. (**2022**). Generalized form of p-bounded variation of sequences of fuzzy real numbers. *Pure and Applied Mathematics Journal*, **11**(3): 47-50.

[14] Paudel, G. P., Pahari, N. P. and Kumar, S. (**2022**). Double sequence space of Fuzzy real numbers defined by Orlicz function. *The Nepali Mathematical Sciences Report*, **39**(2): 85-94

[15] Ruckle. W.H. **(1981)**. *Sequence spaces* . Pitman Advanced Publishing Programme.

[16] Sanchez1, F. , Garcia1, R. and Villanueva, I.**(2000)**. Extension of multilinear operators on Banach spaces. *Extracta Mathematica*; **15**(2): 291 – 334.

[17] Srivastava,J.K. and Pahari,N.P. **(2012)**. On vector valued paranormed sequence space $c_0(X, M, \overline{\lambda}, \overline{p})$ defined by Orlicz function. *Journal of Rajasthan Academy of Physical Sciences*; **11**(2):11-24.

[18] Wilansky, A. **(1978)**. *Modern methods in topological vector spaces*. McGraw-Hill Book Co. Inc. New York.

[19] Yilmaz, Y. and Solak,I.**(2004)**. Operator perfectness and normality of vector-valued sequence spaces. *Thai Journal of Mathematics*, **2** (2) : 247-257 .

□□

Nepal Journal of Mathematical Sciences (NJMS)
ISSN: 2738-9928 (online), 2738-9812 (print)
Vol. 4, No. 2, 2023 (August): 49-58
DOI: https://doi.org/10.3126/njmathsci.v4i2.59536
School of Mathematical Sciences,
Tribhuvan University, Kathmandu, Nepal

Research Article
Received Date: April 9, 2023
Accepted Date: August 13, 2023
Published Date: August 30, 2023

Forecasting Annual Mean Temperature and Rainfall in Bangladesh Using Time Series Data

Keya Rani Das[1*], Preetilata Burman[2], Linnet Riya Barman[3], Mashrat Jahan[4], Mst. Noorunnahar[5]

[1,5]*Dept. of Statistics, Bangabandhu Sheikh Mujibur Rahman Agricultural University Gazipur, Bangladesh.*

[2,3]*Faculty of Agricultural Economics and Rural Development, Bangabandhu Sheikh Mujibur Rahman Agricultural University Gazipur, Bangladesh*

[4]*Dept. of Agricultural Economics, Bangabandhu Sheikh Mujibur Rahman Agricultural University Gazipur, Bangladesh*

Email: [1]*keyadas57@bsmrau.edu.bd*, [2]*preetypbs@gmail.com*, [3]*linnetriya@gmail.com*, [4]*mjahan.aec@bsmrau.edu.bd*, [5]*noorunnahar.stt@bsmrau.edu.bd*

*Corresponding author: Keya Rani Das

Abstract: *Our ability to grow crops is significantly impacted by the weather. Therefore, it is important to make predictions about the weather. Because of its reliance on stable weather conditions, agriculture is highly susceptible to the effects of climate change. Countries like Bangladesh, whose economy is based on agriculture, will be more severely affected by the effects of climate change than others. For this reason, it is crucial to develop a robust forecasting tool to determine the implications of climatic variables, especially temperature and rainfall. In this study, we project the average annual rainfall and temperature in Bangladesh using the Auto-Regressive Integrated Moving Average (ARIMA) model for the next decade, from 2023 to 2032. Bangladesh's precipitation and temperature records from the past 60 years were compiled and analyzed with the help of the R programming language. Annual mean temperatures are forecasted to fall between 24.9 and 26.3 degrees Celsius, while annual mean rainfall is forecasted to fall between 1,550 and 2,650 millimeters.*

Keywords: *Rainfall, Temperature, Agricultural production, Bangladesh, ARIMA.*

Introduction

Agriculture is the backbone of the economies of many developing countries because it provides people with both food and income. Since this sector is highly vulnerable to climate change, Bangladesh, one of the rising developing nations, is in particular jeopardy. Farmers use weather forecasts and climatological trends to determine which crops to plant and when. Climate has a major impact on how often pests need and diseases occur, how easily farmers can get their hands on water, and how much fertilizer they need to use. However, climatic change and variability have an effect on agricultural output and standard of living. Recent climate changes have had multiple effects on crop yields (Lobell et. al, [21]). The threat that climate change posed to small and medium-sized rainfed farmers was significant (Ashalatha et. al, [4]).

Bangladesh typically experiences subtropical monsoon weather. The highest temperature ever recorded in the summer is 37 C (98 F), while there are few spots where it can occasionally reach 41 C (105 F) or more. Between July and October, we get about 80% of our annual precipitation. Precipitation totals typically fall between 1429 and 4338 millimeters per year on average (BBS, [7]).

The effects of the climate affect many facets of agricultural production (Iizumi&Ramankutty, [16]). The primary climatic factors affecting agricultural production include rising temperatures, changed precipitation

patterns, and an increase in atmospheric CO2 concentration (Neenu et. al, [26]). In terms of agriculture, temperature and rainfall are two of the most important climatic parameters. Understanding how temperature and precipitation variations impact crop output is a crucial first step in developing policy and agricultural management choices.

A significant economic factor is the timing of rainfall (Torres et. al, [36]). The effect of rainfall on agricultural productivity could be asymmetric (Mitra, [35]). Long-term changes in natural rainfall patterns might pose a problem for the world's current farming methods (Wei et. al, [38]). Rainfall's impact on crop production can be explained by either its seasonal average quantity or its temporal distribution. Rainfall unpredictability affects food accessibility per capita and raises the percentage of the overall malnourished population in developing countries (Kinda & Badolo, [18]). Rainfall does not directly affect production because it is dependent on the environment, but there are many other factors that do (Yudin et. al, [24]). Precipitation is also responsible for loss of soil nutrients.

It was discovered that brief hot spells can lower the number of seeds or grains that might otherwise contribute to crop yield (Wheeler et. al, [39]). These results imply that temperature rises brought on by climate change may have a significant influence on agricultural yields, which may have consequences for the world's food supply. Depending on how each crop species is affected, heat stress has a negative impact on normal plant growth and development (Bhattacharya, [8]). The pace of phenological development was accelerated by warm temperatures (Hatfield & Prueger, [13]). The benefits of increased planting density for yield are diminished by higher temperatures (Wang et. al, [37]). Efficiency is considerably reduced by increases in yearly temperature fluctuation and long-term temperature (Rahman & Anik, [31]). Yields were reduced by temperatures outside or inside the ideal range (18–22 °C) (Jannat et. al, [17]). In Bangladesh, rising temperatures were linked to declines in the value of small farms (Hossain et. al, [14]). All of Bangladesh's primary food crops' production and cropping areas were negatively impacted by the maximum temperature. But in certain cases, crop yields have typically increased when temperatures have increased. The net crop revenue from crop cultivation in Bangladesh will grow as the temperature and rainfall rise (Hossain et. al, [15]). Crop yields are increased through climate-smart agriculture, which also makes it easier to produce crops in a secure environment (Liliane & Charles, [19]). The production of annual crops like wheat and groundnuts can be drastically reduced by brief high-temperature events that occur at various periods close to blooming (Challinor et. al, [10]). Wheat yields are reduced by around 3–10% for every 1°C increase in temperature throughout the growing season (You et. al, [43]).

In the study district in Ghana, the unpredictable rainfall and rising temperatures have a significant beneficial influence on maize output, underscoring the necessity for ongoing adaptation strategies such cultivating high yielding and drought tolerant maize varieties to improve family food security (Baffour-Ata et. al, [6]). Zhao et. al. [45] discovered that rising temperatures have a detrimental effect on the world's wheat, rice, maize, and soybean crops. According to a study by Lobell and Field, [20] rising temperatures cause a decline in worldwide wheat, maize, and barley yields. According to Schlenker and Roberts, [33] research, maize, soybean, and cotton yields in the US are severely harmed by temperatures that are higher than a particular point. Maize, rice, and soybean crops all benefited from higher minimum temperatures (Yin et. al, [41]). Rainfall has a detrimental impact on rice output during the heading, flowering, ripening, and reproductive stages. Rice breeders should create rice types that use less water and are more productive in hot weather (Abbas & Mayo, [1]). Since there are so many negative impacts of rainfall and temperature fluctuations all over the world like this, it is even more important for Bangladesh to come up with a good forecasting method.
Crops, animals, and pests are all vulnerable to changes in temperature and precipitation patterns, which can have an effect on agricultural output. Predicted shifts in the climate must be taken into account so that farmers and ranchers can adapt and increase their resilience. Climate variability and changes in the frequency of severe events are essential for the yield, its stability, and quality (Porter & Semenov, [28]). That's why it's crucial to know how precipitation and temperature will affect agricultural output. The purpose of this study is to predict annual mean precipitation and temperature for the period 2023-2032 in an effort to alleviate a major agricultural problem.

Methods

The aim of this research is to predict rainfall and mean temperature for the next 10 years from 2023 to 2032. Both forecasting is done using ARIMA. Rainfall and mean temperature records of Bangladesh for the past sixty years (1961-2021) were collected from the Climate Change Knowledge Portal of World Bank (World Bank, [40]). Analysis was done in RStudio with the help of auto.arima() function. In this analysis, lubridate, ggplot2, dplyr, and forecast packages were applied. There are no missing values in this data set. The study is conducted with non-stationary time series data. The Auto-Regressive Integrated Moving Average (ARIMA) model is used to forecast annual mean rainfall and temperature trends in Bangladesh.

ARIMA Model

The Autoregressive (AR) model can be effectively coupled with Moving Average (MA) models to form a general and useful class of time series models called Autoregressive Moving Average (ARMA) models. However, they can only be used when the data are stationary. This class of models can be extended to non-stationary series by allowing differencing of the data series. These are called the Autoregressive Integrated Moving Average (ARIMA) model (Anderson & Theodore, [3]). Thus, an ARIMA model is a combination of an Autoregressive (AR) process and a Moving Average (MA) process applied to a non-stationary data series. The three essential elements of the ARIMA model are autoregressive, integrated, and moving average, which drives the evaluation and selection of coefficients iteratively and recursively. These three elements are known as *p*, *d*, and q, respectively (Aborass et al, [2]).

The general non-seasonal model is known as ARIMA (*p*,*d*,*q*):

AR:*p* =order of the autoregressive part

I:*d* = degree of differencing involved

MA:*q* =order of the moving average part

The equation forth simplest ARIMA (*p*,*d*,*q*) model is as follows:

$$Y_t = c + \varphi_1 Y_{t-1} + \varphi_2 Y_{t-2} + \ldots + \varphi_p Y_{t-p} + e_t - \theta_1 e_{t-1} - \theta_2 e_{t-2} - \ldots - \theta_p e_{t-p} \qquad (1)$$

Where, Y_t = Climatic factor (Annual mean rainfall and temperature)

Y_{t-1}, $Y_{t-2},\ldots,Y_{t-p}$ = Climatic factor (Annual mean rainfall and temperature)at time lags t-1,t-2,…,t-p ,respectively.

The Box Jenkins Methodology

The Box Jenkins methodology is used to find the best-fitted model of time series data for both Univariate and Multivariate ARIMA models (Ljung & Box, [22]). Box-methods Jenkin's have four steps. First, it is necessary to determine whether or not the variables are stationary. The unit root test is used to ensure stationarity. To check the unit root and stationarity of the data, the augmented Dickey-Fuller (ADF) test and the Kwiatkowski, Phillips, Schmidt, and Shin (KPSS) test can be used. If the data is not stationary, it is transformed to be stationary by comparing the original data series. The second step is to develop a preliminary model that specifies the appropriate values of p, d, and q. The AutoCorrelation Function (ACF) and Partial Auto Correlation Function (PACF) plot to assist us in determining the order of the MA and AR processes respectively. The third step is to estimate the model's parameters using likelihood methods such as AIC, AICc, and BIC. Finally, the best-fitted model must be validated by testing the parameters and residuals of the chosen model. The residuals are examined using the ACF and PACF plots, as well as the (Box & Jenkins, [9]) statistics.

Decomposition of Time Series Data

To break down time series data into its component parts, decomposition of data is used. Using RStudio, simple additive decomposition has been performed. It goes like this:

$$Y_t = S_t + T_t + R_t \qquad (2)$$

Where, S = Seasonal Variation

T = Trend or cyclic component

R = Residual or error component

Results and Discussion

Annual Mean Rainfall

The time series plot (figure 1) shows stationary and the parameter values of p, d and q found for the ARIMA model are 0, 1 and 2. The final model chosen with the aid of the "auto.arima()" function is ARIMA (0,1,2).

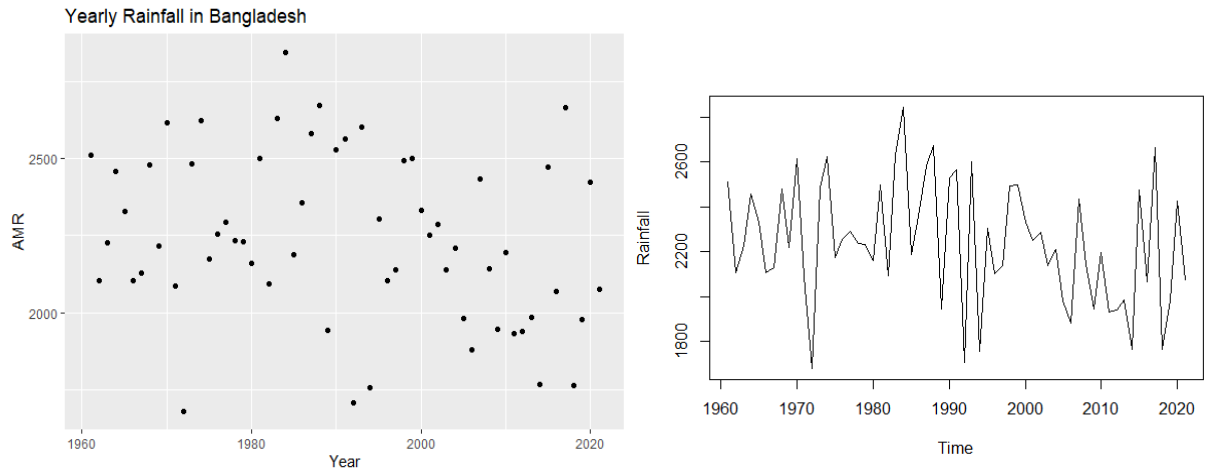

Fig.1: *Time series plot of yearly rainfall in Bangladesh*

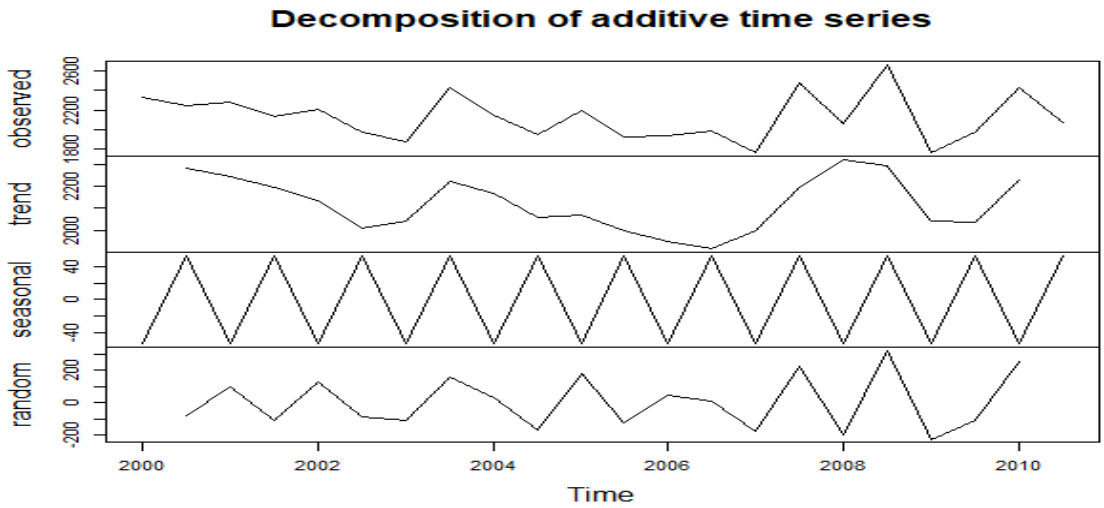

Fig.2: *Decomposition of additive time series of annual mean rainfall data in Bangladesh*

In figure 2, four types of plots are shown. first one is for the observed raw data, the second one shows the trend of the data, the third one depicts the seasonal variation and the last one shows a random component. No specific trend shows in the above plot.

Table 1

Parameter estimation of ARIMA (0,1,2) model

Parameter	Coefficients	St. Error	z value	Pr(>|z|)
MA1	-1.1073	0.1238	-8.9449	<2e-16 ***
MA2	0.2164	0.1250	1.7318	0.0833*

*** *means significant at* 1%, ** *means significant at* 5% *and* * *means significant at* 10% *level of significance*.

The model selection criteria as Akaike Information Criteria (AIC), lowest Corrected Akaike Information Criteria (AICc), Bayesian information criterion (BIC) values are listed in the following table for the yearly average rainfall data.

Table 2

Performance criteria of ARIMA (0,1,2) model

Criteria	ARIMA(0,1,2)
log likelihood	-420.88
$sigma^2$	72730
AIC	847.77
AICc	848.2
BIC	854.05

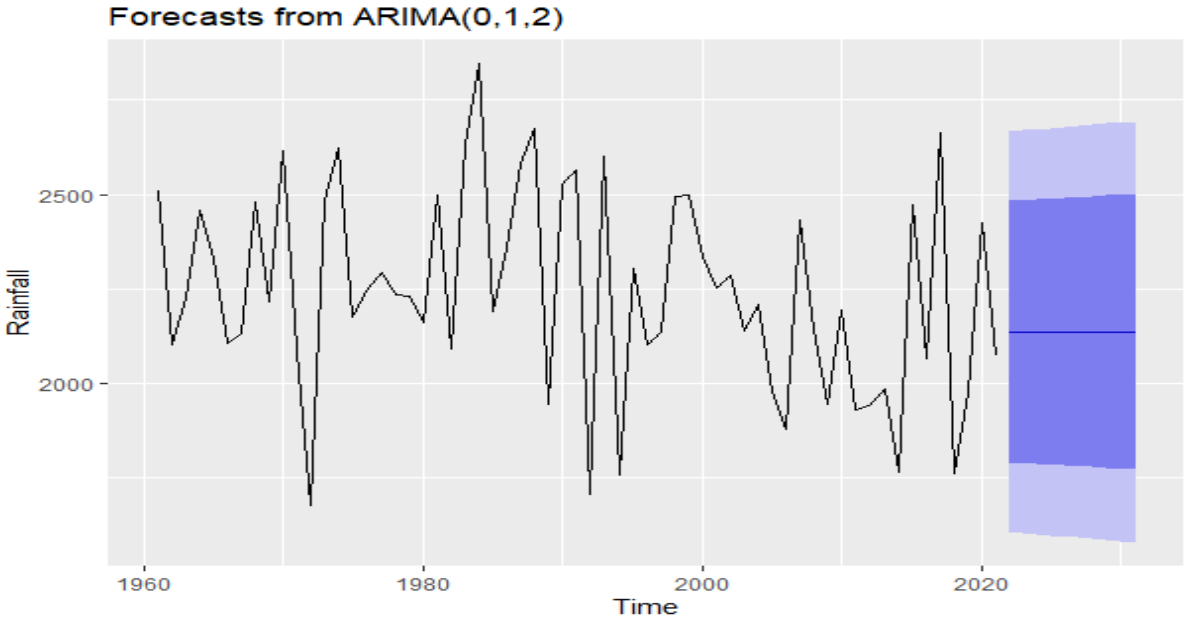

Fig.3: *Forecasting yearly average rainfall in Bangladesh*

Figure 3 focuses the forecasted values of yearly average rainfall in Bangladesh for the next ten years from 2022 to 2032. By using ARIMA(0,1,2) model the deep blue shade in the forecasted part shows 80% confidence interval and light blue shade shows 95% confidence interval for the rainfall in Bangladesh. From the 95% confidence interval it depicts the forecasted average annual rainfall is around 1550 mm to 2650 mm.

Annual Mean Temperature

The parameter values for the ARIMA model are determined to be 0, 1, and 2 according to the time series plot in Figure 4. The final model chosen with the aid of the "auto.arima ()" function is ARIMA (0,1,2).

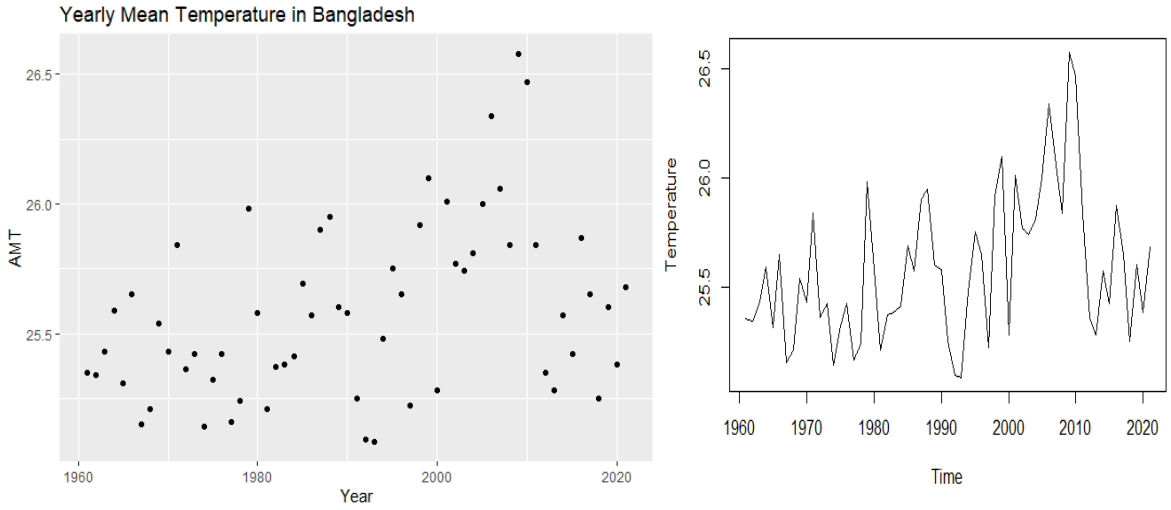

Fig.4: *Time series plot of yearly mean temperature in Bangladesh*

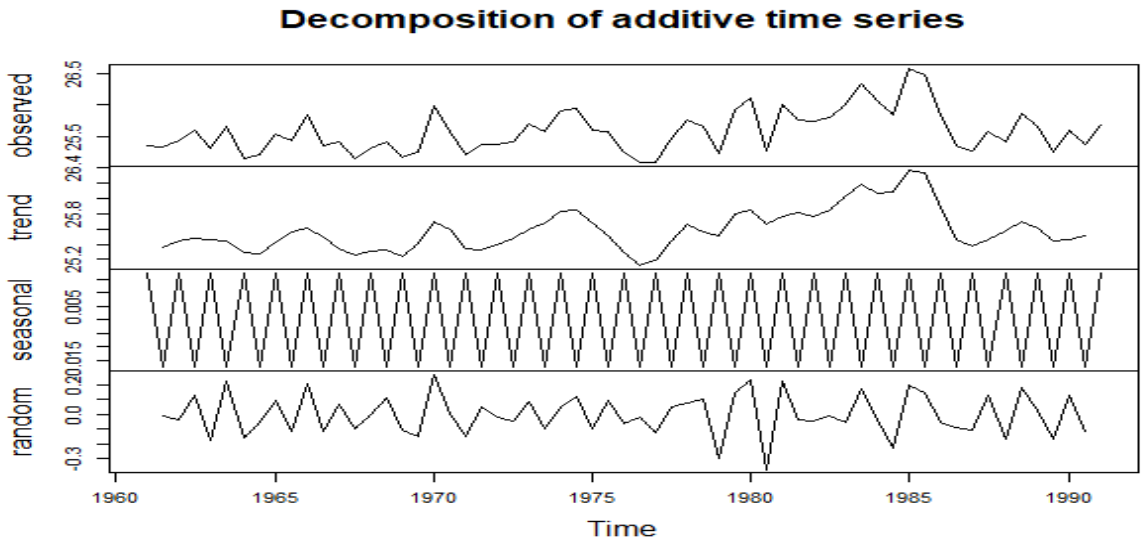

Fig.5: *Decomposition of additive time series of annual mean temperature data in Bangladesh*

Figure 5 displays four different types of plots, the first of which is for the observed raw data, the second of which indicates the data's trend, the third of which shows the seasonal fluctuation, and the fourth of which displays random components. For this data, there is no specific trend in the figure 5.

Table 3

Parameter estimation of ARIMA (0,1,2) model

Parameter	**Coefficients**	**St. Error**	**z value**	**Pr(>|z|)**
MA1	–0.4816	0.1363	–3.5336	0.0004***
MA2	–0.3270	0.1577	–2.0732	0.03816**

*** *means significant at* 1%, ** *means significant at* 5% *and* * *means significant at* 10% *level of significance.*

For the yearly average temperature data, the model selection criteria such as Akaike Information Criterion (AIC), lowest Corrected Akaike Information Criteria (AICc), and Bayesian information criterion (BIC) values are provided in the table below.

Table 4

Performance criteria of ARIMA (0,1,2) model

Criteria	**ARIMA(0,1,2)**
log likelihood	-12.56
$sigma^2$	0.09063
AIC	31.11
AICc	31.54
BIC	37.4

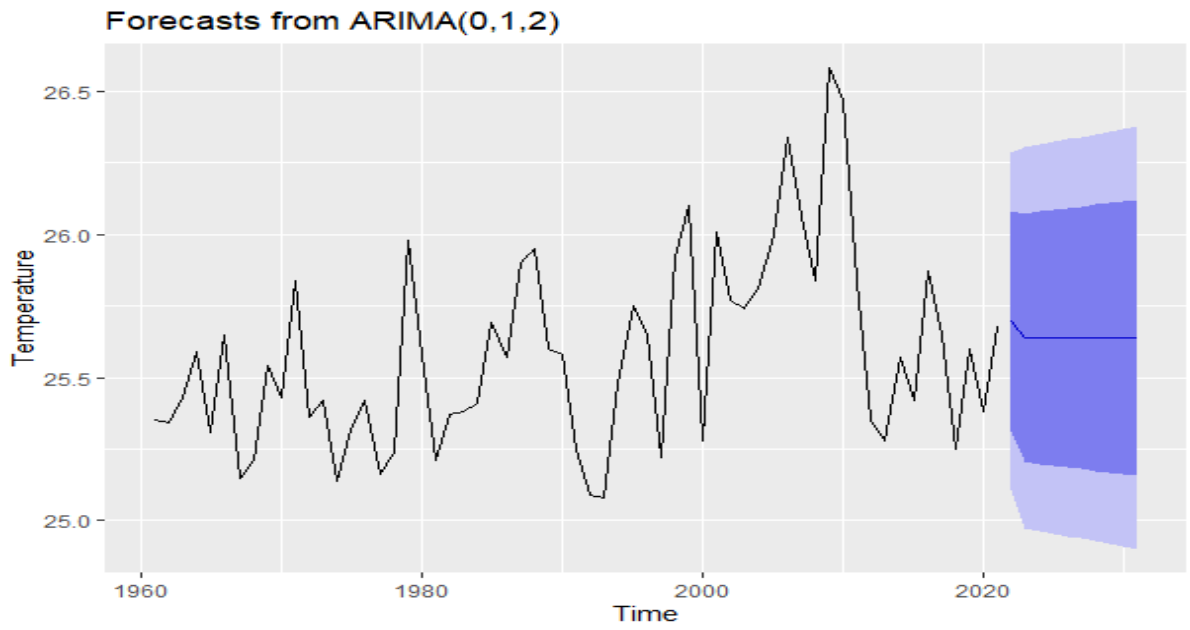

Fig.6: *Forecasting yearly average temperature in Bangladesh*

Figure 6 depicts the anticipated values of yearly average mean temperature in Bangladesh over the next 10 years, from 2023 to 2032. Using the ARIMA(0,1,2) model, the deep blue shade in the predicted portion represents an 80% confidence interval while the light blue shade shows a 95% confidence interval for the temperature in Bangladesh. According to the 95% confidence interval, the anticipated average annual mean temperature ranges between 24.9 ^{0}C and 26.3 ^{0}C.

Over the years, researchers have tried to pin down the best approach to studying climate change's impact on farm yields. The yield of crops is greatly affected by weather fluctuations over time (Yirdew & Yeshiwas [42]). Extreme heat and rain events have been demonstrated to significantly lower crop yields (Powell & Reinhard, [29]). But, accurate weather predictions can reduce planting-stage wages by reducing prior out-migration and can amplify the negative effects of bad meteorology on crop production wages (Rosenzweig & Udry, [32]). In addition, rainfall has both a short-term and long-term negative and considerable influence on agriculture productivity (Zahoor et al, [44]). Again another pair of researchers say that rainfall and economic growth in general appear to be growing in tandem. Temperature, unlike rain, has little effect on agricultural productivity (Erkan&Diken, [11]). But it has been found that more so than rainfall, temperature has an influence on crop productivity (Ochieng et al, [27]). Cotton production is growing in relation to rainfall (Ghanwat et al, [12]) whereas rainfall had little effect on coffee output (Msuya & Mahonge, [25]). With global warming, it is predicted that average temperatures would rise and heat waves will occur more frequently (Asseng et. al, [5]). For most nations, the impacts of heat are equal to or greater than those of water stress (Siebert et al, [34]). Crop performance suffers as a result of rising global temperatures (Zhu et al, [46]). The studies repeatedly demonstrate that agricultural yields are significantly impacted by temperature.

Short- and long-term stresses can significantly influence growth and yield processes when stress occurs at sensitive stages (Prasad et al, [30]). So regulated, steady growth in climatic factors is sometimes good for agricultural production. Bangladesh has witnessed extremes in rainfall and temperature during the previous few decades, affecting both the environment and the agricultural economy. Masum et al, [23] used the ARIMA model to predict and forecast rainfall and temperature in Chattogram, Bangladesh from 1953 to 2070 considering seasonal variations. (Aborass et al. [2]) applied the Box-Jenkins ARIMA methodology and comparative study of ETS model for rainfall forecasting at Birzeit for the period which extended from September -2003 to August-2021. This study predicts annual mean rainfall and temperature with the ARIMA (0,1,2) and ARIMA (0,1,2) model respectively.

Concluding Remarks

The two most important climatic factors are rainfall and temperature. Studies have shown that deviations in temperature from the ideal range can have a significant impact on a country's agricultural output. In a similar vein, inadequate or excessive precipitation will reduce agricultural output. A nation should take adequate measures to prepare for such critical climate elements. Floods, cyclones, droughts, and other extreme weather are becoming more frequent, wreaking havoc on farmlands and agricultural production in Bangladesh, one of the nation's most vulnerable to global warming. The consequences of global change, such as low land submergence, severe floods, cyclones, tidal waves, coastal flooding, and poor socioeconomic situations, especially with regards to everyday living and food security, are having a profound effect on the physical and chemical processes in these areas. Many factors, including but not limited to rising sea levels, rising temperatures, saline intrusion, shrinking cultivable landmass, limited access to clean water and sanitary conditions, infrastructure, plant diseases, limited energy sources, and so on, are making this worse. With increasing temperature and precipitation swings, farmers in Bangladesh can benefit from up-to-date and reliable weather forecasts in order to better manage crops in the field. The 10-year rainfall and mean temperature forecasts from 2023 to 2032 can help farmers make long-term plans and adjustments to their agricultural production processes. Even if climatic conditions may fluctuate due to a number of variables, this prediction will hopefully help them have a secure agricultural production process and avoid the difficult periods. If farmers had access to weather predictions, it might have prevented some of the damage that has been done. These climate services will help the agricultural sector prepare for and respond to extreme weather events, as well as adapt to the long-term effects of climate change. Therefore, this type of forecasting method is essential for ensuring the reliability of agricultural output.

References

[1] Abbas, S., & Mayo, Z. A. **(2021)**. Impact of temperature and rainfall on rice production in Punjab, Pakistan. *Environment*, *Development and Sustainability*, **23**(2): 1706-1728.

[2] Aborass, D., Abu Hassan, H., Sahalash, I., & Al-Rimmawi, H. **(2022)**. Application of ARIMA models in forecasting average monthly rainfall in Birzeit, Palestine. *International Journal of Water Resources and Arid Environments*, **11**(1): 62-80.

[3] Anderson, Theodore. **(1971)**. The Statistical Analysis of Time Series Data. 19. ch8. 10.1002/9781118186428.

[4] Ashalatha, K. V., Munisamy, G., & Bhat, A. R. S. **(2012)**. Impact of climate change on rainfed agriculture in India: a case study of Dharwad. *International Journal of Environmental Science and Development*, **3**(4): 368-371.

[5] Asseng, S., Foster, I. A. N., & Turner, N. C. **(2011)**. The impact of temperature variability on wheat yields. *Global Change Biology*, **17**(2): 997-1012.

[6] Baffour-Ata, F., Tabi, J. S., Sangber-Dery, A., Etu-Mantey, E. E., & Asamoah, D. K. Effect of Rainfall and Temperature Variability on Maize Yield in the Asante Akim North District of the Ashanti Region, Ghana. *SSRN Electronic Journal*. [Preprint] Available at SSRN: https://ssrn.com/abstract=4243569 or http://dx.doi.org/10.2139/ssrn.4243569

[7] BBS. **(2021)**. Yearbook of agricultural statistics, Bangladesh Bureau of Statistics. Statistics and Informatics Division, Ministry of Planning, Government of the People's Republic of Bangladesh. Pp.233. http://www.bbs.gov.bd/

[8] Bhattacharya, A. **(2019)**. Effect of high-temperature stress on crop productivity. Effect of high temperature on crop productivity and metabolism of macro molecules. Academic Press. 1-114. ISBN: 978-0-12-817562-0. DOI: https://doi.org/10.1016/C2018-0-02297-5

[9] Box, G. E. P. & Jenkins, G. M. **(1976)**. Time series analysis: forecasting and control. San Francisco, CA: Holden-Day. 1970: 575

[10] Challinor, A. J., Wheeler, T. R., Craufurd, P. Q., & Slingo, J. M. **(2005)**. Simulation of the impact of high temperature stress on annual crop yields. *Agricultural and Forest Meteorology*, **135**(1-4): 180-189.

[11] Erkan, K. A. R. A., & Diken, A. **(2020)**. Climatic change: The effect of rainfall on economic growth. *Süleyman Demirel Üniversitesi Vizyoner Dergisi*, **11**(28): 665-679.

[12] Ghanwat, P. S., Asewar, B. V., & Jondhale, A. N. **(2022)**. Effect of rainfall variability on cotton production and productivity in Marathwada region. *Pharma Innovation* , **11**(10):536-539.

[13] Hatfield, J. L., & Prueger, J. H. **(2015)**. Temperature extremes: effect on plant growth and development. *Weather Clim Extrem*, **10**: 4–10.

[14] Hossain, M. S., Arshad, M., Qian, L., Kächele, H., Khan, I., Islam, M. D. I., & Mahboob, M. G. **(2020)**. Climate change impacts on farmland value in Bangladesh. Ecological indicators, 112, 106181.

[15] Hossain, M. S., Arshad, M., Qian, L., Zhao, M., Mehmood, Y., & Kächele, H. **(2019)**. Economic impact of climate change on crop farming in Bangladesh: An application of Ricardian method. *Ecological Economics*, 164: 106354.

[16] Iizumi, T., & Ramankutty, N. **(2015)**. How do weather and climate influence cropping area and intensity?. *Global Food Security*, **4**: 46-50.

[17] Jannat, A., Ishikawa-Ishiwata, Y., & Furuya, J. **(2021)**. Assessing the impacts of climate variations on the potato production in Bangladesh: A supply and demand model approach. Sustainability, 13(9), 5011.

[18] Kinda, S. R., & Badolo, F. **(2019)**. Does rainfall variability matter for food security in developing countries?. *Cogent Economics & Finance*, **7**(1): 1640098.

[19] Liliane, T. N., & Charles, M. S. **(2020)**. Factors affecting yield of crops. Agronomy-climate change & food security, 9.

[20] Lobell, D. B., & Field, C. B. **(2007)**. Global scale climate–crop yield relationships and the impacts of recent warming. *Environmental Research Letters*, 2(1), 014002.

[21] Lobell, D. B., Cahill, K. N., & Field, C. B. **(2007)**. Historical effects of temperature and precipitation on California crop yields. *Climatic change*, 81(2), 187.

[22] Ljung, G. M., & Box, G. E. **(1978)**. On a measure of lack of fit in time series models. *Biometrika*, 65(2): 297-303. https://doi.org/10.1093/biomet/65.2.297

[23] Masum, M. H., Islam, R., Hossen, M. A., & Akhie, A. A. **(2022)**. Time Series Prediction of Rainfall and Temperature Trend using ARIMA Model. *Journal of Scientific Research*, **14**(1): 215-227.

[24] Mohamed Yudin, M. F, & Ismail, N. A. **(2018)**. Economical effect of rainfall toward production and cost of production. Plantation Management Exhibition & Seminar (PIMES). Faculty of Plantation and Agrotechnology, KampusJasin, 15: 84.

[25] Msuya, A. M., & Mahonge, C. P. **(2022)**. Impact of climate variability, farmers adaptation and coping strategies on coffee production in highlands of Kigoma District, Tanzania. *Asian Journal of Forestry*, 6(1).

[26] Neenu, S., Biswas, A. K., & Rao, A. S. **(2013)**. Impact of climatic factors on crop production-A review. *Agricultural Reviews*, **34**(2): 97-106.

[27] Ochieng, J., Kirimi, L., & Mathenge, M. **(2016)**. Effects of climate variability and change on agricultural production: The case of small scale farmers in Kenya. *NJAS-Wageningen Journal of Life Sciences*, **77**: 71-78.

[28] Porter, J. R., & Semenov, M. A. **(2005)**. Crop responses to climatic variation. *Philosophical Transactions of the Royal Society B*: *Biological Sciences*, **360**(1463): 2021-2035.

[29] Powell, J. P., & Reinhard, S. **(2016)**. Measuring the effects of extreme weather events on yields. *Weather and Climate Extremes*, **12**: 69-79.

[30] Prasad, P. V. V., Staggenborg, S. A., & Ristic, Z. **(2008)**. Impacts of drought and/or heat stress on physiological, developmental, growth, and yield processes of crop plants. Response of crops to limited water: Understanding and modeling water stress effects on plant growth processes, **1**:301-355. https://doi.org/10.2134/advagricsystmodel1.c11

[31] Rahman, S., & Anik, A. R. **(2020)**. Productivity and efficiency impact of climate change and agro ecology on Bangladesh agriculture. Land Use Policy, **94**: 104507.

[32]Rosenzweig, M. R., & Udry, C. **(2014)**. Rainfall forecasts, weather, and wages over the agricultural production cycle. *American Economic Review*, **104**(5): 278-283.

[33] Schlenker, W., & Roberts, M. J. **(2009)**. Nonlinear temperature effects indicate severe damages to US crop yields under climate change. *Proceedings of the National Academy of Sciences*, **106**(37): 15594-15598.

[34] Siebert, S., Webber, H., &Rezaei, E. E. **(2017)**. Weather impacts on crop yields-searching for simple answers to a complex problem. *Environ. Res. Lett*., **12**(8): 081001.

[35] Subrata Kumar Mitra **(2014).** Nonlinear impact of rain on food grain production in India. *Applied Economics Letters*, **21**(14): 1001-1005, DOI: 10.1080/13504851.2014.904483

[36] Torres, M., Howitt, R., & Rodrigues, L. **(2019)**. Analyzing rainfall effects on agricultural income: Why timing matters. *Economics*, **20**(1): 1-14.

[37] Wang, R., Rejesus, R. M., Tack, J. B., & Aglasan, S. **(2021)**. Do higher temperatures influence how yields respond to increasing planting density?. *Agricultural and Resource Economics Review*, **50**(2): 273-295.

[38] Wei, W., Chen, L., & Fu, B. **(2009)**. Effects of rainfall change on water erosion processes in terrestrial ecosystems: a review. *Progress in Physical Geography*, **33**(3): 307-318.

[39] Wheeler, T. R., Craufurd, P. Q., Ellis, R. H., Porter, J. R., & Prasad, P. V. (**2000)**. Temperature variability and the yield of annual crops. *Agriculture*, *Ecosystems & Environment*, **82**(1-3): 159-167.

[40] World Bank. World Bank Climate Change Knowledge Portal. Summary | Climate Change Knowledge Portal. [online]. Available at: https://climateknowledgeportal.worldbank.org/country/bangladesh

[41] Yin, X. G., Olesen, J. E., Wang, M., Öztürk, I., & Chen, F. **(2016)**.Climate effects on crop yields in the Northeast Farming Region of China during 1961–2010. *Journal of Agricultural Science*, **154**(7): 1190-1208.

[42] Yirdew, A., &Yeshiwas, Y. **(2020)**. Effect of Rainfall and Temperature on Crop Production in Quarit District. *International Journal of Environmental Monitoring and Analysis*, **8**(4): 88-95.
doi: 10.11648/j.ijema.20200804.12

[43] You, L., Rosegrant, M. W., Wood, S., & Sun, D. **(2009)**. Impact of growing season temperature on wheat productivity in China. *Agricultural and Forest Meteorology*, **149**(6-7): 1009-1014.

[44] Zahoor, Z., Shahzad, K., & Mustafa, A. U. **(2022)**. Do Climate Changes influence the Agriculture Productivity in Pakistan? Empirical Evidence from ARDL Technique. *Forman Journal of Economic Studies*, 18(1).

[45] Zhao, C., Liu, B., Piao, S., Wang, X., Lobell, D. B., Huang, Y., Huang, M., Yao, Y., Bassu, S., Ciais, P., Durand, JL., Elliott, J., Ewert, F., Janssens, I. A., Li, T., Lin, E., Liu, Q., Martre, P., Müller, C., Peng, S., Peñuelas, J., Ruane, A.C., Wallach, D., Wang, T., Wu, D., Liu, Z., Zhu, Y., Zhu, Z., & Asseng, S. **(2017)**. Temperature increase reduces global yields of major crops in four independent estimates. *Proceedings of the National Academy of sciences*, **114**(35): 9326-9331.

[46] Zhu, T., Fonseca De Lima, C. F., & De Smet, I. **(2021)**. The heat is on: how crop growth, development, and yield respond to high temperature. *Journal of Experimental Botany*, **72**(21): 7359-7373.

□□

Nepal Journal of Mathematical Sciences (NJMS)
ISSN: 2738-9928 (*online*), 2738-9812 (*print*)
Vol. 4, No. 2, 2023 (August): 59-66
DOI: https://doi.org/10.3126/njmathsci.v4i2.59539

Research Article
Received Date: July 3, 2023
Accepted Date: August 17, 2023
Published Date: August 30, 2023

Collocation Computational Technique For Fractional Integro-Differential Equations

Olumuyiwa James Peter[1,2]*, Mfon O. Etuk[3] , Michael Oyelami Ajisope[4] , Christie Yemisi Ishola[5], Tawakalt Abosede Ayoola[6] , & Hasan S. Panigoro[7]

[1]*Dept. of Math. and Computer Sciences, University of Medical Sciences, Ondo City, Ondo State, Nigeria*
[2]*Dept. of Epidemiology and Biostatistics, School of Public Health, University of Medical Sc., Ondo City, Nigeria*
[3]*Department of Mathematics and Statistics, Federal Polytechnic Bida, Bida, Nigeria*
[4]*Department of Mathematics, Federal University,Oye-Ekiti, Nigeria*
[5]*Department of Mathematics National Open University Jabi, Abuja, Nigeria*
[6]*Department of Mathematics, Osun State University Osogbo, Osun State, Nigeria*
[7]*Biomathematics Research Group, Department of Mathematics, Faculty of Mathematics and Natural Sciences, Universitas Negeri Gorontalo, Bone Bolango* 96554, *Indonesia*

Email: [1,2]*peterjames*4*real@gmail.com*, [3]*etukmfon*16*@gmail.com*, [4]*micsope@gmail.com*, [5]*cyishola@gmail.com*, [6]*tawakalt.alade@uniosun.edu.ng*, [7]*hspanigoro@ung.ac.id*

∗Corresponding Author: Olumuyiwa James Peter

Abstract: *In this study, the collocation method and first-kind Chebyshev polynomials are used to investigate the solution of fractional integral-differential equations. In order to solve the problem, we first convert it to a set of linear algebraic equations, which are then solved by using matrix inversion to get the unknown constants. To demonstrate the theoretical findings, a few numerical examples are given and compared with other results obtained by other numerical techniques. Tables and figures are utilized to demonstrate the accuracy and effectiveness of the method. The outcomes demonstrate that the method improved accuracy more effectively while requiring less labor-intensive tasks.*

Keywords: *First-kind Chebyshev polynomials, Fractional integro-differential equations, Numerical technique, Matrix inversion.*

Introduction

The utilization of fractional integro-differential equations (IDEs) has significantly enhanced the modeling of real-world physical problems. Fractional calculus stands out as the most effective approach for capturing unusual phenomena. Illustrative instances encompass the dispersion of heat within a furnace, the spread of viruses, the positioning of satellites in space, and the memory characteristics of a system, among others. As commonly acknowledged, the collocation method hinges on the notion of approximating the precise solution of a given functional equation using an appropriate approximant selected from a finite-dimensional space, typically a piecewise algebraic polynomial. This approximant precisely satisfies the equation within a specific subset of the integration interval, known as the set of collocation points. [1–8]. According to [9–12], the concept of fractional calculus originated from a question over whether the definition of a derivative to an integer order n could be expanded to still hold true when is not an integer. This question was later forgotten because the formula for fractional derivatives is complex, making it difficult to work with ordinary pencil and paper. However, because we have computers and machines, complexity is no longer an issue.

The majority of fractional integro-diffrential equations (FIDEs) cannot be solved analytically; hence, extensive research has been done to find approximations and numerical methods of solving FIDEs.

Fractional Fredholm IDEs are solved using Laguerre polynomials in [13] and Bernstein polynomials as the basis function in [14, 15] to approximate the solution of FIDEs. In [16–18], collocation techniques were used to solve FIDEs using various basis functions. In [19], the Sumudu transform method and the Hermite spectral collocation method are used to solve FIDEs; When solving Volterra fractional IDEs, [20] used Bernstein modified homotopy perturbation approach; and in [21], approximate solutions of Volterra-Fredholm IDEs of fractional order are introduced. Using Galerkin method and Taylor series expansion, as well as a quick numerical algorithm based on the second kind of Chebyshev polynomials, [22, 23] investigated the numerical solution of fractional singular IDEs. [24, 25] used the least-squares method to solve FIDEs. [26] investigated the solution of linear fractional Fredholm integro-differential equation by using second kind Chebyshev wavelet and [27] employed numerical techiques for the solution of nonlinear integro-differential equations. [28] proposed and investigate a spectral approximation for numerical solutions of fractional integro-differential equations with weakly kernels. In order to eliminate the solution's singularity, the original equations are changed into an equivalent weakly singular Volterra integral equation by incorporating some relevant smoothing transformations. The above work serves as the motivation for the present study.

In this study, we present an innovative and precise numerical method for addressing fractional integro-differential equation systems. Our approach employs the collocation computational technique, utilizing first-kind Chebyshev polynomials as the basis functions for solving these fractional IDEs. This method results in less demanding work in terms of computational cost and better accuracy.

The rest of the paper is structured as follows: Section 2 deals with some relevant basic definitions, section 3 deals with the demonstration of the suggested method. Numerical examples which demonstrate the method's applicability and validity is given in section 4, section 5 deals with results and discussion of results. Finally, the conclusion of the study is presented in section 6. The general form of the class of problem considered in this work is given as:

$$D^{\alpha}\omega(s) = p(s)\omega(s)f(s) + \int_0^s K(s,t)\omega(t)dt; 0 \leq s,t \leq 1, \tag{1}$$

with the following supplementary conditions:

$$\omega^{(j)}(0) = \omega_j; j = 0,1,2,...n-1; n-1 < \alpha \leq n, n \in N. \tag{2}$$

Where $D^{\alpha}\omega(s)$ is the α^{th} Caputo fractional derivative of $\omega(s)$; $p(s)$, $f(s)$ and $K(s,t)$ are given smooth functions, ω_j are real constant, and s are real variables varying [0, 1] and $\omega(s)$ is the unknown function to be determined.

Some relevant basic definitions

Definition 1. Fractional integro-differential equation is an equation in which the unknown $\omega(s)$ appears under the integral sign and contain fractional derivatives $D^{\alpha}\omega(s)$ as well. According to [29], a standard fractional integro-differential equations is defined as:

$$D^{\alpha}\omega(s) = f(s) + \lambda \int_{g(s)}^{h(s)} K(s,t)\omega(s)dt,$$

where $K(s,t)$ is a function of two variables s and t known as the kernel or the nucleus of the integral equation, $g(s)$ and $h(s)$ are the limits of integration, λ is a constant parameter.

Definition 2. The Caputo Factional Derivative is defined as [30]

$$D^{\alpha}\omega(s) = \frac{1}{\Gamma(r-\alpha)} \int_0^s (s-t)^{r-\alpha-1}\omega^{r}(t)dt \tag{3}$$

n is non-negative integer such that, $r-1 < \alpha < n$. For example, if $0 < \alpha < 1$, the Caputo fractional derivative is

$$D^{\alpha}\omega(s) = \frac{1}{\Gamma(1-\alpha)} \int_0^s (s-t)^{r-\alpha-1}\omega^{'}(t)dt. \tag{4}$$

Definition 3. The Chebyshev polynomials [31] of degree r over $[0,1]$ is defined by the relation

$$\upsilon_r^*(s) = cos\left\{Cos^{-1}(2s-1)\right\}; n \geq 0.$$

The recurrence relation is given as,

$$\upsilon_{r+1}^*(s) = 2(2s-1)\upsilon_r^*(s) - \upsilon_{r-1}^*(s); r \geq 1,$$

where

$$\upsilon_0^*(s) = 1, \upsilon_1^*(s) = 2s-1.$$

Implementation of the method

The study considered an estimated solution represented in the form of first-kind Chebyshev polynomials:

$$\omega(s) = \sum_{i=0}^{r} \upsilon_i^*(s) a_i, \tag{5}$$

Here, the constants a_i for $i = 0(1)r$ represent the undisclosed coefficients of the shifted Chebyshev polynomials that need to be ascertained. The approach relies on the approximation of the unknown function $\omega(s)$ by employing equation (3) to equation (1). Additionally, substituting equation (5) into (1) yields,

$$\frac{1}{\Gamma(1-\alpha)} \int_0^s (s-t)^{r-\alpha-1} \frac{d^r}{dt^r} (\sum_{i=0}^{r} \upsilon_i^*(t)) a_i dt - p(x)\upsilon_i^*(s) - \int_0^s k(s,t)\upsilon_i^*(t)dt = f(s) \tag{6}$$

$$Let \quad \zeta(s) = \frac{1}{\Gamma(1-\alpha)} \int_0^s (s-t)^{r-\alpha-1} \frac{d^r}{dt^r} (\sum_{i=0}^{r} \upsilon_i^*(t)) a_i dt,$$

$$\eta(s) = \int_0^s k(s,t)\upsilon_i^*(t).$$

Substituting $\zeta(s)$ and $\eta(s)$ in equation (6), gives

$$\zeta(s) - p(s)\upsilon_i^*(x) - \eta(s) = f(s). \tag{7}$$

Collocating (7) at equally spaced point $s_i = a + \frac{(b-a)i}{r}$, $(i = 0(1)(r))$ results into linear system algebraic of equations in (r+1) unknown constants $a_i's$. Also, additional equations are also derived from (2) and are represented in matrix form:

$$\begin{pmatrix} Q_{11} & Q_{12} & Q_{13} & \cdots & \cdots & \cdots & Q_{1r} \\ Q_{21} & Q_{22} & Q_{23} & \cdots & \cdots & \cdots & Q_{2r} \\ \vdots & \vdots & \vdots & & \vdots & & \\ \vdots & \vdots & \vdots & & \vdots & & \\ Q_{m1} & Q_{m2} & Q_{m3} & \cdots & \cdots & \cdots & Q_{mr} \\ Q_{11}^0 & Q_{12}^0 & Q_{13}^0 & \cdots & \cdots & \cdots & Q_{1r}^0 \\ Q_{21}^1 & Q_{22}^1 & Q_{23}^1 & \cdots & \cdots & \cdots & Q_{2r}^1 \\ \vdots & \vdots & \vdots & & \vdots & & \\ \vdots & \vdots & \vdots & & \vdots & & \\ Q_{m1}^{r-1} & Q_{m2}^{r-1} & Q_{m3}^{r-1} & \cdots & \cdots & \cdots & Q_{mr}^{r-1} \end{pmatrix} \begin{pmatrix} a_0 \\ a_1 \\ \vdots \\ \vdots \\ \vdots \\ \vdots \\ \vdots \\ \vdots \\ a_r \end{pmatrix} = \begin{pmatrix} R_{11} \\ R_{22} \\ \vdots \\ \vdots \\ Rmr \\ R_{11}^0 \\ R_{22}^1 \vdots \\ \vdots \\ R_{mr}^{r-1} \end{pmatrix} \tag{8}$$

where Q_{is} and Q_{is}^{r-1} are the coefficients of a_{is} and R_{is} are values of $f(s_i)$
The matrix inversion approach is then used to solve the system of equations in order to obtain the unknown constants.

$$\begin{pmatrix} a_0 \\ a_1 \\ \vdots \\ \vdots \\ \vdots \\ \vdots \\ \vdots \\ \vdots \\ a_r \end{pmatrix} = \begin{pmatrix} Q_{11} & Q_{12} & Q_{13} & \cdots & \cdots & \cdots & Q_{1r} \\ Q_{21} & Q_{22} & Q_{23} & \cdots & \cdots & \cdots & Q_{2r} \\ \vdots & \vdots & \vdots & & \vdots & & \\ \vdots & \vdots & \vdots & & \vdots & & \\ Q_{m1} & Q_{m2} & Q_{m3} & \cdots & \cdots & \cdots & Q_{mr} \\ Q_{11}^0 & Q_{12}^0 & Q_{13}^0 & \cdots & \cdots & \cdots & Q_{1r}^0 \\ Q_{21}^1 & Q_{22}^1 & Q_{23}^1 & \cdots & \cdots & \cdots & Q_{2r}^1 \\ \vdots & \vdots & \vdots & & \vdots & & \\ \vdots & \vdots & \vdots & & \vdots & & \\ Q_{m1}^{r-1} & Q_{m2}^{r-1} & Q_{m3}^{r-1} & \cdots & \cdots & \cdots & Q_{mn}^{n-1} \end{pmatrix}^{-1} \begin{pmatrix} R_{11} \\ R_{22} \\ \vdots \\ \vdots \\ Rmr \\ R_{11}^0 \\ R_{22}^1 \vdots \\ \vdots \\ R_{mr}^{r-1} \end{pmatrix} \tag{9}$$

The sought-after approximate solution is derived through the solution of equation (9), followed by the insertion of the determined constant values into the assumed approximate solution.

Numerical examples with results and discussion

In this section, three numerical problems are presented to test the efficiency and simplicity of the suggested method. We perform the computation with the help of Maple 18 software.

Example 1. Consider the fractional Volterra integro-differential equation [32]

$$D^{\alpha}\omega(s) = \frac{s^2 e^s}{5}\omega(s) + \frac{6x^{2.25}}{\Gamma(3.25)} + \int_0^s t\,\omega(t)dt, \tag{10}$$

subject to $\omega(0) = 0$, for $\alpha = \frac{3}{4}$, the exact solution is $\omega(s) = s^3$. Applying the proposed technique for different values $\alpha = 0.65, 0.75, 0.85, 0.95$ respectively, we have the following approximate solutions.

$$\begin{aligned}
\omega(s) &= -3\times 10^{-11} + 3\times 10^{-9}s - 3\times 10^{-9}s^2 + 1.0000000001s^3\\
\omega(s) &= 2\times 10^{-11} - 0.027653591s + 0.153378821s^2 + 1.008595542s^3\\
\omega(s) &= -4\times 10^{-11} + 0.034398374s - 0.1426233144s^2 + 0.9903261389s^3\\
\omega(s) &= 1\times 10^{-10} + 0.07693657s - 0.277005541s^2 + 0.9802676637s^3
\end{aligned}$$

Example 2. Consider the fractional Fredholm Integro-differential equation [24]

$$D^{\alpha}\omega(s) = \omega(s) + \frac{8}{3\Gamma(0.5)}s^{1.5} - s^2 - \frac{1}{3}s^3 + \int_0^s \omega(t)dt \tag{11}$$

Subject to $\omega(0) = 0$, for $\alpha = \frac{1}{2}$, the exact solution is $\omega(s) = s^2$. Applying the proposed technique for different values $\alpha = 0.5, 0.65, 0.75, 0.85$ respectively, we have the following approximate solutions.

$$\begin{aligned}
\omega(s) &= 1.16826354\times 10^{-11} - 2.83\times 10^{-9}s + 1.0000000043s^2 - 3.573844333s\times 10^{-9}s^3\\
\omega(s) &= -7.2\times 10^{-11} - 0.0928995883s + 0.8741581798s^2 - 0.1738219395s^3\\
\omega(s) &= -2.7\times 10^{-11} - 0.1234325707s + 0.7798780867s^2 - 0.1944653643s^3\\
\omega(s) &= -1.9\times 10^{-11} - 0.1453990287s + 0.6972345157s^2 - 0.193248671s^3
\end{aligned}$$

Example 3. Consider the fractional Volterra Integro-differential equation [33].

$$D^{1/3}\omega(s) = \frac{3\sqrt{\pi}}{4\Gamma(\frac{13}{6})}s^{\frac{4}{3}} - \frac{2}{63}s^{\frac{9}{2}}(9+7s^2) + \int_0^s (st - s^2t^2)\omega(t)dt, \tag{12}$$

subject to initial conditions $\omega(0) = 0$ with the non-polynomial exact solution $\omega(s) = s^{\frac{3}{2}}$. Applying the proposed technique for different values $\alpha = 0.333333, 0.35, 0.45, 0.55, 0.65$ respectively, we have the following approximate solutions.

$$\begin{aligned}
\omega(s) &= 0.1593261367s - 0.5714144863s^7 + 2.492317064s^6 - 4.596356361s^5\\
&\quad + 4.735599489s^4 - 3.136374607s^3 + 1.917377053s^2 + 3.601\times 10^{-11}\\
\omega(s) &= 0.1468793779s + 2.342527711s^6 - 4.324730514s^5 + 4.464678275s^4\\
&\quad - 0.5389237087s^7 + 1.872627517s^2 - 2.979559309s^3 + 5.184\times 10^{-11}\\
\omega(s) &= 0.08760750183s + 1.540065996s^6 - 2.408\times 10^{11} - 2.864694840s^5\\
&\quad + 2.987408235s^4 - 0.3625998682s^7 + 1.590190322s^2 - 2.088567904s^3\\
\omega(s) &= 0.04859546975s + 0.9314622181s^6 - 1.745512022s^5 + 1.822787227s^4\\
&\quad - 0.2276405006s^7 + 1.310079152s^2 - 1.333448084s^3 - 5.874\times 10^{-11}\\
\omega(s) &= 0.02341269350s + 0.5076386080s^6 - 0.9551665749s^5 + 0.9749333984s^4\\
&\quad - 0.1336620560s^7 + 1.053811826s^2 - .7390996908s^3 + 2.425\times 10^{-11}
\end{aligned}$$

In this section, we present the results and discussion of the study. Tables 1-3 shows comparison of the absolute errors for examples 1-3, while figures 1-3 shows the graphical behaviour of the approximation solutions of example 1-3.

Table 1. Comparison of the absolute errors for example 1

s	Exact	Appro. Solu. n=3	Absol. Error at n =3	Absol. Error n=4 [32]
0.0	0.000	−0.00000000003000	$3.000E-11$	$3.000E-5$
0.2	0.008	0.00800000025800	$2.580E-10$	$3.710E-5$
0.4	0.064	0.06400000035000	$3.540E-10$	$2.400E-5$
0.6	0.216	0.21600000030000	$3.060E-10$	$8.400E-5$
0.8	0.512	0.51200000020000	$1.620E-10$	$4.300E-5$
0.1	1.000	1.00000000000000	$0.000E+00$	$2.800E-5$

Table 2. comparison of the absolute errors for example 2

s	Exact	Appro. Solu. at n=3	Absol. Error n=3	Absol. Error [24]
0.0	0.000	0.00000000001168	$1.168E-11$	$0.000E+00$
0.2	0.040	0.03999999958000	$4.169E-10$	$1.557E-04$
0.4	0.160	0.15999999930000	$6.970E-10$	$2.887E-03$
0.6	0.360	0.35999999890000	$1.000E-09$	$1.681E-02$
0.8	0.640	0.63999999860000	$1.498E-09$	$6.069E-02$
0.1	1.000	0.99999999740000	$2.362E-09$	$1.683E-01$

Table 3. comparison of the absolute errors for example 3

s	Exact	Appro. Solu. n=3	Absol. Error n=3	Absol. Error [33]
0.0	0.0000000000	0.00000000003601	$3.601E-11$	–
0.2	0.0894427191	0.08972763196000	$2.849E-04$	$9.8E-03$
0.4	0.2529822128	0.25321979130000	$2.376E-04$	$4.9E-03$
0.6	0.4647580015	0.46500112560000	$2.431E-04$	$3.2E-03$
0.8	0.7155417528	0.71583758500000	$2.958E-04$	$3.5E-03$
1.0	1.00000000000	1.00047428800000	$4.743E-04$	$3.5E-03$

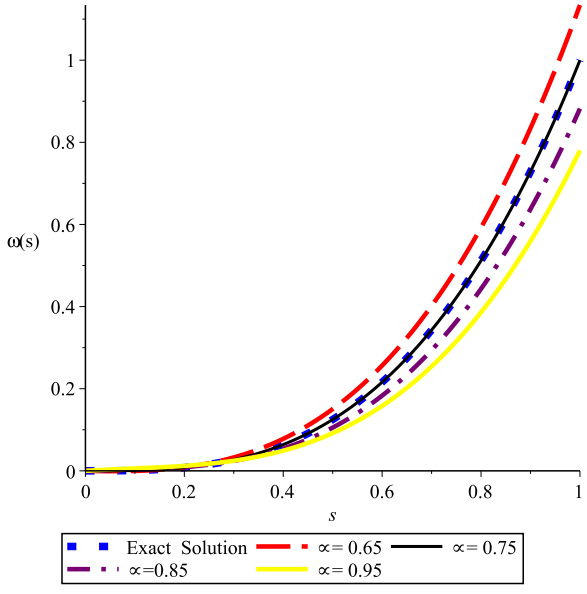

Figure 1. Showing the graphical behaviour of the approximation solutions of example 1

Using the collocation method via cubic B-spline wavelets, example 1 was solved by [31] at $n = 4$, [32] applied the homotopy analysis transform method for solving example 2, and example 3 was solved by [24] using three numerical schemes. By comparing the results, it can be seen from tables 1- 3 that the proposed method performed better when compared with the results obtained by other numerical methods. Also, figures 1-3, demonstrate that the approximate solutions are in excellent agreement with the exact solutions, and as the values of α increase the curve tend to zero.

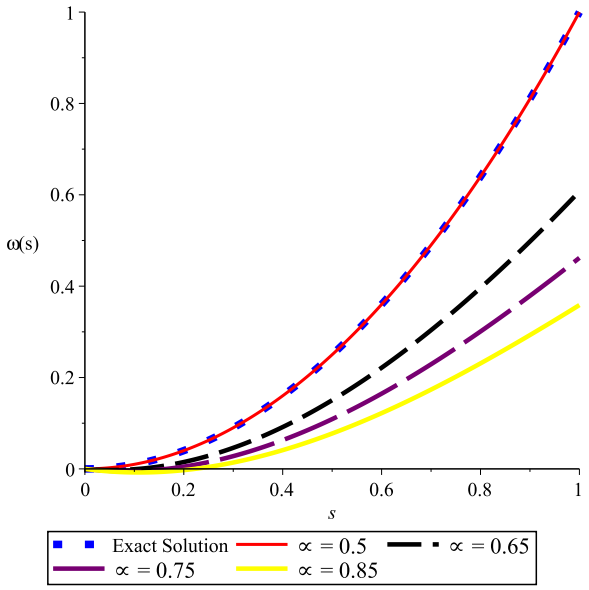

Figure 2. Showing the graphical behaviour of the approximation solutions of example 2

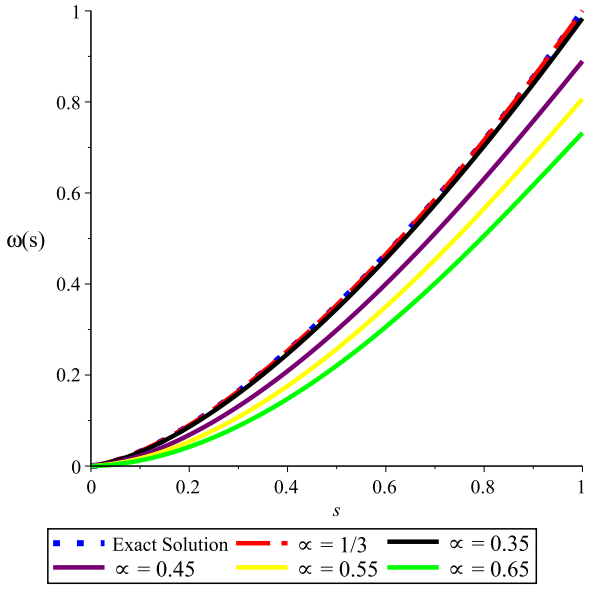

Figure 3. Showing the graphical behaviour of the approximation solutions of example 3

Conclusion

This work demonstrates a numerical solution of fractional integro-differential equations using collocation computational technique. Three examples are used to demonstrate the method's applicability and validity, and it appears that the method produces favourable results. We confirmed that the proposed method is in excellent agreement with the exact solutions, the solution obtained using the proposed method is more accurate than the obtained result in [24, 31, 32]. On the basis of this work, researchers can extend this technique to some other fractional integro-differential equations. The research will be valuable in multidisciplinary fields such as science and engineering, among others. It is helpful because it addresses the challenge of dealing with fractional order integro-differential problems by employing a simple collocation technique. The method has the advantage of being more accurate and requiring less computer time to run. Fractional integro-differential equations can be used to simulate many real life situations.

Data Availability Statement

No data associated in the manuscript.

Conflicts of interest

The authors declare that they have no conflict of interest concerning the publication of this manuscript.

References

[1] Peter, O. J., Yusuf, A., Ojo, M. M., Kumar, S., Kumari, N., and Oguntolu, F. A. **(2022)**. A mathematical model analysis of meningitis with treatment and vaccination in fractional derivatives. *International Journal of Applied and Computational Mathematics*, 8(3):117.

[2] Peter, O. J., Oguntolu, F. A., Ojo, M. M., Olayinka Oyeniyi, A., Jan, R., and Khan, I. **(2022)**. Fractional order mathematical model of monkeypox transmission dynamics. *Physica Scripta*, 97(8):084005.

[3] Peter, O. J. **(2020)**. Transmission dynamics of fractional order brucellosis model using caputo–fabrizio operator. *International Journal of Differential Equations*, 2020:1–11.

[4] Peter, O. J., Yusuf, A., Oshinubi, K., Oguntolu, F. A., Lawal, J. O., Abioye, A. I., and Ayoola, T. A. **(2021)**. Fractional order of pneumococcal pneumonia infection model with caputo fabrizio operator. *Results in Physics*, 29:104581.

[5] Oyedepo, T., Adebisi, A. F., Tayo, R. M., Adedeji, J. A., Ayinde, M. A., and Peter, O. J. **(2020)**. Perturbed least squares technique for solving volterra fractional integro-differential equations based on constructed orthogonal polynomials. *J. Math. Comput. Sci.*, 11(1):203–218.

[6] Uwaheren, O., Adebisi, A., Olotu, O., Etuk, M., and Peter, O. **(2021)**. Legendre galerkin method for solving fractional integro-differential equations of fredholm type. *The Aligarh Bulletin of Mathematics*, 40(1):1–13.

[7] Adebisi, A., Okunola, K., Raji, M., Adedeji, J., and Peter, O. **(2021)**. Galerkin and perturbed collocation methods for solving a class of linear fractional integro-differential equations. *The Aligarh Bulletin of Mathematics*, 40(2):45–57.

[8] Abbaszadeh, M. and Dehghan, M. **(2020)**. A meshless numerical investigation based on the rbf-qr approach for elasticity problems. *AUT Journal of Mathematics and Computing*, 1(1):1–15.

[9] Caputo, M. **(1967)**. Linear models of dissipation whose q is almost frequency independent—ii. *Geophysical Journal International*, 13(5):529–539.

[10] Loverro, A. **(2004)**. Fractional calculus: History. *Definitions and Applications for the Engineer*, 84.

[11] Jaradat, H., Awawdeh, F., and Rawashdeh, E. **(2011)**. Analytic solution of fractional integro-differential equations. *Annals of the University of Craiova-Mathematics and Computer Science Series*, 38(1):1–10.

[12] Setia, A., Liu, Y., and Vatsala, A. **(2014)**. Numerical solution of fredholm-volterra fractional integro-differential equations with nonlocal boundary conditions. *Journal of fractional calculus and applications*, 5(2):155–165.

[13] Daşcıoğlu, A. and Bayram, D. V. **(2019)**. Solving fractional fredholm integro-differential equations by laguerre polynomials.

[14] Huang, L., Li, X.-F., Zhao, Y., and Duan, X.-Y. **(2011)**. Approximate solution of fractional integro-differential equations by taylor expansion method. *Computers & Mathematics with Applications*, 62(3):1127–1134.

[15] Nanware, J., Goud, P. M., and Holambe, T. **(2020)**. Solution of fractional integro-differential equations by bernstein polynomials. *Malaya Journal of Matematik*, 5(1):581–586.

[16] Dilkel, V. and Aysegül, D. **(2018)**. Applied collocation method using laguerre polynomials as the basis functions. *Advances in difference equations a Springer Open Journal*, pages 1–11.

[17] Rawashdeh, E. **(2006)**. Numerical solution of fractional integro-differential equations by collocation method. *Applied mathematics and computation*, 176(1):1–6.

[18] Ma, X. and Huang, C. **(2014)**. Spectral collocation method for linear fractional integro-differential equations. *Applied Mathematical Modelling*, 38(4):1434–1448.

[19] Amer, Y., Mahdy, A., and Youssef, E. **(2018)**. Solving fractional integro-differential equations by using sumudu transform method and hermite spectral collocation method. *Computers, Materials and Continua*, 54(2):161–180.

[20] Oyedepo, T., Adebisi, A., Raji, M., Ajisope, M., Adedeji, J., Lawal, J., and Uwaheren, O. **(2021)**. Bernstein modified homotopy perturbation method for the solution of volterra fractional integro-differential equations,". *Pasifi Journal of Science and Technology*, 22(1):30–36.

[21] Alkan, S. and Hatipoglu, V. F. **(2017)**. Approximate solutions of volterra-fredholm integro-differential equations of fractional order.

[22] Mohamed, D. **(2014)**. Numerical solution of fractional singular integrodifferential equation using taylor series expansion and galerkin method. *Journal of Pure and Applied Mathematics*, pages 129–143.

[23] Nemati, S., Sedaghat, S., and Mohammadi, I. **(2016)**. A fast numerical algorithm based on the second kind chebyshev polynomials for fractional integro-differential equations with weakly singular kernels. *Journal of Computational and Applied Mathematics*, 308:231–242.

[24] Mohamed, S., Muteb, R., and Refah, A. **(2016)**. Solving fractional integro-differential equations by homotopy analysis transform method. *International Journal of pure and Applied Mathematics*, 106(4):1037–1055.

[25] Abdulmutallab, D. S. M. **(2014)**. Numerical solution of fractional integro-differential equations by least squares method and shifted chebyshev polynomial. *Hindawi Publishing Corporation*, 2014:5.

[26] Setia, A., Liu, Y., and Vatsala, A. S. **(2014)**. Solution of linear fractional fredholm integro-differential equation by using second kind chebyshev wavelet. In *2014 11th International Conference on Information Technology: New Generations*, pages 465–469. IEEE.

[27] Sharif, A., Hamoud, A., and Ghadle, K. **(2020)**. Solving nonlinear integro-differential equations by using numerical techniques. *Acta Univ. Apulensis*, 61:45–53.

[28] Shi, X. et al. **(2022)**. Spectral collocation methods for fractional integro-differential equations with weakly singular kernels. *Journal of Mathematics*, 2022.

[29] Wazwaz, A.-M. **(2010)**. *Partial differential equations and solitary waves theory*. Springer Science & Business Media.

[30] Peter, O. J., Shaikh, A. S., Ibrahim, M. O., Nisar, K. S., Baleanu, D., Khan, I., and Abioye, A. I. **(2021)**. Analysis and dynamics of fractional order mathematical model of covid-19 in nigeria using atangana-baleanu operator.

[31] Mason, J. C. and Handscomb, D. C. **(2002)**. *Chebyshev polynomials*. Chapman and Hall/CRC.

[32] Maleknejad, K., Sahlan, M. N., and Ostadi, A. **(2013)**. Numerical solution of fractional integro-differential equation by using cubic b-spline wavelets. In *Proceedings of the World Congress on Engineering*, volume 1, pages 3–5.

[33] Kumar, K., Pandey, R. K., and Sharma, S. **(2017)**. Comparative study of three numerical schemes for fractional integro-differential equations. *Journal of Computational and Applied Mathematics*, 315:287–302.

Nepal Journal of Mathematical Sciences (NJMS)
ISSN: 2738-9928 (*online*), 2738-9812 (*print*)
Vol. 4, No. 2, 2023 (August): 67-76
DOI: https://doi.org/10.3126/njmathsci.v4i2.59538

Research Article
Received Date: July 3, 2023
Accepted Date: August 17, 2023
Published Date: August 30, 2023

Numerical Analysis of Fractional-Order Diffusion Equation

Jeevan Kafle[1] , Deepak Bahadur Bist[1] , & Shankar Pariyar[1,2,*]

[1] *Central Department of Mathematics, Tribhuvan University, Kathmandu, Nepal*
[2] *Trichandra Multiple Campus , Tribhuvan university, Kathmandu, Nepal*
* Correspondence to: Shankar Pariyar
Email: *shankar.pariyar@trc.tu.edu.np*

Abstract: *Fractional diffusion equations serve as fundamental tools for addressing the non-local properties and long range memory effects that observed in diffusion processes within complex media. This works focuses on solving non-integer order (fractional) diffusion equations by employing the natural decomposition approach which gives the solution in series form. Some numerical examples of one dimensional and two dimensional fractional order diffusion equations are presented to demonstrate its application and obtained solutions are interpreted with the help of the computational software. Compared to other analytical and numerical techniques, the fractional natural decomposition method demonstrates advantages such as reduced computational complexity and faster convergence. Additionally, it can also be readily applied to address linear as well as non-linear problems. The application of natural decomposition approach to solve non-integer order (fractional) diffusion equations provides the most comprehensive understanding of the anomalous diffusion process occurring within complex media, as the fractional model accurately captures the non-local properties and long-range memory effects associated with such processes. To support the technique, we have taken into account a few problems and analyzed their solution by fractional natural decomposition method (FNDM) with solutions for the classical diffusion equations. Keywords: Fractional derivative, Riemann-Liouville (R-L) derivative, Caputo derivative, natural transform, Adomian decomposition, Fractional diffusion.*

Keywords: *Fractional derivative, Riemann-Liouville (R-L) derivative, Caputo derivative, Natural transform, Adomian decomposition, Fractional diffusion*.

1 Introduction:

Diffusion is a common process that is essential to many fields of science, including physics, chemistry, biology, and engineering [15]. It describes the process by which the particles, energy, or other quantities spread and mix in a medium due to random thermal motion. Fick's law, which bears the name of the German scientist Adolf Fick and was created in the middle of the 19th century, serves as the foundation for the traditional definition of diffusion [14]. The traditional explanation of diffusion, based on Fick's law, offers a fundamental framework for understanding the spreading of substances in homogeneous systems [14]. However, in recent years, researchers have uncovered anomalous diffusion phenomena that deviate from the classical diffusion behavior, exhibiting peculiar characteristics, such as non-local behavior, memory effects, and long-range interaction phenomena [15, 20]. To capture and describe these anomalous diffusion processes, a more generalized mathematical framework is required. This is where fractional calculus and the fractional diffusion process come into play [3, 15]. By extending the idea of differentiation and integration to non-integer orders, fractional calculus makes it possible to describe non-local and long-range interaction phenomena [3, 13, 15]. The fractional diffusion equation arises from the incorporation of fractional derivatives into the classical diffusion equation, providing a mathematical framework to describe and analyze complex diffusion phenomena in fractal media, heterogeneous environments, and systems with memory effect. This capability attracted significant interest from a variety of scientific disciplines [15, 19]. Within the realm of anomalous diffusion, the fractional diffusion equations have been

independently developed by considering various non-integer orders (fractional) derivatives in time, space, and both time-space domains [19]. The time-fractional diffusion equation, inspired by studies by Metzler et al. [10], introduces a fractional derivative in the time domain by considering the continuous time random walk. This equation extends the traditional diffusion equation incorporating time derivative of fractional order, enabling the description of memory effects and long-range correlations observed in time-dependent diffusion processes. Similarly, the space fractional diffusion equation, as described in works by Meerschaert et al. (2006), incorporates a fractional order spatial derivative. It allows for the characterization of diffusion processes in non-homogeneous media and fractal geometries. The equation captures sub-diffusion or super-diffusion phenomena, where the spreading behavior is slower or faster than classical diffusion, respectively, in spatial domains [8]. Furthermore, the space-time non-integer (fractional) order diffusion equation, studied by Gorenflo et al. [4], and Meerschaert et al. [9] combines fractional derivatives in both time and space domains. This is particularly relevant for describing anomalous diffusion in highly heterogeneous environments, where temporal and spatial correlations play significant roles.

Several fundamental methods have been developed by renowned mathematicians for solving non-integer order diffusion equations. Abbasbandy et al. [1] proposed the variational iteration method (VIM) to construct an approximation solution. Lin et al. [7] employed the finite difference scheme method (FDSM) for constructing approximations of fractional diffusion. Additionally, other approaches like homotopy analysis method (HAM) [5], homotopy perturbation transform method (HPTM) [6], natural decomposition method (NDM), [11], Adomian decomposition method (ADM) [18], and so on have been utilized in this context [15]. In this this work, we utilize the natural decomposition method to solve the non-integer order diffusion equations. The natural transform with Adomian decomposition approach for non-linear partial differential equations was first used by Rawashdesh and Matima [16]. Through our investigation, we reveal the numerical solution to the time-fractional diffusion equation, which is a critical step toward developing a general framework to model anomalous diffusion phenomena. This framework captures the intricacies of long-range correlations, memory effects, and time-dependent system dynamics[19, 20].

1.1 Riemann-Liouville (R-L) Derivative

The Riemann-Liouville (R-L) derivative for non-integer order is defined in terms of the fractional integration called R-L fractional integral [3]. The R-L integral of $\phi(\xi)$, $\xi \geq -1$ of non-integer order $\alpha > 0$ is formulated as [3, 15]

$$ {}_aI_\xi^\alpha(\phi(\xi)) = \frac{1}{\Gamma(\alpha)} \int_a^\xi \frac{\phi(\tau)}{(\xi-\tau)^{1-\alpha}} d\tau, \quad \alpha > 0, \quad \xi > a \tag{1} $$

where Γ is gamma function. With fractional integral, R-L derivative is given by

$$ {}_a^R D_\xi^\alpha(\phi(\xi)) = \begin{cases} \frac{1}{\Gamma(p-\alpha)} \frac{d^p}{d\xi^p} \int_a^\xi \frac{\phi(\tau)}{(\xi-\tau)^{1-p+\alpha}} d\tau, & \text{if } \alpha \in \mathbb{R}^+, \ p-1 < \alpha < p \\ \frac{d^p}{d\xi^p}\phi(\xi), & \text{if } \alpha = p \end{cases} $$

1.2 Caputo Derivative

The Caputo definition is defined by interchanging the order of derivative and fractional integration [3].

$$ {}_a^C D_\xi^\alpha(\phi(\xi)) = \begin{cases} \frac{1}{\Gamma(p-\alpha)} \int_a^\xi \frac{\phi^{(p)}(u)}{(\xi-u)^{1-p+\alpha}} du & \text{if } \alpha \in \mathbb{R}^+, \ p-1 < \alpha < p \\ \phi^{(p)}(\xi) & \text{if } \alpha = p \in \mathbb{N} \end{cases} $$

1.3 Natural Transform

The fractional natural transform of a function $\phi(\tau)$ is given by [2, 17]

$$\mathscr{N}^{+}[\phi(\tau)] = \psi(s,u) = \int_0^{\infty} e^{-s\tau}\phi(u\tau)d\tau, \quad s,u \in \mathbb{R} \tag{2}$$

where the variables s and u represent the transformation variable. The definition of the inverse of natural transform for a function is [17];

$$\mathscr{N}^{-}[\psi(s,u)] = \phi(\tau) = \frac{1}{2\pi i}\int_{a-i\infty}^{a+i\infty} e^{s\tau}\psi(s,u)ds \tag{3}$$

where the variables s and u represent the transformation variable, a is a real constant, and the integration is taken along line $Re(P) = a$ in a complex plane $P = \xi + i\tau$.

1.4 Adomian Decomposition Method (ADM)

Consider a non-linear ordinary fractional differential equation [11],

$${}_a^c D_\tau^\alpha \phi(\tau) + R\phi(\tau) + G\phi(\tau) = \psi(\tau),\ p-1 < \alpha \le p,\ \ p \in \mathbb{N} \tag{4}$$

with initial conditions

$$\phi^{(j)}(0) = \frac{d^j\phi(0)}{d\tau^j},\ j = 0,1,...,p-1.$$

${}_a^c D_\tau^\alpha$ denote the fractional derivative with respect to τ in Caputo sense and it is an invertible linear operator, R is the operator for liner remainders, G represent the non-linear operator that is considered as analytic, and $\psi(\tau)$ is a known function. As per ADM algorithm, the solution of (4) is an infinite series

$$\phi(\tau) = \sum_{i=0}^{\infty}\phi_i(\tau). \tag{5}$$

Taking the fractional integral (inverted operator of ${}_a^c D_\tau^\alpha$) on both side of (5),

$$I_\tau^\alpha\, {}_a^c D_\tau^\alpha \phi(\tau) + I_\tau^\alpha R\phi(\tau) + I_\tau^\alpha G\phi(\tau) = I_\tau^\alpha \psi(\tau) \tag{6}$$

Using the initial condition,

$$\phi(\tau) = \sum_{j=0}^{p-1}\frac{\tau^j}{j!}\phi^{(j)}(0) + I_\tau^\alpha\psi(\tau) - I_\tau^\alpha R\phi(t) - I_t^\alpha G\phi(\tau) \tag{7}$$

and the expression for the non linear expression $G\phi(\tau)$ is given by

$$G\phi(\tau) = \sum_{k=0}^{\infty} A_k(\tau) \tag{8}$$

where $A_k(\tau)$,depending on $\phi_0, \phi_1...$, are Adomian polynomials and can be calculated for non-linearity $G\phi = f(\phi(\tau))$ as,

$$A_k(\tau) = \frac{1}{k!}\left[\frac{d^k}{d\lambda^k} f\left(\sum_{i=0}^{k}\phi_i(\tau)\lambda^i\right)\right]_{\lambda=0} \tag{9}$$

From (5), (8) and (9), equation (7) becomes;

$$\sum_{n=0}^{\infty}\phi_n(\tau) = \sum_{j=0}^{p-1}\frac{\tau^j}{j!}\phi^{(j)}(0) + I_\tau^\alpha\left[\phi(\tau)\right] - I_\tau^\alpha\left[R\sum_{n=0}^{\infty}\phi_n(\tau)\right] - I_\tau^\alpha\left[\sum_{k=0}^{\infty}A_k(\tau)\right] \tag{10}$$

Then, from (10), we find the iterative scheme and then the approximate solution to equation (5) is the sum of thus obtained term.

2 Natural Decomposition Method (NDM)

The fractional natural transform method (FNTM) and Adomian decomposition method (ADM) are combined to create a new method natural decomposition method (NDM) [12]. Let $\Omega = S \times I$, where $S = [0, L]$ be spatial domain and $I = [0, T]$ be time domain. Then an equation of one-dimensional time-fractional diffusion is [7, 11];

$$ {}^{c}D_{\tau}^{\alpha}\mathscr{U}(\xi,\tau) = K\frac{\partial^2 \mathscr{U}(\xi,\tau)}{\partial \xi^2} + \psi(\xi,\tau), \quad (\xi,\tau) \in \Omega, \;\; 0 < \alpha \leq 1 \tag{11} $$

with initial and boundary conditions

$$ \mathscr{U}(\xi,0) = h(\xi), \;\; 0 \leq \xi \leq L \tag{12} $$

$$ \mathscr{U}(0,\tau) = \mathscr{U}(L,\tau) = 0, \;\; \tau > 0 \tag{13} $$

where ${}^{c}D_{\tau}^{\alpha} = \dfrac{\partial^{\alpha}}{\partial \tau^{\alpha}}$ is non-integer order (fractional) derivative in Caputo sense, $\mathscr{U}(\xi,\tau)$ is solute concentration , $\psi(\xi,\tau)$ is the source function, and K represents the diffusion coefficient (constant or function of ξ) which controls the anomalous diffusion in complex medium.
The solution of non-integer order diffusion equation by NDM, taking natural transform of (11)

$$ \mathscr{N}^{+}\left[{}^{c}D_{\tau}^{\alpha}\mathscr{U}(\xi,\tau)\right] = \mathscr{N}^{+}\left[K\frac{\partial^2 \mathscr{U}(\xi,\tau)}{\partial \xi^2} + \psi(\xi,\tau)\right] \tag{14} $$

Using the natural transform's differentiation property

$$ \begin{aligned} \left(\frac{s}{u}\right)^{\alpha}\mathscr{N}^{+}\left[\mathscr{U}(\xi,\tau)\right] - \frac{s^{\alpha-1}}{u^{\alpha}}\mathscr{U}(\xi,0) &= \mathscr{N}^{+}\left[K\frac{\partial^2 \mathscr{U}}{\partial \xi^2} + \psi(\xi,\tau)\right] \\ \implies \mathscr{N}^{+}\left[\mathscr{U}(\xi,\tau)\right] &= \frac{1}{s}h(\xi) + \frac{u^{\alpha}}{s^{\alpha}}\mathscr{N}^{+}\left[K\frac{\partial^2 \mathscr{U}}{\partial \xi^2} + \psi(\xi,\tau)\right] \end{aligned} $$

$\mathscr{U}(\xi,\tau)$ can be written as an infinite series by using the ADM technique.

$$ \mathscr{U}(\xi,\tau) = \sum_{k=0}^{\infty}\mathscr{U}_k(\xi,\tau) = \sum_{k=0}^{\infty}\mathscr{U}_k \tag{15} $$

The Adomian polynomials infinite series is used in this problem to represent any existent non-linear components

$$ G\mathscr{U}(\xi,\tau) = \sum_{k=0}^{\infty}A_k \tag{16} $$

where $A_k = \dfrac{1}{k!}\left[\dfrac{d^k}{d\lambda^k}G\left[\sum_{k=0}^{\infty}(\lambda^k \mathscr{U}_k)\right]\right]_{\lambda=0}$ $k = 0, 1, 2...$, are adomian polynomials
From equation (15) and (16)

$$ \mathscr{N}^{+}\left[\sum_{k=0}^{\infty}\mathscr{U}_k\right] = \frac{1}{s}h(\xi) + \frac{u^{\alpha}}{s^{\alpha}}\mathscr{N}^{+}\left[K\sum_{k=0}^{\infty}\frac{\partial^2 \mathscr{U}_k}{\partial \xi^2} + \psi(\xi,\tau)\right] $$

Using the Adomian decomposition and inverse natural transform,
$\mathscr{U}_0(\xi,\tau) = \mathscr{N}^{-}\left[\dfrac{1}{s}h(\xi)\right] + \mathscr{N}^{-}\left[\dfrac{u^{\alpha}}{s^{\alpha}}\mathscr{N}^{+}\left[\psi(\xi,\tau)\right]\right]$ and $\mathscr{U}_{k+1}(\xi,\tau) = \mathscr{N}^{-}\left[\dfrac{u^{\alpha}}{s^{\alpha}}\mathscr{N}^{+}\left[K\dfrac{\partial^2 \mathscr{U}_k}{\partial \xi^2}\right]\right]$
for k=0,1,2,..., the NDM method's solution is derived by substituting the values of $\mathscr{U}_k(\xi,\tau)$ in (15)

3 Result and Discussion

In this section, we use the NDM approach to illustrate a few time-fractional diffusion equations.

Ex.1. Consider the following fractional diffusion equation in one dimension [11]

$$\frac{\partial^{\alpha}\mathscr{U}(\xi,\tau)}{\partial\tau^{\alpha}}=\frac{\xi^{2}}{2}\frac{\partial^{2}\mathscr{U}(\xi,\tau)}{\partial\xi^{2}},\quad(\xi,\tau)\in\Omega,\quad 0<\alpha\leq 1 \tag{17}$$

with initial condition

$$\mathscr{U}(\xi,0)=\xi^{2},\ \ 0\leq\xi\leq 2 \tag{18}$$

By employing natural transform on (18)

$$\mathscr{N}^{+}\left[\frac{\partial^{\alpha}\mathscr{U}(\xi,\tau)}{\partial\tau^{\alpha}}\right]=\mathscr{N}^{+}\left[\frac{\xi^{2}}{2}\frac{\partial^{2}\mathscr{U}}{\partial\xi^{2}}\right]$$

Using the differentiation property of natural transform,

$$\mathscr{N}^{+}\left[\mathscr{U}(\xi,\tau)\right]=\frac{1}{s}\mathscr{U}(\xi,0)+\frac{u^{\alpha}}{s^{\alpha}}\mathscr{N}^{+}\left[\frac{\xi^{2}}{2}\frac{\partial^{2}\mathscr{U}}{\partial\xi^{2}}\right]=\frac{\xi^{2}}{s}+\frac{u^{\alpha}}{s^{\alpha}}\mathscr{N}^{+}\left[\frac{\xi^{2}}{2}\frac{\partial^{2}\mathscr{U}}{\partial\xi^{2}}\right] \tag{19}$$

Then by ADM algorithm, the solution $\mathscr{U}(\xi,\tau)$ can be expressed in infinite series as

$$\mathscr{U}(\xi,\tau)=\sum_{k=0}^{\infty}\mathscr{U}_{k}(\xi,\tau)=\sum_{k=0}^{\infty}\mathscr{U}_{k} \tag{20}$$

From equation (19) and (20)

$$\mathscr{N}^{+}\left[\sum_{k=0}^{\infty}\mathscr{U}_{k}(\xi,\tau)\right]=\frac{\xi^{2}}{s}+\frac{u^{\alpha}}{s^{\alpha}}\mathscr{N}^{+}\left[\frac{\xi^{2}}{2}\sum_{k=0}^{\infty}\frac{\partial^{2}\mathscr{U}_{k}}{\partial\xi^{2}}\right]$$

Taking inverse natural transform

$$\sum_{k=0}^{\infty}\mathscr{U}_{k}(\xi,\tau)=\mathscr{N}^{-}\left[\frac{\xi^{2}}{s}\right]+\mathscr{N}^{-}\left[\frac{u^{\alpha}}{s^{\alpha}}\mathscr{N}^{+}\left[\frac{\xi^{2}}{2}\sum_{k=0}^{\infty}\frac{\partial^{2}\mathscr{U}_{k}}{\partial\xi^{2}}\right]\right]$$

By ADM algorithm

$$\mathscr{U}_{0}(\xi,\tau)=\mathscr{N}^{-}\left[\frac{\xi^{2}}{s}\right]=\xi^{2}$$

and

$$\mathscr{U}_{k+1}(\xi,\tau)=\mathscr{N}^{-}\left[\frac{u^{\alpha}}{s^{\alpha}}\mathscr{N}^{+}\left[\frac{\xi^{2}}{2}\frac{\partial^{2}\mathscr{U}_{k}}{\partial\xi^{2}}\right]\right],\quad for\quad k=0,1,2,...$$

For all values of $k=0,1,2,...$, equation (20) becomes;

$$\mathscr{U}(\xi,\tau)\ \ =\ \ \xi^{2}\left(1+\frac{\tau^{\alpha}}{\Gamma(\alpha+1)}+\frac{\tau^{2\alpha}}{\Gamma(2\alpha+1)}+\frac{\tau^{3\alpha}}{\Gamma(3\alpha+1)}+\frac{\tau^{4\alpha}}{\Gamma(4\alpha+1)}+...\right) \tag{21}$$

Using computational software, figure 1 shows that the three-dimensional plot that visually represents the NDM solution for different values of the variable α. On the other hand, figure 2 presents a two-dimensional plot illustrating the solution for various values of α specifically when τ is fixed at 1. Notably, by observing both figures, it becomes evident that as the value of α progressively approaches 1, the solution curve increasingly converges towards the curve corresponding to $\alpha=1$. The figures provide clear evidence that the non-integer (fractional) order diffusion equation effectively captures the diffusive

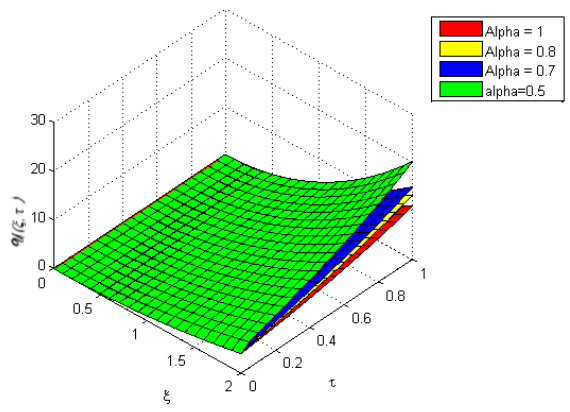

Figure 1: 3D plot of numerical solution of example 1 for different values α

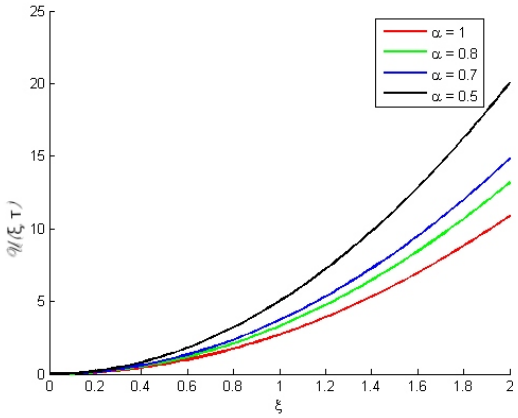

Figure 2: 2D plot of solution of example 1 at $\tau = 1$

behavior in continuous time. This property enables it to accurately represent the non-local nature and long-range memory effects observed in anomalous diffusion processes occurring within complex medium.

When $\alpha = 1$, (21) gives;

$$\mathscr{U}(\xi,\tau) \quad = \quad \xi^2\left(1+\tau+\frac{\tau^2}{2!}+\frac{\tau^3}{3!}+\frac{\tau^4}{4!}+...\right)$$

This is the somewhat like exact solution in closed form

$$\mathscr{U}(\xi,\tau) = \xi^2 e^{\tau}$$

By computational software,

Figure 3 shows that three-dimensional plot illustrating the error of the solution across different values of the variable α. This plot visually demonstrates how the error changes with varying α. On the other hand, Figure 4 presents a two-dimensional graph that specifically focuses on the error of the solution for different α values when τ is fixed at 1. Notably, both figures provide clear evidence that as α approaches 1, the corresponding error consistently decreases. This observation suggests a strong correlation between the proximity of α to 1 and the reduction of error in the solution.

Ex.3. Consider following two dimensional fractional diffusion equation [11]

$$\frac{\partial^{\alpha}\mathscr{U}(\xi,y,\tau)}{\partial\tau^{\alpha}} = \frac{y^2}{2}\frac{\partial^2\mathscr{U}(\xi,y,\tau)}{\partial\xi^2} + \frac{\xi^2}{2}\frac{\partial^2\mathscr{U}(\xi,y,\tau)}{\partial y^2}, \quad (\xi,y,\tau)\in\Omega, \quad 0<\alpha\leq 1 \tag{22}$$

with initial

$$\mathscr{U}(\xi,y,0) = y^2, \quad 0\leq y\leq 1 \tag{23}$$

Applying the natural transform on both side of (23)

$$\mathscr{N}^{+}\left[\frac{\partial^{\alpha}\mathscr{U}}{\partial\tau^{\alpha}}\right] = \mathscr{N}^{+}\left[\frac{y^2}{2}\frac{\partial^2\mathscr{U}}{\partial\xi^2}+\frac{\xi^2}{2}\frac{\partial^2\mathscr{U}}{\partial y^2}\right]$$

By differentiation property of natural transform and using initial condition

$$\mathscr{N}^{+}\left[\mathscr{U}(\xi,y,\tau)\right] = \frac{y^2}{s}+\frac{u^{\alpha}}{s^{\alpha}}\mathscr{N}^{+}\left[\frac{y^2}{2}\frac{\partial^2\mathscr{U}}{\partial\xi^2}+\frac{\xi^2}{2}\frac{\partial^2\mathscr{U}}{\partial y^2}\right] \tag{24}$$

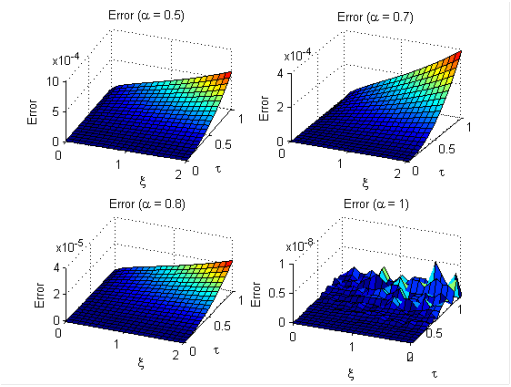

Figure 3: Error plots of the solution by NDM for different α in 3D.

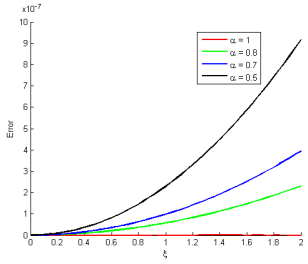

Figure 4: Error plots of the solution by NDM for $\tau = 1$ in 2D.

Using ADM algorithm, solution $\mathscr{U}(\xi, y, \tau)$ is given by infinite series

$$\mathscr{U}(\xi, y, \tau) = \sum_{k=o}^{\infty} \mathscr{U}_k(\xi, y, \tau) \tag{25}$$

From equation (24) and (25)

$$\mathscr{N}^+\left[\sum_{k=o}^{\infty} \mathscr{U}_k\right] = \frac{y^2}{s} + \frac{u^\alpha}{s^\alpha}\mathscr{N}^+\left[\frac{y^2}{2}\sum_{k=0}^{\infty}\frac{\partial^2 \mathscr{U}_k}{\partial \xi^2} + \frac{\xi^2}{2}\sum_{k=0}^{\infty}\frac{\partial^2 \mathscr{U}_k}{\partial y^2}\right]$$

Taking inverse natural transform

$$\sum_{k=o}^{\infty} \mathscr{U}_k = \mathscr{N}^-\left[\frac{y^2}{s}\right] + \mathscr{N}^-\left[\frac{u^\alpha}{s^\alpha}\mathscr{N}^+\left[\frac{y^2}{2}\sum_{k=0}^{\infty}\frac{\partial^2 \mathscr{U}_k}{\partial \xi^2} + \frac{\xi^2}{2}\sum_{k=0}^{\infty}\frac{\partial^2 \mathscr{U}_k}{\partial y^2}\right]\right]$$

By ADM algorithm

$$\mathscr{U}_0(\xi, y, \tau) = \mathscr{N}^-\left[\frac{y^2}{s}\right] = y2$$

and

$$\mathscr{U}_{k+1}(\xi, y, \tau) = \mathscr{N}^-\left[\frac{u^\alpha}{s^\alpha}\mathscr{N}^+\left[\frac{y^2}{2}\frac{\partial^2 \mathscr{U}_k(\xi,\tau)}{\partial \xi^2} + \frac{\xi^2}{2}\sum_{k=0}^{\infty}\frac{\partial^2 \mathscr{U}_k}{\partial y^2}\right]\right], \quad for \quad k = 0, 1, 2, ...$$

putting different values of k

$$\mathscr{U}_{2k-1}(\xi, y, \tau) = \xi^2 \frac{\tau^{(2k-1)\alpha}}{\Gamma((2k-1)\alpha + 1)}, \quad for \ \ k = 1, 2, ...$$

and

$$\mathscr{U}_{2k-2}(\xi, y, \tau) = y^2 \frac{\tau^{(2k-2)\alpha}}{\Gamma((2k-2)\alpha + 1)}, \quad for \ \ k = 1, 2, ...$$

From all above, equation (25) becomes;

$$\mathscr{U}(\xi, y, \tau) = \xi^2\left(\frac{\tau^\alpha}{\Gamma(\alpha+1)} + \frac{\tau^{3\alpha}}{\Gamma(3\alpha+1)} + ...\right) + y^2\left(1 + \frac{\tau^{2\alpha}}{\Gamma(2\alpha+1)} + \frac{\tau^{4\alpha}}{\Gamma(4\alpha+1)} + ...\right)$$

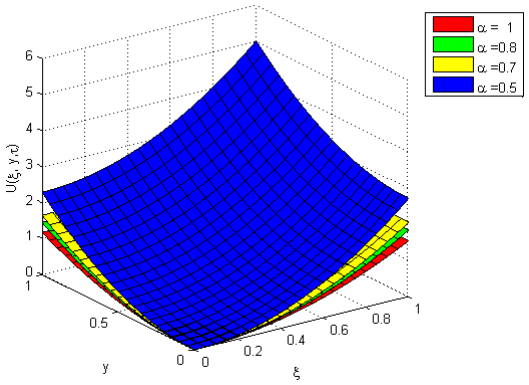

Figure 5: Solution of two dimensional fractional diffusion Equation by NDM

Now, by using computational software,

Figure 5 shows that the three-dimensional plot that visually represents the NDM solution of two dimensional fractional order diffusion equation for different values of the variable α. Notably, by observing figure, it becomes evident that whenever value of α progressively approaches 1, the solution curve increasingly converges towards the curve corresponding to $\alpha = 1$ and at $\alpha = 1$ it coincides with the exact solution in closed form.

When $\alpha = 1$, above gives;

$$\mathscr{U}(\xi, y, \tau) = \xi^2 \left(\frac{\tau}{1!} + \frac{\tau^3}{3!} + ... \right) + y^2 \left(1 + \frac{\tau^2}{2!} + \frac{\tau^4}{4!} + ... \right) = \xi^2 \sinh \tau + y^2 \cosh \tau.$$

This is the somewhat like exact solution in closed form Plotting the error by using computational software Figure 6 shows that three-dimensional plot illustrating the error of the solution of two dimensional

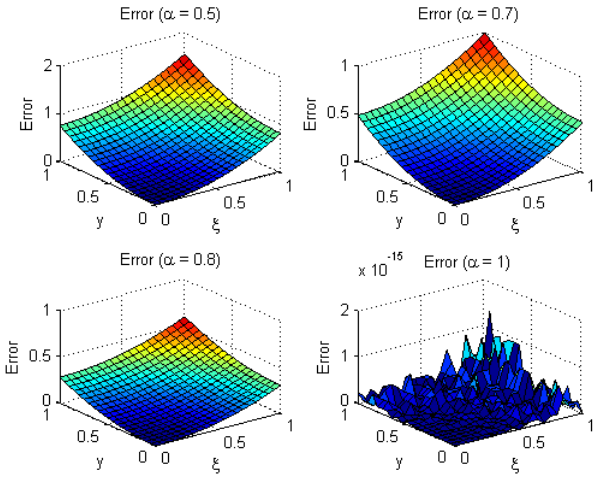

Figure 6: Error plot of the solution by NDM

diffusion equation by NDM across different values of the variable α. This plot visually demonstrates how the error changes with varying α. Notably, figures provide clear evidence that as α approaches 1, the corresponding error consistently decreases. This observation suggests a strong correlation between the proximity of α to 1 and the reduction of error in the solution.

Acknowledgement: Jeevan Kafle acknowledges the University Grants Commission (UGC), Nepal, for the financial support provided as a faculty research grant(FRG) [FRG,079/80 - S & T -08]. Shankar Pariyar is sincerely thankful to the **Institute of Science and Technology, TU, Kathmandu,Nepal** for the faculty Mini-research Grant.

4 Conclusion

In this work, we have examined the numerical analysis of the non-integer (fractional) order diffusion equation by employing the natural decomposition method (NDM). Proposed method offers a valuable approach for approximating solutions to fractional differential equations, including the fractional diffusion equation, which exhibits anomalous diffusion behavior. The fractional diffusion equations are the best tools to capture the diffusion in complex media where non-local property and and long-range memory effect plays a crucial role. Through the application of the NDM, we have successfully illustrated the numerical solutions for one dimensional and two dimensional fractional diffusion equations and from the result we discovered that whenever on-integer order α tends towards integer order, the non-integer order solutions converge rapidly close to exact solution. Therefore the accuracy and convergence of the NDM have been validated through our numerical experiments. The application of NDM to illustrative instances has further proved that, when comparing the integer-order model with fractional order model, it becomes apparent that the fractional-order mathematical model provides the most effective approach for capturing the non-local property and long-range memory effect that exhibit by anomalous diffusion process. In conclusion, the non integer order diffusion equation offers a best mathematical framework to capture the anomalous diffusion process in complex media and the fractional natural decomposition method (NDM) is regarded as the best tool for solving linear as well as non-linear fractional partial differential equations due to its superior convergence and accuracy compared to other methods.

References

[1] Abbasbandy, S. **(2007)**. An approximation solution of a nonlinear equation with riemann–liouville's fractional derivatives by he's variational iteration method. *Journal of Computational and Applied Mathematics*, 207(1): 53-58.

[2] Belgacem, F. B. M. and Silambarasan, R. **(2012)**. Advances in the natural transform. In AIP conference proceedings, volume 1493. *American Institute of Physics*, https://doi.org/10.1063/1.4765477

[3] Gorenflo, R. and Mainardi, F. **(1997).** Fractional calculus. In Fractals and fractional calculus in continuum mechanics, 223-276.

[4] Gorenflo, R. and Mainardi, F. **(2001).** Random walk models approximating symmetric space-fractional diffusion processes. In Problems and Methods in Mathematical Physics: The Siegfried Pr¨ossdorf Memorial Volume Proceedings of the 11th TMP, Chemnitz (Germany), March 25–28, 1999. Springer.

[5] Kafle J, Bagale L, KC, D **(2020).** Numerical Solution of Parabolic Partial Differential Equation by Using Finite Difference Method. *Journal of Nepal Physical Society,* **6**(2):57-65. https://doi.org/10.3126/jnphyssoc.v6i2.34858

[6] Li, X., Xu, M., and Jiang, X. **(2009).** Homotopy perturbation method to time-fractional diffusion equation with a moving boundary condition. *Applied Mathematics and Computation,* **208**(2).

[7] Lin, Y. and Xu, C. **(2007).** Finite difference/spectral approximations for the time-fractional diffusion equation. *Journal of computational physics,* **225**(2).

[8] Meerschaert, M. M. and Tadjeran, C. **(2004).** Finite difference approximations for fractional advection–dispersion flow equations. *Journal of computational and applied mathematics,* **172**(1).

[9] Meerschaert, M. M. and Tadjeran, C. (2006). Finite difference approximations for two-sided space-fractional partial differential equations. *Applied numerical mathematics,* **56**(1).

[10] Metzler, R. and Klafter, J. **(2000).** The random walk's guide to anomalous diffusion: a fractional dynamics approach. *Physics reports,* **339**(1).

[11] Momani, S. **(2005).** Analytical approximate solution for fractional heat-like and wave-like equations with variable coefficients using the decomposition method. *Applied Mathematics and Computation,* **165**(2).

[12] Pariyar,S. **(2023).** Numerical Analysis for Fractional Calculus. M.Phil's thesis, Central Department of Mathematics, Tribhuvan University, Nepal.

[13] Pariyar, S. and Kafle, J. **(2022).** Approximation solutions for solving some special functions of fractional calculus via caputo-fabrizio sense. *Nepal Journal of Mathematical Sciences*, **3**(2): 71-80.DOI: 10.3126/njmathsci.v3i2.49203

[14] Pariyar, S. and Kafle, J. **(2023).** Caputo-Fabrizio approach to numerical fractional derivatives. *BIBECHANA,* **20**(2): 126-133.

[15] Podlubny, I. **(1999).** An introduction to fractional derivatives, fractional differential equations, to methods of their solution and some of their applications. *Math. Sci. Eng,* **198**.

[16] Rawashdeh, M. and Maitama, S. **(2017).** Finding exact solutions of nonlinear pdes using the natural decomposition method. *Mathematical Methods in the Applied Sciences,* **40**(1).

[17] Rawashdeh, M. S. **(2017).** The fractional natural decomposition method: theories and applications. *Mathematical Methods in the Applied Sciences,* **40**(7).

[18] Ray, S. S. and Bera, R. **(2006).** Analytical solution of a fractional diffusion equation by adomian decomposition method. *Applied Mathematics and Computation,* **174**(1).

[19] Schneider, W. R. and Wyss, W. **(1989).** Fractional diffusion and wave equations. *Journal of Mathematical Physics,* **30**(1).

[20] Wyss, W. **(1986).** The fractional diffusion equation. *Journal of Mathematical Physics,* **27**(11).

Nepal Journal of Mathematical Sciences (*NJMS*)
ISSN: 2738-9928 (*online*), 2738-9812 (*print*)
Vol. 4, No. 2, 2023 (*August*): *77-82*
DOI: https://doi.org/10.3126/njmathsci.v4i2.59537

Research Article
Received Date: May 3, 2023
Accepted Date: August 9, 2023
Published Date: August 30, 2023

On a New Application of Almost Increasing Sequence to Laguerre Series Associated with Strong Summability of Ultrapherical Series

Suresh Kumar Sahani[1] , Jagat Krishna Pokharel[2] ,Gyan Prasad Paudel[3] , & S.K. Tiwari[4]

[1]*Department of Mathematics, MIT Campus, Tribhuvan University, Janakpurdham,Nepal*
[2]*Department of Mathematics Education, Sanothimi Campus, Tribhuvan University, Bhaktapur, Nepal*
[3]*Central Campus of Science and Technology, Mid-West University, Surkhet, Nepal*
[4]*Department of Mathematics, Dr C.V.Raman University,Bilaspur, India*

Email: [1]*sureshkumarsahani35@gmail.com*[*], [2]*jagatpokhrel.tu@gmail.com*, [3]*gyan.math725114@gmail.com*, & [4]*sk10tiwari@gmail.com*

Corresponding Author: Suresh Kumar Sahani

Abstract: *The concept of summability of infinite series has been utilized in virtually every field of scientific application, including the enhancement of signals in filters, the acceleration of the rate of convergence, orthogonal series, and approximation theory, to name just a few. In addition, by making use of the main theorem, a collection of new well-known arbitrary findings have been obtained. Taking into account the appropriate conditions of a prior result, which result was produced, verifies the conclusions of the current study.*

Keywords: *Matrix summability, Laguerre series, Ultraspherical series*.

AMS Subject Classification (2020): 40C05, 40F05

1. Introduction

Cauchy's monumental "course d'analyses algebriaic" published in 1821 and Abel's investigations (see [8, 10-18]) into the binomial series (published in 1826) provided a solid foundation for the antiquated and esoteric concept of convergence infinite series. In Dynamical Astronomy, in particular, there were a few non-convergent series that gave close to the right answers. In 1890, a theory of divergent series was formulated for the first time by Cesàro, who wrote a paper on the multiplication of a series. From there, the theory of series emerged as the hub of mathematical analysts' ingenuity, explaining why the sequence of partial sums of a function varies in a periodic fashion. Mathematicians like Holder, Hausdorff, Riesz, Nörlund, etc. worked tirelessly to develop effective solutions, and only in the last decade of the twentieth century and the first year of the twenty-first century have they succeeded. Cauchy's idea of convergence is intended to have a tight relationship with this method through process. In a fair fashion, we can refer to these values as their sums. The process of linking generalized sums, known as summability (Szasz 1946; Hardy 1949), offers a natural generalization of the classical notion of convergence (Hobson 1909).

2. Definitions

Before proceeding with the main work, we now give some notations and definitions that are used in the paper.

2.1 Regular triangular matrix (see [17]**)**

The matrix of triangles $(\Lambda) = (r_{a,b})$ where a = 0, 1, 2, 3, … and b = 0, 1, 2, 3, …and $r_{a,b} = 0$ for $0 < a < 1$,(defines a regular sequence-to-sequence transformation) b, is regular) if

$\lim_{a\to\infty} r_{a,b} = 0$, for every fixed b; … (1)

$\sum_{b=0}^{a} | r_{a,b} | \leq K$, independent of a; … (2)

and $\lim_{a\to\infty} \sum_{b=0}^{a} r_{a,b} = 1.$ … (3)

2.2 Strongly summable (see [5,17]**);**

An infinite series $\sum v_a$ with the sequence of partial sums $\{ S_a \}$ is said to be strongly summable (Λ) to a fixed finite sums S, if $\sum_{b=0}^{a} r_{a,b} | S_b - S | = o(1),$ as $a \to \infty$. … (4)

2.3 We have the following three cases (see [5,20,21]**);**

(a) $r_{a,b} = \frac{1}{(a+1)} (b \leq a)$

(b) $r_{a,b} = \frac{1}{\{(b+1) \sum_{m=0}^{a} \frac{1}{m+1}\}} \quad (b \leq a)$

(c) $r_{a,b} = \frac{1}{(1 - b + a) \sum_{m=0}^{a} \frac{1}{m+1}} \quad (b \leq a)$

Summability (Λ) becomes respectively Cesàro summability, Riesz summability and Nörlund summability.

2.4 Ultraspherical series (see [5,20,21]**);**

Let $f(\theta, \phi)$ be a function defined in range $0 \leq \theta \leq \pi$ and $0 \leq \phi \leq 2\pi$. The ultraspherical series corresponding to $f(\theta, \phi)$ on the sphere S is given by

$$f(\theta, \phi) \sim \frac{1}{2\pi} \sum_{a=0}^{\infty} (a + \alpha) \int_S \int \frac{f(\theta', \phi') Q_n^{(\alpha)} (\cos \omega) \sin \theta' \, d\theta' \, d\phi'}{[\sin^2 \theta' \sin^2 (\phi - \phi')]^{\frac{1-2\alpha}{2}}} \quad \dots \quad (5)$$

Where, $\cos \omega = \cos \theta \cos \theta' + \sin \theta \sin \theta' \cos (\phi - \phi')$. … (6)

2.5 Ultraspherical polynomial (see [18,20]**);**

The ultraspherical polynomial $Q_a^{(\alpha)}(x)$ is defined by generating function

$$(1 - 2xt + t^2)^{-\alpha} = \sum_{a=0}^{\infty} t^a \, Q_a^{(\alpha)}(x), \ \alpha > 0 \quad \dots \quad (7)$$

A generalized mean value of $f(\theta, \phi)$ on the sphere S has been defined Gupta (see [4]) as follows:

$$f(\omega) = \frac{1}{2\pi (\sin \omega)^{2\alpha}} \int_{C_\omega} \frac{f(\theta', \phi') \, ds'}{[\sin^2 \theta' \sin^2 (\phi - \phi')]^{\frac{1-2\alpha}{2}}} \quad \dots \quad (8)$$

where the integral is taken along the small circle C whose center is (θ, ϕ) on the sphere S and whose curvilinear radius is ω.

The series (5) reduces to

$$f(\theta, \phi) \sim \frac{\Gamma(\alpha)}{\Gamma\left(\frac{1}{2}\right) \Gamma(\frac{1}{2} + \alpha)} \sum_{a=0}^{\infty} (a + \alpha) \int_0^{\pi} f(\omega) \sin^{2\alpha} \omega \, Q_a^{(\alpha)} (\cos \omega) \, d\omega \, . \quad \dots \quad (9)$$

Also, we write

$\phi(\omega) = \{ f(\omega) - A \} (\sin \omega)^{2\alpha - 1}$ … (10)

where A is a fixed constant.

Various researchers have explored various intriguing generalizations; here we list just a handful (see [1-9, 19-21]). The following theorem on the summability of Laguerre series in matrices was proved by them (see [6]):

2.6 Known Theorem:

Let the non- negative real sequence $\{r_{a,b}\}$ be none decreasing with respect to b

and

$$\lim_{a\to\infty}\sum_{b=0}^{a}\lambda_{a,b} = 1 \quad \dots \quad (11)$$

If $\left|\ \phi\ \right|$ is integrable in the sense of Lebesgue integral in any bounded interval (0, ω)

and if,

$$\int_1^{\infty} e^z\, z^{\frac{-1}{5}}\ \left|\ \phi\ (z)\right|\ dz\ <\ \infty\ . \quad \dots \quad (12)$$

Then for $-2<2\alpha<-1$, the Leguerre series corresponding to the function $f\ \in L\ [0,\infty]$ given by

$$f(x) \sim \sum_{a=0}^{\infty} v_n\, L_a^{(\alpha)}(x) \quad \dots \quad (13)$$

where

$$v_a = \left\{\Gamma(\alpha+1)\binom{a+\alpha}{\alpha}\right\}^{-1} \int_0^{\infty} e^{-z} z^{\alpha} f(z) L_a^{(\alpha)}(z)\ dz \quad \dots \quad (14)$$

and $L_a^{(\alpha)}(z)$ denotes the a^{th} Laguerre polynomial of order $-\alpha<1$ which is defined as

$$\sum_{a=0}^{\infty} L_a^{(\alpha)}(x)\ \omega^n = (1-\omega)^{-\alpha-1} e^{\frac{-x\omega}{1-\omega}} \quad \dots \quad (15)$$

and

$$\phi\ (z) = (\Gamma(\alpha+1))^{-1} e^{-z} z^{\alpha}\{f(z)-f(0)\} \quad \dots \quad (16)$$

is summable (Λ) at $x = 0$ to the sum $f(0)$.

3. Main Theorem

We prove the following theorem

3.1 Theorem:

Let $\{r_{a,b}\}$ be non-negative, monotone increasing sequence with respect to b, and

$$\lim_{a\to\infty}\sum_{b=0}^{a} r_{a,b} = 1. \quad \dots \quad (17)$$

Let μ be a large constant and δ be such that

$$1>\alpha(1+\delta)\ >\alpha, \quad \alpha\in(0,1). \quad \dots \quad (18)$$

Let ϕ be a function ω which is bounded variation in open interval (ξ,π) i.e.$|\phi(\omega)|\ \in(\xi,\pi)$where ξ is defined as follows:

$$\xi = \mu\, a^{-\delta},\ (\ 0<\xi<\pi) \quad \dots \quad (19)$$

and, if

$$\int_0^t\ \left|\ \phi(\omega)\right|\ d\omega\ = O(t^{\varepsilon+1})\ ,\ \ \text{as } t\to 0 \quad \dots \quad (20)$$

and $\varepsilon = \frac{2\alpha+1}{\delta} - 1.$ … (21)

Then the given ultraspherical series corresponding$f(\theta,\phi)$ on the sphere S is strongly summable (Λ) to the sum A.

3.2 Lemmas:

The following lemmas are necessary for us to prove our theorem:

Lemma 1 (see [22]) : We have for $\alpha>0$,

$$Q_a^{(\alpha)}\ (\cos\theta\ ) = \theta^{-\alpha}\ O\ (\ a^{\alpha-1}),\ \frac{C}{a} \le \theta \le \frac{\pi}{2} \quad \dots \quad (22)$$

and,

$Q_a^{(\alpha)}(\cos\theta) = O\left(\frac{1}{a^{1-2\alpha}}\right)$, $0 \leq \theta \leq \frac{c}{a}$ … (23)

Lemma 2 (see [22]) : For $a \geq 0$, we have

$\frac{d}{dx}\{ Q_a^{(\alpha)}(x) \} = 2\,\alpha Q_a^{(\alpha+1)}(x)$, … (24)

Where $Q_{-1}^{(\alpha)}(x) = 0$

Lemma 3 : Under the condition of theorem, we have

$\sum_{b=0}^{a} r_{a,b} K^{\alpha-1} = O(a^{\alpha-1})$, … (25)

and similarly,

$\sum_{b=0}^{a} r_{a,b} K^{2\alpha+1} = O(a^{2\alpha+1})$, as $a \to \infty$. … (26)

The proof obviously follows on using (17).

3.3 Proof of the theorem:

Let σ_a denote the a^{th} partial sum of the series (5) .Then we have (see [22]).

$\sigma_a = \frac{\Gamma(\alpha)}{\sqrt{\pi}\,\Gamma(\alpha+\frac{1}{2})} \int_0^{\pi} f(\omega) \sum_{m=0}^{a} (m+\alpha)\, Q_a^{(\alpha)}(\cos\omega)\,(\sin\omega)^{2\alpha} d\omega$

$\sigma_a = \frac{\Gamma(\alpha)}{\sqrt{\pi}\,\Gamma(\alpha+\frac{1}{2})} \int_0^{\pi} f(\omega)\, sin^{2\alpha}\omega \left[\frac{d}{dx}\left\{Q_{a+1}^{(\alpha)}(x) + Q_a^{(\alpha)}(x)\right\}\right]_{x=cos\omega} d\omega$. … (27)

Therefore, with view of (10), we have

$\sigma_a - A = \frac{\Gamma(\alpha)}{\sqrt{\pi}\,\Gamma\left(\alpha+\frac{1}{2}\right)} \int_0^{\pi} \phi(\omega) \frac{d}{d\omega}\{ Q_{a+1}^{(\alpha)}(\cos\omega) + Q_a^{(\alpha)}(\cos\omega) \}\, d\omega$

$\sigma_a - A = O\left[\int_0^{\pi} \phi(\omega) \frac{d}{d\omega}(Q_{a+1}^{(\alpha)}(\cos\omega)\, d\omega\right] + O\left[\int_0^{\pi} \phi(\omega) \frac{d}{d\omega}(Q_a^{(\alpha)}(\cos\omega))\, d\omega\right]$,

$= I_1 + I_2$, … (28)

In order to establish our theorem, we must demonstrate that

$\sum_{b=0}^{a} r_{a,b} \left|\sigma_a - A\right|^p = O(1)$, as $a \to \infty$. … (29)

Now applying Minkowski's inequality, we get

$\{\sum_{b=0}^{a} r_{a,b} \left|\sigma_a - A\right|^p\}^{\frac{1}{p}} \leq \{\sum_{b=0}^{a} r_{a,b} \left|I_1\right|^p\}^{\frac{1}{p}} + \{\sum_{b=0}^{a} r_{a,b} \left|I_2\right|^p\}^{\frac{1}{p}}$

$= (M)^{\frac{1}{p}} + (N)^{\frac{1}{p}}$ (say) … (30)

Let us first consider I_1,

$\left|I_1\right| = O\left[\int_0^{\pi} \left|\phi(\omega)\right| \left|\frac{d}{d\omega}\{Q_{b+1}^{(\alpha)}(\cos\omega)\right| d\omega\right]$

$= O\left[\left(\int_0^{\xi} + \int_{\xi}^{\pi}\right) \left|\phi(\omega)\right| \left|\frac{d}{d\omega}\{ Q_{b+1}^{(\alpha)}(\cos\omega) \right| d\omega$

$= O(I_{1,1}) + O(I_{1,2})$, (say) . … (31)

We have,

$I_{1,1} = \int_0^{\xi} \left|\phi(\omega)\right| \left|\frac{d}{d\omega}\{ Q_{b+1}^{(\alpha)}(\cos\omega) \right| d\omega$

$= \int_0^{\xi} \left|\phi(\omega)\right| 2\alpha \left|Q_{b+1}^{(\alpha+1)}(\cos\omega) \right|$, using (24)

$= \int_0^{\xi} \left|\phi(\omega)\right| 2\alpha\, O\{ (b+1)^{2\alpha+1} \}\, d\omega$, using (23)

$= O(b^{2\alpha+1}) \int_0^{\xi} \left|\phi(\omega)\right| d\omega$

$= O(b^{2\alpha+1})\, O(\xi^{\varepsilon+1})$, using (20).

Hence,

$\sum_{b=0}^{a} r_{a,b}\ \mathrm{O}(I_{1,1}) = \sum_{b=0}^{a} r_{a,b}\mathrm{O}(b^{2\alpha+1})\ \mathrm{O}(\xi^{\varepsilon+1})$

$= \mathrm{O}\left(\sum_{b=0}^{a} r_{a,b}\, b^{2\alpha+1}\right) \mathrm{O}(\xi^{\varepsilon+1})$

$= \mathrm{O}(a^{2\alpha+1})\ \mathrm{O}(a^{-\delta(\varepsilon+1)})$, using(26) and (19)

$= \mathrm{O}(\ a^{2\alpha+1-\varepsilon\delta-\delta})$

$=\mathrm{O}(1)$, as $a\to\infty$, using (21) . … (32)

Again,

$I_{1,2} = \int_{\xi}^{\pi} \left|\phi(\omega)\right| \left|\frac{d}{d\omega}\{Q_{b+1}^{(\alpha)}(\cos\omega)\right| d\omega$

$= [\phi(\omega)Q_{b+1}^{(\alpha)}(\cos\omega)]_{\xi}^{\pi} - \int_{\xi}^{\pi} d\phi(\omega)\, Q_{k+1}^{(\alpha)}(\cos\omega)\, d\omega$

$= \mathrm{O}(b^{\alpha-1})\ \xi^{-\alpha}$, using (22)

and $\phi(\omega) \in \mathrm{BV}(\xi,\pi)$.

Hence,

$\sum_{b=0}^{n} r_{a,b}\ \mathrm{O}(I_{1,2}) = \sum_{b=0}^{a} r_{a,b}\mathrm{O}(b^{\alpha-1})\ \xi^{-\alpha}$

$= \mathrm{O}\left(\sum_{b=0}^{a} r_{a,b}\, b^{\alpha-1}\right) \xi^{-\alpha}$

$= \mathrm{O}\ (a^{\alpha-1})\ (\mu a^{-\delta})^{-\alpha}$, using (25) and (19)

$= \mathrm{O}\ (\ a^{\alpha-1+\alpha\delta})$

$= \mathrm{O}(1)$, as $a\to\infty$ by (27) and (19). … (33)

Therefore, $M = \sum_{b=0}^{a} r_{a,b}\ \left|I_1\right|^p = \mathrm{O}\{\sum_{b=0}^{a} r_{a,b}\}$

$(M)^{\frac{1}{p}} = \mathrm{O}(1)$, as $a\to\infty$ by (3). … (34)

We can also demonstrate that

$(N)^{\frac{1}{p}} = \mathrm{O}(1)$ as $n\to\infty$. … (35)

Combining (34) and (35), we get the required result (29).

Conclusion

In this article, we have used the Generalization procedure to establish advanced systems. Summability methods are instructed to reduce the error. Some new result can be generated by using suitable conditions in the main result. The results [10-22] can be found by applying conditions on the main result.

Acknowledgement

Authors are highly thankful to the referee for his valuable suggestions in improvement of this paper.

Data Availability

All the data used in this study “Degree of approximation of signals by strong summability of ultraspherical series” supports the findings and are cited within the article.

References

[1] Alladi, S. **(2019)**. A Multiplier theorem for ultraspherical polynomials, *Studia Mathematica*, **47**:1-43.

[2] El- Hawary, H.M., Salim,M.S. and Hussien, H.S.. **(2000).** An optional ultraspherical approximation of integrals, *Int. J. Comput. Math.*, **76**(2): 219-237.

[3] Elbert,Á., A.Loforgia, and P. Siafarikas, **(2001)**. A conjecture of the zeros of ultraspherical polynomial, *Journal of Computational and Applied Mathematics*, **133**(1): 684.

[4] Gupta, D.P. **(1962)**. The absolute summability (A) of ultraspherical series, *Annali di Mathematica pura ed Applicata*, **59**: 179-188.

[5] Hamilton, H.J. and Hill, J.D. **(1938)**. On strong summability, *The American Journal of Mathematics*, **60**(3): 588-594.

[6] Khare, S.P., Srivastava, P.K., and Mishra, N.P. **(1994)**. Matrix summability of Laguerre series, *Proc. N. A. S*, **64**(A)(II) , 223-227.

[7] Krasikov, I. **(2017)**. On approximation of ultraspherical polynomials in the oscillatory region, *Journal of Approximation Theory*, **222**: 143-156.

[8] Nigam, H.K. **(2013)**. Birth and growth of summability and approximation theory, *International Journal of Pure and Applied Mathematics*, **83**(5): 639-641.

[9] Prasad, K. **(1980)**. On the strong matrix summability of ultraspherical series, *Indian Journal of Pure Applied Math*., **11**(9): 1170-1175.

[10] Sahani, S.K.,Mishra, V.N.,and Pahari,N.P. **(2021)**.Some problems on approximation of function (Signals) in matrix summability of Legendre series, *Nepal Journal of Mathematical Sciences*,**2**(1): 43-50.

[11] Sahani, S.K.,Mishra, V.N.,and,Pahari,N.P. **(2020)**. On the degree of approximations of a function by N*ö*rlund means of its Fourier Laguerre series, *Nepal Journal of Mathematical Sciences*, **1**: 65-70.

[12] Sahani, S.K.and Mishra,L.N. **(2021)**.Degree of approximation of signals by N*ö*rlund summability of derived Fourier series, *The Nepali Math.Sc.Report*, **38**(2):13-19.

[13] Sahani, S.K., Paudel,Paudel,G.P.,and Thakur, A.K. **(2022)**. On a new application of positive and decreasing sequences to double Fourier series associated with (N,$p_m^{(1)}$,$p_n^{(2)}$) ,*Journal of Neapl Mathematicial Society*,**5**(2): 58-64.

[14] Sahani, S.K. et al. **(2022)**. On certain series to series transformation and analytic continuation by matrix method, *Nepal Journal of Mathematical Sciences*,**3**(1): 75-80.

[15] Sahani, S.K.and Mishra, V.N. **(2023)**.Degree of approximation of function by N*ö*rlund summability of double Fourier series, *Mathematical Sciences and Applications E- Notes*,**11**(2): 80-88.

[16] Sahani, S.K. and Jha, D. **(2021)**. A certain studies on degree of approximation of functions by matrix transformation,*The Mathematics Education*, **LV**(2): 21-33.

[17] Sahani, S.K. and Prasad, K.S. **(2022)**. On a new application of almost non-increasing sequence to ultrasphericial series associated with (N ,p, q)$_k$ means ,**XXIV**(1):1-11.

[18] Sahani, S.K.,Mishra, V.N., and Rathour,L. **(2022)**. On N*ö*rlund summability of double Fourier series, *Open Journal of Mathematical Sciences*, **6**(1): 99-107.

[19] Sharapudinov, I. **(2003)**. Mixed series in ultraspherical polynomials and their approximation properties, *Russian Academy of Science Sbornik Mathematics*, **194**(3): 423- 456.

[20] Singhai, B.C. **(1961)**. On the Cesàro summability of the ultraspherical series, *Bulletino dell' Vnione Mathematica Italiana*,**16**(3): 207-217.

[21] Singhai, B.C. **(1962)**. On the Cesàro summability of the ultraspherical serie, *Annali di Mathematica pura ed Applicata*, **59**: 27-39.

[22] Szegö G. **(1959)**. Orthogonal polynomials colloq. Publ., *Amer. Math. Soc.* New York.

□□

Nepal Journal of Mathematical Sciences (NJMS)
***ISSN*: 2738-9928 (*online*), 2738-9812 (*print*)**
Vol. 4, No. 2, 2023 (August): 83-88
DOI: https://doi.org/10.3126/njmathsci.v4i2.60177

Research Article
Received Date: August 7,2023
Accepted Date: August 25,2023
Published Date: August 30,2023

Connection Formulas on Kummer's Solutions and their Extension on Hypergeometric Function

Madhav Prasad Poudel[1,4],Narayan Prasad Pahari[2], Ganesh Bahadur Basnet[3], & Resham Poudel[3]

[1]*School of Engineering, Pokhara University, Pokhara-30, Kaski, Nepal*

[2]*Central Department of Mathematics, Tribhuvan University, Kirtipur, Kathmandu, Nepal*

[3]*Department of Mathematics, Tribhuvan University, Tri-Chandra Campus, Kathmandu, Nepal*

[4]*Nepal Sanskrit University, Beljhundi, Dang, Nepal*

Corresponding Author: Madhav Prasad Poudel

Email: [1] *pdmadav@gmail.com,* [2]*nppahari@gmail.com* [3]*gbbmath@gmail.com*, & [4]*reshamprdpaudel@gmail.com*

Abstract: *Hypergeometric functions are transcendental functions that are applicable in various branches of mathematics, physics, and engineering. They are solutions to a class of differential equations called hypergeometric differential equations. Kummer obtained six solutions for the hypergeometric differential equation and twenty connection formulae. This research work has extended those connection formulas to other six solutions* $y_1(x), y_2(x), y_3(x), y_4(x), y_5(x), and\, y_6(x)$ *to show that each solution can be expressed in terms of linear relationship among three of the other solutions.*

Keywords: *Hypergeometric function, Kummer's formula, Connection formula*

1. Introduction and Motivation

Before Proceeding with the main work, we shall now introduce some basic notations,definitions and preliminaries that are used in this paper.

1.1 Hypergeometric Function[12]

The Gaussian hypergeometric function ${}_2F_1(a,b;c;x)$ is a special function represented by the hypergeometric series,

$$ {}_2F_1(a,b;c;x) = {}_2F_1\left[\begin{matrix} a & b; \\ & c; \end{matrix}\; x\right] = 1+\sum_{n=1}^{\infty}\frac{(a)_n(b)_n}{(c)_n}\frac{x^n}{n!} \qquad ...(1.1.1)$$

Where $(a)_n$ is called the Pochhammer symbol and is defined as

(i) $(a)_n = a(a+1)(a+2)(a+3)....a+(n-1) = \prod_{k=1}^{n}(a+k-1) = \frac{\Gamma(a+k)}{\Gamma(a)}$ …(1.1.2)

(ii) $(a)_0 = 1, \text{for}\, a \neq o$

If the value of $a,b,c \in Z^+$ in (1.1.1) then it is convergent for $|z|<1$ [13] and if $a,$ and b are the positive integers, $c \in \{0,-1,...,a+1\}$ and $c \in \{0,-1,...,b+1\}$, then the hypergeometric series (1.1.1) is a

polynomial of degree $|a|$ or $|b|$, If $c = a$ and $b = c$ then it is not possible to define ${}_2F_1(a,b;c;z)$ [3]. In this case,

$$ {}_2F_1(a,b;c;x) = \sum_{k=0}^{\infty} \frac{(b)_k}{k!} x^k = (1-x)^{-b} \qquad \ldots(1.1.3) $$

If $\mathrm{Re}(c-a-b) > 0$, $\mathrm{Re}(c) > \mathrm{Re}(b) > 0$ in (1.1.1) then it can be expressed in the form of gamma function through the Guass Kummer identity;

$$ \frac{\Gamma(c)\Gamma(c-a-b)}{\Gamma(c-a)\Gamma(c-b)} \qquad \ldots (1.1.4) $$

The series (1.1.1) is a solution of a second-order linear ordinary hypergeometric differential equation known as Guass Hypergeometric differential equation[12],

$$ x(1-x)y''+(c-(a+b+1)x)y'-aby = 0 \qquad \ldots(1.1.5) $$

1.2 The solutions at the singularities

The equation (1.1.5) has a regular singularity at $x = 0, 1$, and infinity [5, 16]. The table given below, commonly known as Riemann Scheme table, shows the of local exponents of the hypergeometric differential equations at the variate values of x

$x=0$	$x=1$	$x=\infty$
0	0	a
$1-c$	$c-a-b$	b

According to Riemann scheme, the difference of the local exponent is not an integer. This condition is called the generic condition. In this condition the fundamental system of solutions are defined at each singular points.[4]. The fundamental solutions of this differential equation in different singular points are as below.[2]

(i) For singularity at $x = 0$,

$$ y_1(x) = {}_2F_1(a,b;c;x) \qquad \ldots (1.2.1) $$

and $$ y_2(x) = x^{1-c}\, {}_2F_1(a-c+1, b-c+1; 2-c; x) \qquad \ldots(1.2.2) $$

(ii) For singularity at $x = 1$,

$$ y_3(x) = {}_2F_1(a,b;a+b+1-c;1-x) \qquad \ldots(1.2.3) $$

and $$ y_4(z) = x^{c-a-b}\, {}_2F_1(c-a, c-b; c-a-b+1; 1-x) \qquad \ldots(1.2.4) $$

(iii) For singularity at $x = \infty$,

$$ y_5(x) = x^{-a}\, {}_2F_1(a, a-c+1; a-b+1; \frac{1}{x}) \qquad \ldots(1.2.5) $$

and $$ y_6(x) = x^{-b}\, {}_2F_1(b, b-c+1; b-a+1; \frac{1}{x}) \qquad \ldots(1.2.6) $$

1.3 Local Solutions and Connection formula

These six solutions published by Kummer, has four forms related to one another by Euler transformation giving twenty four forms in total [11]. These twenty four solutions are known as Kummer's solution of hypergeometric differential equation. For details, we refer [2, 8].

1.4 Connection Formulas

The six formulas as mentioned by Kummer [2, 8] for three parameters a, b, c and combination of three solutions,[14,15] with the property (1.1.4) will give ${}_6C_3 = 20$ connection formulae as the principle branches of Kummer's solution[1, 2, 10]. They are listed as follows;

$$y_3(x) = \frac{\Gamma(1-c)\Gamma(a+b-c+1)}{\Gamma(a-c+1)\Gamma(b-c+1)} y_1(x) + \frac{\Gamma(c-1)\Gamma(a+b-c+1)}{\Gamma(a)\Gamma(b)} y_2(x) \quad \dots (1.4.1)$$

$$y_4(x) = \frac{\Gamma(1-c)\Gamma(c-a-b+1)}{\Gamma(1-a)\Gamma(1-b)} y_1(x) + \frac{\Gamma(c-1)\Gamma(c-a-b+1)}{\Gamma(c-a)\Gamma(c-b)} y_2(x) \quad \dots (1.4.2)$$

$$y_5(x) = \frac{\Gamma(1-c)\Gamma(a-b+1)}{\Gamma(a-c+1)\Gamma(1-b)} y_1(x) + e^{(c-1)\pi i} \frac{\Gamma(c-1)\Gamma(a-b+1)}{\Gamma(a)\Gamma(c-b)} y_2(x) \quad \dots (1.4.3)$$

$$y_6(x) = \frac{\Gamma(1-c)\Gamma(b-a+1)}{\Gamma(b-c+1)\Gamma(1-a)} y_1(x) + e^{(c-1)\pi i} \frac{\Gamma(c-1)\Gamma(b-a+1)}{\Gamma(b)\Gamma(c-a)} y_2(x) \quad \dots (1.4.4)$$

$$y_1(x) = \frac{\Gamma(c)\Gamma(c-a-b)}{\Gamma(c-a)\Gamma(c-b)} y_3(x) + \frac{\Gamma(c)\Gamma(a+b-c)}{\Gamma(a)\Gamma(b)} y_4(x) \quad \dots (1.4.5)$$

$$y_2(x) = \frac{\Gamma(2-c)\Gamma(c-a-b)}{\Gamma(1-a)\Gamma(1-b)} y_3(x) + \frac{\Gamma(2-c)\Gamma(a+b-c)}{\Gamma(a-c+1)\Gamma(b-c+1)} y_4(x) \quad \dots (1.4.6)$$

$$y_5(x) = e^{a\pi i} \frac{\Gamma(a-b+1)\Gamma(c-a-b)}{\Gamma(1-b)\Gamma(c-b)} y_3(x) + e^{(c-b)\pi i} \frac{\Gamma(a-b+1)\Gamma(a+b-1)}{\Gamma(a)\Gamma(a-c+1)} y_4(x) \quad \dots (1.4.7)$$

$$y_6(x) = e^{b\pi i} \frac{\Gamma(b-a+1)\Gamma(c-a-b)}{\Gamma(1-a)\Gamma(c-a)} y_3(x) + e^{(c-a)\pi i} \frac{\Gamma(b-a+1)\Gamma(a+b-c)}{\Gamma(b)\Gamma(b-c+1)} y_4(x) \quad \dots (1.4.8)$$

$$y_1(x) = \frac{\Gamma(c)\Gamma(b-a)}{\Gamma(b)\Gamma(c-a)} y_5(x) + \frac{\Gamma(c)\Gamma(a-b)}{\Gamma(a)\Gamma(c-b)} y_6(x) \quad \dots (1.4.9)$$

$$y_2(x) = e^{(1-c)\pi i} \frac{\Gamma(2-c)\Gamma(b-a)}{\Gamma(1-a)\Gamma(b-c+1)} y_5(x) + e^{(1-c)\pi i} \frac{\Gamma(2-c)\Gamma(a-b)}{\Gamma(1-b)\Gamma(a-c+1)} y_6(x) \quad \dots (1.4.10)$$

$$y_3(x) = e^{-a\pi i} \frac{\Gamma(a+b-c+1)\Gamma(b-a)}{\Gamma(b)\Gamma(b-c+1)} y_5(x) + e^{-b\pi i} \frac{\Gamma(a+b-c+1)\Gamma(a-b)}{\Gamma(a)\Gamma(a-c+1)} y_6(x) \quad \dots (1.4.11)$$

$$y_4(x) = e^{(b-c)\pi i} \frac{\Gamma(c-a-b+1)\Gamma(b-a)}{\Gamma(1-a)\Gamma(c-a)} y_5(x) + e^{(a-c)\pi i} \frac{\Gamma(c-a-b+1)\Gamma(a-b)}{\Gamma(1-b)\Gamma(c-b)} y_6(x) \dots (1.4.12)$$

$$y_1(x) = e^{b\pi i} \frac{\Gamma(c)\Gamma(a-c+1)}{\Gamma(a+b-c+1)\Gamma(c-b)} y_3(x) + e^{(b-c)\pi i} \frac{\Gamma(c)\Gamma(a-c+1)}{\Gamma(b)\Gamma(a-b+1)} y_5(x) \quad \dots (1.4.13)$$

$$y_1(x) = e^{a\pi i} \frac{\Gamma(c)\Gamma(b-c+1)}{\Gamma(a+b-c+1)\Gamma(c-a)} y_3(x) + e^{(a-c)\pi i} \frac{\Gamma(c)\Gamma(b-c+1)}{\Gamma(a)\Gamma(b-a+1)} y_6(x) \quad \dots (1.4.14)$$

$$y_2(x) = e^{(b-c+1)\pi i} \frac{\Gamma(2-c)\Gamma(a)}{\Gamma(a+b-c+1)\Gamma(1-b)} y_3(x) + e^{(b-c)\pi i} \frac{\Gamma(2-c)\Gamma(a)}{\Gamma(a-b+1)\Gamma(b-c+1)} y_5(x) \dots (1.4.15)$$

$$y_2(x) = e^{(a-c+1)\pi i} \frac{\Gamma(2-c)\Gamma(b)}{\Gamma(a+b-c+1)\Gamma(1-a)} y_3(x) + e^{(a-c)\pi i} \frac{\Gamma(2-c)\Gamma(b)}{\Gamma(b-a+1)\Gamma(a-c+1)} y_6(x) \dots (1.4.16)$$

$$y_1(x) = e^{(c-a)\pi i}\frac{\Gamma(c)\Gamma(1-b)}{\Gamma(a)\Gamma(c-a-b+1)}y_4(x) + e^{-a\pi i}\frac{\Gamma(c)\Gamma(1-b)}{\Gamma(a-b+1)\Gamma(c-a)}y_5(x) \quad \ldots (1.4.17)$$

$$y_1(x) = e^{(c-b)\pi i}\frac{\Gamma(c)\Gamma(1-a)}{\Gamma(b)\Gamma(c-a-b+1)}y_4(x) + e^{-b\pi i}\frac{\Gamma(c)\Gamma(1-a)}{\Gamma(b-a+1)\Gamma(c-b)}y_6(x) \quad \ldots (1.4.18)$$

$$y_2(x) = e^{(1-a)\pi i}\frac{\Gamma(2-c)\Gamma(c-b)}{\Gamma(a-c+1)\Gamma(c-a-b+1)}y_4(x) + e^{-a\pi i}\frac{\Gamma(2-c)\Gamma(c-b)}{\Gamma(a-b+1)\Gamma(a-1)}y_5(x) \quad \ldots (1.4.19)$$

$$y_2(x) = e^{(1-b)\pi i}\frac{\Gamma(2-c)\Gamma(c-a)}{\Gamma(b-c+1)\Gamma(c-a-b+1)}y_4(x) + e^{-b\pi i}\frac{\Gamma(2-c)\Gamma(c-a)}{\Gamma(b-a+1)\Gamma(1-b)}y_6(x) \quad \ldots (1.4.20)$$

2. Research Objective

In 1837, Kummer introduced the solution to the Kummer differential equation which is known as Confluent hypergeometric function. In the meantime he had discovered twenty four solutions for the same, which subsequently formed the twenty formulas as the branches of Kummer solution [13]. They are listed in relations (1.4.1-1.4.20). In this paper, our objective is to find the relations between any four sets of solutions and also to express any one of them as the linear combination of the other three solutions.

3. Main Result

In section 1.4, the connection formulas for six different solutions, each consisting of two different solutions are presented. The extension of connection formula refers to the combination of any three solutions for a given solution. Each extension formulas is obtained as the combination of three different solutions. The combination of six formulas taken four at a time constitute of ${}^6C_4 = 12$ solutions. The six extension of connection formula are already evaluated by Poudel et.al [9] The remaining six connection formulas will be obtained in this research paper. Those results are presented as follows.

2.1 Extension formula

1. $$y_1(x) = \frac{\Gamma(a-c+1)\Gamma(b-c+1)}{\Gamma(1-c)}\left[\begin{array}{l} e^{-a\pi i}\dfrac{\Gamma(b-a)}{\Gamma(b)\Gamma(b-c+1)}y_5(x) \\ +e^{-b\pi i}\dfrac{\Gamma(a-b)}{\Gamma(a)\Gamma(a-c+1)}y_6(x) - \dfrac{\Gamma(c-1)}{\Gamma(a)\Gamma(b)}y_2(x)\end{array}\right] \quad \ldots(2.1.1)$$

2. $$y_2(x) = \frac{1}{\Gamma(c-1)}\left[\begin{array}{l} e^{-a\pi i}\dfrac{\Gamma(b-a)\Gamma(a)}{\Gamma(b-c+1)}y_5(x) + e^{-b\pi i}\dfrac{\Gamma(a-b)\Gamma(b)}{\Gamma(a-c+1)}y_6(x) \\ -\dfrac{\Gamma(1-c)\Gamma(a)\Gamma(b)}{\Gamma(a-c+1)\Gamma(b-c+1)}y_1(x)\end{array}\right] \quad \ldots(2.1.2)$$

3. $$y_3(x) = \frac{\Gamma(a+b-c+1)\Gamma(c-b)}{\Gamma(a-c+1)}\left[\begin{array}{l} e^{(c-2b)\pi i}\dfrac{\Gamma(1-a)y_4(x)}{\Gamma(b)\Gamma(c-a-b+1)} + e^{-2b\pi i}\dfrac{\Gamma(1-a)y_6(x)}{\Gamma(b-a+1)\Gamma(c-b)} \\ -e^{-c\pi i}\dfrac{\Gamma(a-c+1)y_5(x)}{\Gamma(b)\Gamma(a-b+1)}\end{array}\right] \quad \ldots(2.1.3)$$

4. $$y_4(x)=\frac{\Gamma(a)\Gamma(c-a-b+1)}{\Gamma(1-b)}\begin{bmatrix} e^{(2a-c)\pi i}\ \dfrac{\Gamma(b-c+1)y_3(x)}{\Gamma(a+b-c+1)\Gamma(c-a)}+e^{2(a-c)\pi i}\ \dfrac{\Gamma(b-c+1)y_6(x)}{\Gamma(a)\Gamma(b-a+1)} \\ -e^{-c\pi i}\ \dfrac{\Gamma(1-b)y_5(x)}{\Gamma(a-b+1)\Gamma(c-a)} \end{bmatrix} \quad \ldots(2.1.4)$$

5. $$y_5(x)=e^{(c-b)\pi i}\ \frac{\Gamma(a-b+1)\Gamma(b-c+1)}{\Gamma(2-c)\Gamma(a)}\begin{bmatrix} \dfrac{(e^{(1-b)\pi i})\Gamma(c-a)y_4(x)}{\Gamma(b-c+1)\Gamma(c-a-b+1)}+\dfrac{(e^{-b\pi i})\Gamma(c-a)y_6(x)}{\Gamma(b-a+1)\Gamma(1-b)} \\ -\dfrac{(e^{(b-c+1)\pi i})\Gamma(a)y_3(x)}{\Gamma(a+b-c+1)\Gamma(1-b)} \end{bmatrix} \quad \ldots(2.1.5)$$

6. $$y_1(x)=e^{(c-1)\pi i}\ \frac{\Gamma(1-b)\Gamma(a-c+1)}{\Gamma(a-b)}\begin{bmatrix} \dfrac{\Gamma(c-a-b)y_3(x)}{\Gamma(1-a)\Gamma(1-b)}+\dfrac{\Gamma(a+b-c)y_4(x)}{\Gamma(a-c+1)\Gamma(b-c+1)} \\ -e^{(1-c)\pi i}\ \dfrac{\Gamma(b-a)y_5(x)}{\Gamma(1-a)\Gamma(b-c+1)} \end{bmatrix} \quad \ldots(2.1.6)$$

The proof of the above extension formulas are as follows;

2.1 Derivation of the extension formula for (2.1.1)

From (1.4.1) and (1.4.11), we get

$$\frac{\Gamma(1-c)\Gamma(a+b-c+1)}{\Gamma(a-c+1)\Gamma(b-c+1)}y_1(x)+\frac{\Gamma(c-1)\Gamma(a+b-c+1)}{\Gamma(a)\Gamma(b)}y_2(x)$$

$$=e^{-a\pi i}\ \frac{\Gamma(a+b-c+1)\Gamma(b-a)}{\Gamma(b)\Gamma(b-c+1)}y_5(x)+e^{-b\pi i}\ \frac{\Gamma(a+b-c+1)\Gamma(a-b)}{\Gamma(a)\Gamma(a-c+1)}y_6(x)$$

or, $$\frac{\Gamma(1-c)}{\Gamma(a-c+1)\Gamma(b-c+1)}y_1(x)$$

$$=e^{-a\pi i}\ \frac{\Gamma(b-a)}{\Gamma(b)\Gamma(b-c+1)}y_5(x)+e^{-b\pi i}\ \frac{\Gamma(a-b)}{\Gamma(a)\Gamma(a-c+1)}y_6(x)-\frac{\Gamma(c-1)}{\Gamma(a)\Gamma(b)}y_2(x)$$

or, $$y_1(x)=\frac{\Gamma(a-c+1)\Gamma(b-c+1)}{\Gamma(1-c)}\left[e^{-a\pi i}\ \frac{\Gamma(b-a)}{\Gamma(b)\Gamma(b-c+1)}y_5(x)+e^{-b\pi i}\ \frac{\Gamma(a-b)}{\Gamma(a)\Gamma(a-c+1)}y_6(x)-\frac{\Gamma(c-1)}{\Gamma(a)\Gamma(b)}y_2(x)\right]$$

This proves the extension formula (2.1.1).

Applying the similar derivations from the given relations we obtain the formulae (2.1.2)-(2.1.6). From formulas (1.4.2) and (1.4.12), we get the connection formula for $y_2(x)$ in(2.1.2), Similarly using the formulas (1.4.13) and (1.4.18) we get the connection formula for $y_3(x)$ in (2.1.3),from (1.4.14) and (1.4.17), we get the connection formula for $y_4(x)$ in(2.1.4), from (1.4.15) and (1.4.20), we get the connection formula for $y_5(x)$ in (2.1.5) and finally from (1.4.6) and (1.4.10), we get the formula for $y_6(x)$ in (2.1.6).

3. Conclusion

The hypergeometric function is the solution of the Gaussian hypergeometric differential equation[1]. Kummer has obtained six solutions and twenty connecting formulas for the second-order hypergeometric differential equation. By the help of these formulas listed in (1.3.1-1.7.6) and (1.4.1-1.4.20) respectively, for the hypergeometric differential equation, we have obtained additional six extensions [(2.1.1)-(2.1.6)] of the connecting formulas for $y_1(x)$, $y_2(x)$ $y_3(x)$, $y_4(x)$, $y_5(x)$ and $y_6(x)$. Every solution are expressed as the linear combination of other three solutions. These solutions are highly applicable in various branches of applied sciences.

4. References

[1] Barnes, E. W. **(1908)**. A new development of the theory of the hypergeometric functions. *Proceedings of the London Mathematical Society*, **2**(1): 141-177.

[2] Kummer, E. E. **(1836)**. Über die hypergeometrische Reihe., *Journal Four Math*., **15** :39-83

[3] Haraoka, Y. **(2022)**. Complete list of connection relations for Gauss hypergeometric differential equation. *Kumamoto Journal. Math.*, **35**: 1-60.

[4] Haraoka, Y., & Haraoka, Y. **(2020)**. Analysis at a regular point. *Linear differential equations in the complex domain: from classical theory to forefront*, 21-27.

[5] Lievens, S., Srinivasa Rao, K., & Van der Jeugt, J. (2005). The finite group of the Kummer solutions. *Integral Transforms and Special Functions*, **16**(2): 153-158.

[6] Mathews Jr, W. N., Frerick, M. A., Teoh, Z., &Frerick, J. K. **(2021)**. A physicist's guide to the solution of Kummer's equation and confluent hypergeometric functions. *ArXiv preprint arXiv:*2111.04852.

[7] Morita, T., & Sato, K. I. **(2016)**. Kummer's 24 solutions of the hypergeometric differential equation with the aid of fractional calculus. *Advances in Pure Mathematics*, **6**(3): 180-191.

[8] Olver, F. J., Daalhuis, A.B., Lozier, D.W., Schneider, B.I., Boisvert, R.F., Clark, C.W., Miller, B.R., Saunders, B.V.&Cohl, H.S. **(2022)**. *NIST Digital Library of Mathematical Functions*.

[9] Poudel, M. P., Harsh, H. V., Pahari, N. P., & Panthi, D. **(2023)**. Kummer's theorems, popular solutions and connecting formulas on Hypergeometric function. *Journal of Nepal Mathematical Society*, **6**(1): 48-56.

[10] Poudel, M. P., Harsh, H. V., & Pahari, N. P. **(2023)**. Laplace transform of some Hypergeometric functions. *Nepal Journal of Mathematical Sciences*, **4**(1).

[11] Prosser, R. T. (1994). On the Kummer solutions of the hypergeometric equation. *The American Mathematical Monthly*, **101**(6): 535-543.

[12] Rainville, E. D. **(1960)**. *Special functions*. Macmillan.

[13] Rao, K. S., & Lakshmi Narayanan, V. **(2018)**. *Generalized Hypergeometric functions: transformations and group theoretical aspects*. IOP Publishing.

[14] Slater, L. J. **(1966)**. *Generalized hypergeometric functions*. Cambridge University Press.

[15] Weisstein, E. W. **(2003)**.Confluent hypergeometric function of the first kind. *https://mathworld. wolfram. com/*.

[16] Weisstein, E. W. **(2003)**. Confluent hypergeometric function of the second kind. *https://mathworld. wolfram. com/*.

□□

Instruction to Authors
Nepal Journal of Mathematical Sciences (NJMS)

1. Scope

Nepal Journal of Mathematical Sciences (NJMS) is the official peer-reviewed journal published by the School of Mathematical Sciences, Tribhuvan University. It is devoted to publish the original research papers as well as critical survey articles related to all branches of pure and applied mathematical sciences. The journal aims to reflect the latest developments in issues related to Applied Mathematics, Mathematical Modelling, Industrial Mathematics, Biomathematics, Pure and Applied Statistics, Applied Probability, Operations Research, Theoretical Computer Science, Information Technology, Data Science, Financial Mathematics, Actuarial Science, Mathematical Economics and many more disciplines. NJMS is published in English and it is open to authors around the world regardless of the nationality. It is published two times in a year. NJMS articles are freely available on online and print form.

2. Editorial Policy

NJMS welcomes high-quality original research papers and survey articles in all areas of Mathematical Sciences and real - life applications at all levels including new theories, techniques and applications to science, industry and society. The authors should justify that the theoretical as well as computational results they claim really contribute to Mathematical Sciences or in real- life applications. A complete manuscript be no less than 5 pages and no more than 20 pages (11pt, including figures, tables, and references) as mentioned in the paper Template. However, this can be extended with the acceptance of the respective referees and the Editor-in- Chief. The submitted manuscript should meet the standard of the NJMS.

3. Manuscript Preparation

Manuscript must be prepared in Microsoft Word format (see Template) and LATEX (see template) in the prescribed format with given page limit .

4. Title of the Paper

The title of the paper should be concise, specific, not exceeding 20 words in length.

5. Authors Names and Institutional Affiliations

This should include the full names, institutional addresses and email addresses of authors. The corresponding author should also be indicated.

6. Abstract and Keywords

Each article is to be preceded by an abstract up to maximum 250 words with 4-6 key pertinent words.

7. Introduction

The introduction briefly describes the problem, purpose, significance and output of the research work, including hypotheses being tested. The current state of the research field should be reviewed carefully and key publications should be cited.

8. Materials and Methods

It describes the research plan, the materials (or subjects), and the method used. It explains in detail the data, sample and population, and the variables used.

9. Results and Discussions

Results section should provide details of all of the experiments that are required to support the conclusions. Discussion can also be combined with results.

10. Figures and Tables

Figures and Tables are to be separately numbered, titled in the text serially.

11. Conclusions and Acknowledgments

Not mandatory, but can be added to the manuscript.

12. References

• Journal Citation

[1] Faraji, H. & Nourouzi, K. (2017). Fixed and common fixed points for (ψ, ⊠)-weakly contractive mappings inb-metric spaces. Sahand Communications in Mathematical Analysis.7(1): 49-62.

• Doctoral Dissertation Citation

[1] Oliver, T. H. (2009). The Ecology and Evolution of Ant-Aphid Interactions (Doctoral dissertation Imperial College London).

• Research Book Citation

[1] Mursaleen, M. and Başar, F. (2020). Topics in Modern Summability Theory. BocaRaton : CRC Press.

13. Manuscript Submission

At the time of submission, authors are requested to include the list of 3-5 panellists of experts of the related research area. All information, submissions and correspondence of the articles should be addressed to

Editor-in- Chief:

Prof. Dr. Narayan Prasad Pahari

Director, School of Mathematical Sciences,
Tribhuvan University, Kathmandu, Nepal
Email: njmseditor@gmail.com

Nepal Journal of Mathematical Sciences (NJMS)
ISSN: 2738-9928 (Online), 2738-9812 (Print)
Volume 4, Number 2, August 2023

CONTENTS

1.	On a Generalization of Chatterjee's Fixed Point Theorem in b-metric Space *Chhabi Dhungana, Kshitiz Mangal Bajracharya, Narayan Prasad Pahari, & Durgesh Ojha* *DOI: https://doi.org/10.3126/njmathsci.v4i2.59526*	1-6
2.	High School Performance Based Engineering Intake Analysis and Prediction Using Logistic Regression and Recurrent Neural Network *Govinda Pandey, Nanda Bikram Adhikari, & Subarna Shakya* *DOI: https://doi.org/10.3126/njmathsci.v4i2.59524*	7-16
3.	The Gradshteyn and Ryzhik's Integral and the Theoretical Computation of involving the Continuous Whole Life Annuities *Ogungbenle Gbenga Michael, Ihedioha Silas Abahia, & Ogungbenle Oluwatoyin Gladys* *DOI: https://doi.org/10.3126/njmathsci.v4i2.59527*	17-30
4.	Computational Analysis of Fractional Reaction-Diffusion Equations that Appear in Porous Media *Vinod Gill, Harsh Vardhan Harsh, & Tek Bahadur Budhathoki* *DOI: https://doi.org/10.3126/njmathsci.v4i2.59534*	31-40
5.	On New Space of Vector-Valued Generalized Bounded Sequences Defined on Product Normed Space *Jagat Krishna Pokharel, Narayan Prasad Pahari, & Jhavi Lal Ghimire* *DOI: https://doi.org/10.3126/njmathsci.v4i2.59531*	41-48
6.	Forecasting Annual Mean Temperature and Rainfall in Bangladesh Using Time Series Data *Keya Rani Das,Preetilata Burman, Linnet Riya Barman, Mashrat Jahan, & Mst. Noorunnahar* *DOI: https://doi.org/10.3126/njmathsci.v4i2.59536*	49-58
7.	Collocation Computational Technique For Fractional Integro-Differential Equations *Olumuyiwa James Petera, Mfon O. Etukb, Michael Oyelami Ajisopec, Christie Yemisi Isholad, Tawakalt Abosede Ayoolae, & Hasan S. Panigoro* *DOI: https://doi.org/10.3126/njmathsci.v4i2.59539*	59-66
8.	Numerical Analysis of Fractional-Order Diffusion Equation *Jeevan Kafle, Deepak Bahadur Bist, & Shankar Pariyar* *DOI: https://doi.org/10.3126/njmathsci.v4i2.59538*	67-76
9.	On a New Application of Almost Increasing Sequence to Laguerre Series Associated with Strong Summability of Ultrapherical Series *Suresh Kumar Sahani,Jagat Krishna Pokharel, Gyan Prasad Paudel &S.K. Tiwari* *DOI: https://doi.org/10.3126/njmathsci.v4i2.59537*	77-82
10.	Connection Formulas on Kummer's Solutions and their Extension on Hypergeometric Function *Madhav Prasad Poudel, Narayan Prasad Pahari, Ganesh Basnet, & Resham Poudel* *DOI: https://doi.org/10.3126/njmathsci.v4i2.60177*	83-88

Mailing Address:
Nepal Journal of Mathematical Sciences
School of Mathematical Sciences
Tribhuvan University, Kirtipur, Kathmandu, Nepal
Phone: (00977) 01-6200207
Website: www.sms.tu.edu.np
Email: *njmseditor@gmail.com*
The Nepal Journal of Mathematical Sciences (NJMS) is now available on NepJOL at https://www.nepjol.info/index.php/njmathsci/index